

EXPERIMENTAL AND THEORETICAL INVESTIGATION OF
OIL RETENTION IN A CARBON DIOXIDE AIR-CONDITIONING SYSTEM

by

Jun-Pyo Lee

Dissertation submitted to the Faculty of the Graduate School of the
University of Maryland, College Park in partial fulfillment
of the requirements for the degree of
Doctor of Philosophy
2003

Advisory Committee:

Professor Reinhard Radermacher, Chair/Advisor
Professor Michael Ohadi
Professor Tien-Mo Shih
Professor Kenneth Kiger
Professor Gary Pertmer

ABSTRACT

Title of dissertation: EXPERIMENTAL AND THEORETICAL
 INVESTIGATION OF OIL RETENTION IN A
 CARBON DIOXIDE AIR-CONDITIONING SYSTEM

Jun-Pyo Lee, Doctor of Philosophy, 2003

Dissertation directed by: Professor Reinhard Radermacher
 Department of Mechanical Engineering

In a closed loop vapor compression cycle, a small portion of the oil circulates with the refrigerant flow through the cycle components while most of the oil stays inside the compressor. The worst scenario of oil circulation in the refrigeration cycle is when large amounts of oil become logged in the system. Each cycle component has different amounts of oil retention. Because oil retention in refrigeration systems can affect performance and compressor reliability, it receives continuous attention from manufactures and operators. Thus, the objective of this dissertation is to develop and use a method to experimentally and theoretically investigate the oil retention behavior in a refrigeration system on a component by component level.

The test facility for the oil retention study mainly consists of a refrigeration loop and an oil loop. An oil injection-extraction method was developed to measure the oil retention at each component of the cycle. As the oil circulation ratio increases, the oil retention volume in the heat exchanger and suction line also increases. 16% and 10% of

the total oil amount charged initially is retained in heat exchangers at 5 wt.% of oil circulation ratio for the refrigerant mass flux, 290 kg/m²s and 414 kg/m²s, respectively. The effect of oil on pressure drop was found to be most profound at high vapor qualities where the local oil mass fractions are the highest.

An analytical model for the annular flow pattern to estimate the oil retention was developed. According to the analysis of CO₂ and oil flow in the suction line, the interfacial friction factor should be expressed as the function of CO₂ gas Reynolds number as well as the dimensionless oil film thickness. Furthermore, an empirical interfacial friction factor based on experimental results was developed. All simulation results for the suction line are bounded by $\pm 20\%$ from experimental results. In the case of heat exchangers, void fraction models were used to estimate the oil retention. Due to the changing oil properties, the heat exchangers were divided into segments. Then the oil retention volume in the heat exchangers was calculated from the oil fraction and the length of the corresponding segment. Void fraction models by Hughmark (1962) and Premoli *et al.* (1971), show good agreement with current experimental results of oil retention at the evaporator and the gas cooler, respectively. Simulation results at the evaporator and the gas cooler are bounded by $\pm 20\%$ of experimental results.

To minimize the oil retention in system components, several design guidelines are suggested.

LIST OF ACCOMPLISHMENTS

Several accomplishments are derived from experimental and modeling efforts.

The list of accomplished tasks is as follows:

1. Oil extraction-injection method was developed to measure the oil retention. Test facility was designed and constructed to investigate the oil retention at each cycle component.
2. Extensive experiment was accomplished with several parameters; refrigerant mass flux, oil circulation ratio, evaporator inlet vapor quality, and system components.
3. The oil distribution in the CO₂ air-conditioning systems was experimentally analyzed. For the higher refrigerant mass flux, less oil volume is retained in the heat exchangers, and this also results in a lower pressure drop penalty factor.
4. An oil retention model for each cycle component was developed to generalize the oil retention in various conditions. An analytical model with empirically correlated friction factor used in the suction line while void fraction models were used to estimate oil retention in the heat exchangers.
5. Most simulation results in the suction line and heat exchangers were bounded by $\pm 20\%$ from experimental results.
6. Parametric studies were conducted with the validated models to investigate the influence of different variables on oil retention.

DEDICATION

To My Wife Okyoung Lim

ACKNOWLEDGEMENT

I greatly appreciate to Dr. Reinhard Radermacher for his guide, supporting and encouragement throughout this research. My appreciation goes also to the committee members Dr. M. Ohadi, Dr. K. Kiger, Dr. T. Shih, and Dr. G. Pertmer. I would like to express my deep gratitude to Dr. Y. Hwang, who helps to settle down in Maryland and encourage completing this work.

I am so happy to work with Lorenzo, Amr, Hayo, Layla, Aydin, and Mr. Hong in Heat Pump Laboratory. I also thank to CEEE former and present students. My appreciation also goes to the member of Refrigerant Alternatives Consortium in CEEE to support this project.

I wish to express my deep appreciation to Okyoung, my parents, and my wife's parent who have supported and encouraged me.

TABLE OF CONTENTS

List of Tables	vii
List of Figures	viii
Nomenclature	xi
CHAPTER 1 Introduction	1
1.1 Overview	1
1.2 Literature Review.....	2
1.2.1 Vertical Upward Flow.....	3
1.2.2 Oil Return in Refrigeration Systems	5
1.2.3 Pressure Drop and Performance Degradation Due to Oil Retention	8
1.2.4 Refrigerant/Oil Mixture Properties	10
1.2.5 Oil Return Research at CEEE, University of Maryland	13
1.3 Objectives of this Research.....	15
CHAPTER 2 Working Fluids	18
2.1 Refrigerants	18
2.1.1 Refrigerant Replacement Issues.....	18
2.1.2 Carbon Dioxide as a Refrigerant	19
2.2 Lubricants.....	20
2.2.1 Mineral Oils	21
2.2.2 Polyol Ester Oils	21
2.2.3 Polyalkylene Glycol Oils	22
2.3 Polyalkylene Glycol Oils with CO ₂ Air-Conditioning Systems	22
2.3.1 Solubility.....	23
2.3.2 Miscibility.....	23
2.3.3 Viscosity.....	25
2.3.4 Chemical Stability.....	25
2.3.5 Lubricity.....	26
CHAPTER 3 Experimental Facility	29
3.1 Test Facility.....	29
3.1.1 Refrigeration Loop	30
3.1.2 Oil Loop	33
3.2 Measurement and Data Acquisition.....	36
3.2.1 Measurements	36
3.2.2 Data Acquisition	41
3.3 Uncertainty Analysis.....	42

CHAPTER 4	Experimental Methods	49
4.1	Methodology of Oil Retention Measurement	49
4.2	Experimental Procedures	50
CHAPTER 5	Experimental Results	55
5.1	Oil Retention.....	55
5.1.1	Oil Retention in the Suction Line & Evaporator	56
5.1.2	The Effects of Refrigerant Flow Rate	59
5.1.3	The Effect of Inlet Vapor Quality	60
5.1.4	Oil Retention in the Gas Cooler	61
5.1.5	Oil Distribution in CO ₂ Air-Conditioning Systems	63
5.2	Pressure Drop	64
5.3	Conclusions	67
CHAPTER 6	Modeling of Oil Retention in the Suction Line	74
6.1	Introduction.....	74
6.2	Modeling of Oil Retention in the Suction Line	74
6.2.1	Flow Patterns in the Suction Line	75
6.2.2	Analytical Model.....	77
6.2.3	Oil Film Analysis	78
6.2.4	CO ₂ Core Analysis	80
6.2.5	Interfacial Friction Factor	81
6.2.6	Oil Retention Volume	86
6.3	Verification of Model.....	86
6.4	Parametric Study.....	87
6.4.1	The Effects of CO ₂ Solubility	87
6.4.2	The Effects of Tube Diameter.....	88
6.4.3	The Effects of Suction Line Superheating	89
6.5	Conclusions	89
CHAPTER 7	Modeling of Oil Retention in Heat Exchangers	98
7.1	Introduction.....	98
7.2	Modeling of Oil Retention.....	98
7.2.1	Flow Patterns in Heat Exchangers	98
7.2.2	Oil Retention in the Header	101
7.2.3	Oil Retention in Microchannel Tubes	103
7.2.4	Void Fraction Models	106
7.2.5	Sensitivity to Number of Segments	111
7.3	Simulation Results for the Evaporator.....	111
7.3.1	Oil Retention in the Evaporator	112
7.3.2	Verification of Model.....	112
7.3.3	The Effects of Superheating in the Evaporator Outlet	115
7.3.4	The Effects of Inlet Vapor Quality of the Evaporator	116
7.4	Simulation Results for the Gas Cooler.....	117
7.4.1	Oil Retention in the Gas Cooler	117
7.4.2	Verification of Model.....	119

7.4.3	The Effects of Approach Temperature.....	120
7.4.4	The Effects of Gas Cooling Pressure	121
7.5	Conclusions	121
CHAPTER 8 Conclusions and Design Recommendations		134
8.1	Conclusions from Experimental Research.....	134
8.1.1	Development of an Experimental Facility	134
8.1.2	Experimental Results	135
8.2	Conclusions from the Modeling Efforts	136
8.2.1	Modeling of Oil Retention in the Suction Line and Heat Exchangers	136
8.2.2	Modeling Results	137
8.3	Recommended Design Guidelines.....	138
8.3.1	Suction line	138
8.3.2	Heat Exchangers	138
CHAPTER 9 Future Work		141
Appendix A Summary of Oil Retention Tests.....		142
References.....		150

List of Tables

Table 2.1 Environmental Effects of Refrigerants (Hwang, 1997)	18
Table 2.2 Characteristics and Properties of Refrigerants (Hwang, 1997)	20
Table 2.3 Miscibility of CO ₂ and PAG (Denso Corporation, 1998)	24
Table 3.1 Specifications of Heat Exchangers	31
Table 3.2 Specifications of Gear Pump	34
Table 3.3 Specifications of Thermocouples.....	37
Table 3.4 Specifications of Absolute Pressure Transducers.....	38
Table 3.5 Specifications of Differential Pressure Transducers.....	38
Table 3.6 Specifications of Refrigerant Mass Flow Meter	39
Table 3.7 Specifications of Oil Mass Flow Meter	39
Table 3.8 Specifications of Oil Level Sensor	41
Table 3.9 Estimates of the Uncertainty of Measured Quantities	44
Table 3.10 Uncertainties for Oil Circulation Ratio and Oil Retention.....	44
Table 5.1 Properties of Oil and CO ₂ in Heat Exchangers (G=290 kg/m ² s).....	62
Table 5.2 Summary of Test Condition (MFR _{ref} =14g/s, OCR=5 wt.%).....	63
Table 7.1 Average and Standard Deviations of Oil Retention in the Evaporator	115
Table 7.2 Average and Standard Deviations of Oil Retention in the Gas cooler	120

List of Figures

Figure 2.1 Solubility of CO ₂ and PAG Oil (Hauk and Weidner, 2000)	27
Figure 2.2 Miscibility of CO ₂ and PAG Oil (Denso Corporation, 1998)	27
Figure 2.3 Viscosity of PAG Oil with Dissolved CO ₂ (Kawaguchi <i>et al.</i> , 2000).....	28
Figure 3.1 Indoor-Side Air Loop for the Evaporator.....	45
Figure 3.2 Outdoor-Side Air Loop for the Gas Cooler.....	45
Figure 3.3 Schematic Diagram of Refrigeration Loop	46
Figure 3.4 Flow Visualization Section.....	46
Figure 3.5 Schematic Diagram of Oil Loop.....	47
Figure 3.6 Oil Injection Ports in Refrigeration Loop.....	47
Figure 3.7 Oil Extractor	48
Figure 3.8 LabView Software for DAS	48
Figure 4.1 Oil Retention Characteristics.....	54
Figure 5.1 Oil Retention in Evaporator and Suction Line ($G = 290 \text{ kg/m}^2\text{s}$)	68
Figure 5.2 Oil Retention in Evaporator and Suction Line ($G = 352 \text{ kg/m}^2\text{s}$)	68
Figure 5.3 Oil Retention in Evaporator and Suction Line ($G = 414 \text{ kg/m}^2\text{s}$)	69
Figure 5.4 Oil Retention in Evaporator and Suction Line ($G = 559 \text{ kg/m}^2\text{s}$)	69
Figure 5.5 Effect of Refrigerant Mass Flux on Oil Retention in Evaporator	70
Figure 5.6 Effect of Evaporator Inlet Vapor Quality on Oil Retention	70
Figure 5.7 Oil Retention in Gas Cooler ($G = 290 \text{ kg/m}^2\text{s}$)	71
Figure 5.8 Oil Retention in Gas Cooler ($G = 414 \text{ kg/m}^2\text{s}$)	71
Figure 5.9 Oil Retention in Heat Exchangers	72

Figure 5.10 Oil Distribution in CO ₂ Air-Conditioning Systems	72
Figure 5.11 Pressure Drop Penalty Factor in Evaporator	73
Figure 5.12 Pressure Drop Penalty Factor in Heat Exchangers	73
Figure 6.1 Baker’s Flow Pattern Map For Horizontal Flow (1954)	91
Figure 6.2 Flow Pattern Map (Taitel and Dukler, 1976)	91
Figure 6.3 Visualized CO ₂ /Oil Flow in Suction Line	92
Figure 6.4 Force Balance of Annular Flow	92
Figure 6.5 Interfacial Shear Stress vs. Refrigerant Gas Velocity	93
Figure 6.6 Interfacial Friction Factor vs. Reynolds Number	93
Figure 6.7 Interfacial Friction Factor vs. Dimensionless Oil Film Thickness	94
Figure 6.8 Interfacial Friction Factor with New Correlation.....	94
Figure 6.9 Comparisons of Oil Retention Volume Ratios between Measured and Calculated Values	95
Figure 6.10 Effects of CO ₂ Solubility in Suction Line	96
Figure 6.11 Effects of Tube Diameter in Suction Line.....	96
Figure 6.12 Effects of Superheating of the Suction Line	97
Figure 7.1 Flow Pattern Map for Two-Phase Flow in Microchannel.....	124
Figure 7.2 CO ₂ /Oil Mixture Flows in the Evaporator.....	124
Figure 7.3 Modeling of Oil Retention in Outlet Header of the Evaporator.....	125
Figure 7.4 CO ₂ /Oil Mixture Flows in the Gas Cooler	125
Figure 7.5 Modeling of Oil Retention in a Microchannel of Heat Exchangers	126
Figure 7.6 Sensitivity to Number of Segments to Oil Retention.....	126

Figure 7.7 Calculated Oil Retention Volume Ratio and Vapor Quality in the Evaporator	127
Figure 7.8 Calculated Oil Retention Volume Ratio in the Evaporator Header	127
Figure 7.9 Volume Ratios in the Evaporator using Various Void Fraction Models	128
Figure 7.10 Effects of Superheating in the Evaporator Outlet.....	129
Figure 7.11 Effects of Vapor Inlet Quality in the Evaporator	129
Figure 7.12 Calculated Oil Retention Volume Ratio and Temperature in the Gas Cooler	130
Figure 7.13 Calculated Length of Segment and Oil Fraction in the Gas Cooler	130
Figure 7.14 Volume Ratio in the Gas Cooler using Various Void Fraction Models	131
Figure 7.15 Calculated and Measured Oil Retention Volume Ratio in System	132
Figure 7.16 Effects of Approach Temperature in the Gas Cooler	132
Figure 7.17 Effects of Gas Cooling Pressure	133
Figure 8.1 Proposed Designs of Heat Exchangers	140

Nomenclature

Roman symbols

A	Area [m^2]
AB	Alkylbenzene
AN	Alkyl Naphthalene
ASHRAE	American Society of Heating, Refrigeration and Air- Conditioning Engineers
ASTM	American Society for Testing and Materials
C	Capacitance [pF]
CEEE	Center for Environmental Energy Engineering
CFC	Chlorofluorocarbon
D	Tube Diameter [m]
DAS	Data Acquisition System
f	Friction Factor
F	Parameter Defined by Equation (7-16)
Fr	Froude Number
G	Mass Flux [$\text{kg}/\text{m}^2\text{-s}$]
GWP	Global Warming Potential
h	Enthalpy [kJ/kg]
HCFC	Hydrochlorofluorocarbon
HFC	Hydrofluorocarbon

HTC	Heat Transfer Coefficient [kW/m ² K]
j	Superficial Gas Flux [m/s]
K	Dielectric Constant
L	Length [m]
MO	Mineral Oil
\dot{m}	Mass Flow Rate [kg/s]
n	Number of Segment
OCR	Oil Circulation Ratio [wt.%]
ODP	Ozone Depletion Potential
P	Pressure [kPa]
PAG	Polyalkylene Glycol
PAO	Poly Alpha Olefin
POE	Polyol Ester
PVE	Poly Vinyl Ether
\dot{Q}	Heat Transfer Rate [kW]
R	Tube Radius [m], Thermal Resistant or Fouling per Unit Length [m/(kW/k)]
Re	Reynolds Number
RH	Relative Humidity
RPM	Revolution Per Minute
S	Slip Ratio
SLHX	Suction Line Heat Exchanger

T	Temperature [$^{\circ}\text{C}$]
TAN	Total Acid Number
u	Velocity [m/s]
U	Overall Heat Transfer Coefficient [$\text{kW}/\text{m}^2\text{K}$]
V	Oil Volume [ml]
We	Weber Number
X	Martinelli Parameter Defined by Equation (6-2)
x	Quality
z	Length [m]

Greek symbols

α	Void Fraction
β	Volume Flow Ratio
d	Oil Film Thickness [m]
ε	Error
λ	Parameter Defined by Equation (6-1)
μ	Dynamic Viscosity [$\text{N}/\text{m}\cdot\text{s}$]
ν	Kinetic Viscosity [m^2/s]
ρ	Density [kg/m^3]
σ	Surface Tension [N/m], Deviation
τ	Shear Stress [N/m^2]
ψ	Parameter Defined by Equation (6-1)

Subscripts

<i>a</i>	air
<i>c</i>	core
<i>cal</i>	calculation
<i>exp</i>	experiment
<i>g</i>	gas
<i>i</i>	Interface
<i>in</i>	inlet
<i>l</i>	liquid
<i>LMTD</i>	Log Mean Temperature Difference
<i>o</i>	oil
<i>out</i>	outlet
<i>r</i>	refrigerant, radial
<i>w</i>	water

CHAPTER 1 Introduction

1.1 Overview

The compressor in a refrigeration system needs oil to lubricate its mechanical parts. The function of a lubricant is to prevent surface-to-surface contact in the compressor, to remove heat, to provide sealing, to keep out contaminants, to prevent corrosion, and to dispose of debris created by wear (Vaughn, 1971). In a closed loop vapor compression cycle, a small portion of the oil circulates with the refrigerant flow through the cycle components while most of the oil stays in the compressor. The lubricant is necessary for the compressor, but is not necessary for the other components of the refrigeration system. To fulfill its duty, the dynamic viscosity of the refrigerant/oil mixture must be high enough to provide the proper lubrication and sealing effects. On the other hand, it is important that the viscosity of the refrigerant/oil mixture in the heat exchangers and tubes is not too high, so that an adequate feedback of the oil into the compressor is possible (Kruse and Schroeder, 1984).

Successful operation of the refrigeration system requires sufficient oil return into the compressor to avoid eventual trouble from a lack of proper lubrication that may cause compressor failure. In fact, the oil return behavior is a complex function of fluid properties as well as system components and configuration aspects. Since the temperature and pressure conditions are varied depending upon each system component, such as the gas cooler, the evaporator and the suction line, the oil return characteristics in the cycle components are also specific to the system component.

The worst scenario of oil circulation in the refrigeration cycle is when large amounts of oil become logged in the system. The circulating oil, which is missing from the compressor, exists as an oil film on the tube wall, and the oil film thickness is affected by the system conditions. Thus, each cycle component has different amounts of oil retention. Large amounts of oil retention cause a decrease in heat transfer and an increase in pressure drop. As a result, the system performance can be degraded. Because oil retention in refrigeration systems can affect performance and reliability, it receives continuous attention from manufactures and operators.

1.2 Literature Review

One of the important issues in refrigeration systems for the reliability and the system life is oil return, so the literature on this issue is abundant. Some researchers have focused on the vertical upward flow of the refrigerant gas/oil mixture. In these cases, the refrigerant gas velocity is a major parameter in ensuring oil transport. Several research papers on the miscible or immiscible pairs of refrigerant/oil mixture also have been published because of the legally mandated phase-out of Chlorofluorocarbon (CFC) and Hydrochlorofluorocarbon (HCFC) refrigerants. These researchers evaluated oil return performance at a single component. In addition, several other studies have been conducted to study oil properties and pressure drop due to oil retention.

However, studies of the oil distribution in each cycle component for proper oil management in refrigeration systems currently have not been found. Moreover, oil return research with CO₂, one of the most promising candidates for alternative refrigerants, has

not yet been investigated. The published literature for oil return as well as oil's effect on system performance and oil properties is summarized below.

1.2.1 Vertical Upward Flow

The vertical suction line is considered to be a weak place for oil return because the refrigerant has to overcome gravity to carry the oil vertically upward. Thus, many papers have been already published to propose guidelines for, or to solve oil return problems.

Wallis (1969) correlated oil transport by experimental results for R-12 and R-22 with mineral oil (MO). He suggested the dimensionless superficial velocity as a conservative bound to guarantee oil transport for the vertical upward flow.

Riedle *et al.* (1972) summarized the open literature for oil transport using various topics: flow pattern, pressure drop, and entrainment. From a literature review of vertical upward flow, an analytical model was chosen. It describes the phenomenon of oil transport in a refrigerant line. However, no experimental tests were performed to verify their proposed model.

The American Society of Heating, Refrigeration and Air-Conditioning Engineers (ASHRAE) Handbook (1976, 1994) contains tables that give minimum refrigeration capacities for suction risers. The minimum refrigeration capacity was calculated from the minimum refrigerant velocity required to ensure oil transport upward in the suction riser. However, the ASHRAE data on oil transport in vertical pipes was thought by some critics to have insufficient experimental verification. Jacobs *et al.* (1976) conducted an experimental study to verify the ASHRAE data. Oil was injected into the test section, and the critical refrigerant mass flux needed to transport oil upward was obtained using sight

glasses. The refrigerant was always in the vapor phase in the test section. They suggested a dimensionless number, which is a function of refrigerant velocity and of the properties of oil and refrigerant, for guarantee of oil transport. They also simulated typical compressor suction and discharge conditions.

Another verification of the ASHRAE data for R-134a/oil mixture was studied by Kesim *et al.* (2000). The minimum refrigerant velocity to guarantee oil transport to the vertical upward flow was simulated. The minimum velocity was found by using the conditions of zero oil flow rate and equal oil and refrigerant shear stresses at the interface. They prepared minimum refrigeration capacity tables for R-134a at the suction line and discharge line. In their simulation, oil film thickness was assumed to be 4% of tube radius. However, this result of this calculation was not validated with experimental results.

Fukuta *et al.* (2000) conducted an oil return study for a suction line with vertical upward flow. Two-phase flow of the oil and air was used to examine basic characteristics of the oil film transport in vertical upward flow. This was done by observing flow patterns and measuring oil film thickness. The oil film thickness was measured using a capacitance sensor with various parameters: air and oil flow rate, oil viscosity, and tube diameter. The average oil film thickness was shown to decrease with an increase of the air velocity and the pressure. It also increased slightly with an increase of the oil viscosity and flow rate. An empirical correlation satisfying the criteria for the oil transport was proposed, using experimental results for the air-oil two-phase flow.

Blankenberger *et al.* (2002) investigated the flow reversal for the vertical annular flow. Their paper describes a study aimed at characteristics of the dynamic behavior of an annular oil film layer driven by air upward through a 50.8 mm pipe. An optical film

thickness sensor was used to obtain oil film thickness data for air-oil flow. They found that the correlations created using air-water systems did not predict the flow behavior of the air-oil system. Two separate layers in the liquid film, a bubbly layer along the wall and a wavy layer, were observed. Their experiments supported a model developed by Mehendale and Radermacher (2000).

1.2.2 Oil Return in Refrigeration Systems

Introducing Hydrofluorocarbon (HFC) refrigerants as alternative refrigerants for CFCs and HCFCs has raised a refrigerant and oil miscibility issue. It is widely believed that without significant mutual miscibility between refrigerant and oil in a low temperature component such as the evaporator or suction line, the compressor would lack oil and eventually result in compressor failure. Related to this issue, several research results on the oil return characteristics of miscible and immiscible pairs of refrigerant/oil mixtures have been published and are summarized below.

Oil return characteristics of a refrigerant blend of R-404A with two lubricants, MO and Polyol Ester (POE) oil, were evaluated by Fung and Sundaresan (1994) in a low temperature display case refrigeration system. They measured the oil level in the compressor crankcase to determine oil return. In the case of low condensing temperature and high evaporative temperature, better oil return characteristics were shown based on the observation of higher oil levels in the compressor crankcase. The refrigerant lubricant combination of R-404A and POE showed significantly better oil return characteristics when compared to R-502/MO and R-404A/MO. Moreover, the evaporation heat transfer for the system, R-404A/POE, performed better than R-502/MO and R-404A/MO.

Sunami *et al.* (1994) evaluated the application of Alkylbenzene (AB), which has been used for many years as a refrigerant oil, to a high-pressure, dome-type rotary compressor. They conducted tests of oil return performance with R-134a with AB and POE. POE showed good oil return characteristics, but the oil return performance of lower-viscosity AB was nearly as good as that of POE. This was because lower-viscosity AB maintained its low viscosity even at low temperatures. They also concluded that lower viscosity AB provides better durability and reliability than conventional MO.

Biancardi *et al.* (1996) conducted experimental and analytical efforts to determine the lubricant circulation characteristics of HFC/POE pairs and HFC/MO pairs in a residential heat pump system and to compare their behavior with an R-22/MO pair. The minimum flow velocities for “worst-case,” in which velocities occurred in the vertical vapor line, were determined by visual observations in an operating heat pump. In addition, they developed on-line oil circulation ratio measurement instrumentation. Biancardi *et al.* reported that minimum flow velocities ranging from 1.8 to 1.9 m/s were required in cooling, and that the use of immiscible oil with R-407C did not result in any worst-case oil return scenario.

Oil return performance comparisons between MO and POE were evaluated by Reyes-Gavilan *et al.* (1996). They experimentally investigated the oil return and lubricant flow characteristics for R-134a with POE and MO at different evaporating temperatures in domestic refrigeration systems. Their study showed that refrigerant gas velocities played an important role in proper oil return to the compressor, and lubricant flow characteristics were similar for both refrigerant/oil pairs at suction conditions.

Sunami *et al.* (1998) conducted oil return tests and durability tests with an HFC refrigerant/AB pair in a split air conditioner. They observed exceptional oil return for ABs, and reported no significant difference among the different viscosity oils. In addition, an immiscible refrigerant pair, R-407C/AB, showed superior anti-wear properties in the compressor compared to miscible refrigerant/oil pairs, such as R-22/MO and R-407C/POE.

Sumida *et al.* (1998) tested R-410A/AB to observe flow patterns in the liquid line and evaluate oil return characteristics. Since, in the liquid line, the oil moving velocity is smaller than the liquid refrigerant velocity, oil accumulates in the liquid line. From their test, it was found that non-accumulation of oil in the liquid line was achieved by keeping the oil circulation ratio under 1 wt.%. Through a sight glass in the compressor, they observed oil levels to evaluate oil return characteristics in a split air-conditioner. They reported that the R-410A/AB pair had reliable oil return characteristics, and the cycle performance with R-410A/low viscosity AB was the same as that of R-410A/POE.

From the literature review, it is clear that many studies have been conducted to evaluate oil return characteristics with HFC refrigerant and miscible or immiscible oil pairs. However, there is no study, which investigates the oil distribution in system components. Moreover, no research about oil return characteristics with CO₂ as a refrigerant has been published yet, even though many studies already have been conducted on system performance or improvement of system components after CO₂ was considered to be an environmentally friendly refrigerant.

1.2.3 Pressure Drop and Performance Degradation Due to Oil Retention

Oil retention in heat exchangers affects heat transfer as well as pressure drop. The presence of oil causes the roughness of the interface between refrigerant and oil to increase, which results in pressure drop increases. The open literature with regard to pressure drop due to oil retention is summarized here.

Green (1971) studied the pressure loss for a R-12/oil mixture with 6 to 12% oil content compared with oil-free R-12 and R-22. The friction factor was roughly double because of the oil content, resulting in a doubling of the frictional pressure loss in the systems containing oil compared to that of a similar oil-free system.

Scheideman and Macken (1975) and Macken *et al.* (1979) investigated the pressure drop caused by oil in the compressor suction and discharge line of a refrigeration system. The refrigeration loop was an all-vapor system in which a reciprocating compressor pumped vapor into the loop. Computations to predict pressure drop were also conducted for R-502 and R-500. The experimental data showed that the existing oil in the tube resulted in a significant increase of the pressure drop under many typical suction conditions. They correlated the pressure drops for 12.5 mm to 75 mm horizontal pipes.

Alofs and Hassan (1990) investigated pressure drop due to the presence of oil in a horizontal pipe under suction line conditions in the refrigeration system. They proposed a flux model, which was modified from the model by Macken *et al.* (1979). The model indicated that the presence of oil increases the pressure drop by as much as a factor of 10.

Zurcher *et al.* (1998) studied pressure drop due to the presence of oil during evaporation. The oil, especially at high vapor qualities, increased the two-phase pressure drop. The influence of oil was strongest at high vapor qualities where the local oil mass

fractions were the highest. However, small amounts of oil, 0.5% and 1%, had almost no effect on pressure drop for vapor qualities below 95%.

The oil also affects system performance because the evaporator capacity is decreased by oil retention. The oil deteriorates the evaporation heat transfer resulting in an increase in evaporator temperature.

Eckels and Pate (1991) studied the effects of oil on two-phase heat transfer. They found that the presence of oil up to 3% improved evaporation heat transfer compared to that of pure refrigerant. In the condenser, the heat transfer was reduced by the presence of oil. The reduction in the condenser performance indirectly degraded the system performance.

The degradation of evaporator capacity due to oil was investigated by Grebner and Crawford (1993). A test facility was constructed to measure the pressure-temperature-concentration relations for mixtures of R-12 with two MOs and R-134a with two synthetic oils such as POE and Polyalkylene Glycol (PAG). Assuming standard operating conditions and neglecting pressure drop in the evaporator, significant reductions in evaporator capacities were predicted due to the increase in saturation temperature resulting from the presence of oil. The effects of oil solubility on evaporator capacity reduction were found to be greater for systems containing R-12/MO mixtures than for those containing R-134a/POE or PAG mixtures.

Popovic (1999) experimentally measured system performance for R-134a with MO and POE. The major impact of a lubricant on system performance was reflected through the magnitude of evaporation heat transfer rate. The author found that a small amount of circulating oil could significantly alter the evaporation heat transfer. In

contrast to the evaporator performance, the effects of oil type on compressor efficiencies were not substantial. The coefficient of performance could be improved by as much as 5% by selecting a miscible oil over an immiscible oil. Popovic concluded that oil selection should not only to be based on system reliability, but also on system performance and efficiency, based on the fact that the use of miscible and lower-viscosity oil resulted in improved performance.

Hwang *et al.* (2002) investigated the effect of the oil circulation ratio on the system performance in a CO₂ climate control system for a vehicle. The oil circulation ratio was measured by a capacitance sensor. They reported that the capacitance of CO₂/PAG mixture depended on the pressure and temperature of the oil in the CO₂/PAG mixture and the oil circulation ratio. The coefficient of performance was degraded by 8% and 11% for idling (1,000 RPM) and driving (1,800 RPM) conditions, respectively, if the oil circulation ratio increased from 0.5 wt.% to 7 wt.%.

1.2.4 Refrigerant/Oil Mixture Properties

Since the circulating oil in a refrigeration system has a dissolved fraction of refrigerant in the oil, the viscosity, density and surface tension of the oil in the mixture are not same as those of pure oil. Several researchers have been interested in the changes of oil properties in the refrigerant/oil solution.

Cooper (1971) investigated the solubility for R-12 and R-22 with MO. The test results showed that oil viscosity increased with an increase of temperature because of the boiling away of the refrigerant which is dissolved in the oil. The maximum oil viscosity did not necessarily occur in the evaporator, but at some specific level of superheat, which most likely was in a suction line.

Short and Cavestri (1992) reported data on the chemical and physical properties of high-viscosity esters and interactions with R-134a. Viscosity of oil-refrigerant solutions was also presented to evaluate the lubricant for hydrodynamic lubrication and sealing of compressor areas.

Thomas and Pham (1992) presented solubility and miscibility results for R-134a with PAGs and modified PAGs, which have different viscosities. The lower viscosity lubricants had higher solubility and were completely miscible with refrigerant. As the viscosity rose, immiscibility appeared and extended to lower temperatures, with further increases in viscosity.

Yokozeki *et al.* (1994, 2000) developed the general model, based on thermodynamics, for refrigerant/oil solubility. The solubility data of partially miscible HFC refrigerants and AB mixtures were correlated with the use of a special binary mixing rule. By combining these solubility and viscosity models, they constructed a viscosity chart as a function of the temperature and solubility.

Even though the number of studies using CO₂ as a refrigerant has significantly increased due to the current environmental issues, few studies have been conducted to evaluate proper oil pairs for CO₂ system. The available papers for oil properties with CO₂ are summarized below.

The solubility, lubricity, and miscibility of CO₂ with a number of synthetic lubricants were studied by Seeton *et al.* (2000). They reported that POE lubricant showed good miscibility characteristics. On the other hand, PAG, Poly Alpha Olefin (PAO), and AB were not miscible with CO₂ at high concentrations of CO₂. However, PAG showed

the best lubricity for transcritical applications because PAG maintained the highest mixture viscosity.

Li and Rajewski (2000) evaluated various lubricants, such as PAO, MO, PAG, POE, and Alkyl Naphthalene (AN), for their interactions with CO₂. Their experimental study included miscibility, solubility, working viscosity, sealed tube stability and lubricity. They found that the lubricants studied varied in their miscibility with CO₂, and that the working viscosities of the solutions were significantly decreased due to the solubility with CO₂.

Kawaguchi *et al.* (2000) measured oil viscosity, solubility, and miscibility for PAG, Poly Vinyl Ether (PVE), and POE oils with CO₂. They also tested lubricity and wear characteristics with different oil types. They reported that PAG is the best oil to use as CO₂ refrigerating oil because it is partially miscible. It has excellent lubricity in boundary lubrication under CO₂ supercritical conditions. It also showed good stability under CO₂ supercritical conditions.

Another study on the miscibility issue with CO₂ was conducted by Hauk and Weidner (2000). They conducted miscibility tests between CO₂ and PAG, POE, and PAO oils. POE showed good miscibility with CO₂, but a phase separation between PAG or PAO and CO₂ occurred. They also developed a solubility chart based on pressure and temperature for three different oil types and CO₂. From their solubility chart, around 30 wt.% of CO₂ can be dissolved into PAG oil under an evaporator condition, which is around 4 MPa pressure.

1.2.5 Oil Return Research at CEEE, University of Maryland

Recently, oil return issues as well as oil's effect on heat transfer measurement have been studied by the Center for Environmental Energy Engineering (CEEE) at the University of Maryland. The published literature by CEEE is summarized below.

Sundaresan and Radermacher (1996) experimentally investigated oil return characteristics of R-407C/MO in comparison with R-407C/ POE and R-22/MO in a split three-ton heat pump. They modified a compressor to install a sight tube, which was fitted with a scale grade so that oil level in the compressor could be observed. For each refrigerant, a charge optimization was conducted to determine the maximum performance. R-22/MO and R-407C/POE showed very similar oil return characteristics and were expected to be equally reliable. However, in the case of R-407C/MO a significant amount of oil was logged in the system outside of the compressor. The study suggested that further experiments were needed to better determine the oil return characteristics.

Oil return characteristics in vertical upward flow were experimentally and theoretically investigated by Mehendale (1998)/Mehendale and Radermacher (2000). The critical mass flow rate for preventing oil film reversal in a vertical pipe for vapor refrigerant with R-22, R-407C, and R-410A with MO and POE was pinpointed and was compared with the results by Jacobs *et al.* (1976). An annular flow model with a vapor core was developed to predict the onset of lubricant film flow reversal. This accounted for lubricant concentration and viscosity variations. At refrigerant mass flow rates below those for zero wall shear stress, the net pressure force was insufficient to balance the weight of the fluid. The oil film immediately adjacent to the wall started flowing in a downward direction. Whenever the refrigeration system is operated at a mass flow rate

lower than the critical mass flow rate, some oil will always flow downward instead of being fully transported upward. Predictions were within + 9% and – 6% of the experimental data. From the parametric studies, the pipe's inside diameter has the greatest effect on the critical refrigerant mass flow rate. This is followed by the vapor density, the film viscosity and the film density.

Hwang *et al.* (2000) and Lee *et al.* (2001) conducted an experimental study of oil return characteristics in the vertical upward suction line of a residential refrigerator and freezer. Their study investigated flow patterns and oil accumulation characteristics of R-134a/immiscible oil pairs, AB and MO, with three different refrigerant and oil flow rates. From the visualization tests, flow patterns of all oils were either a churn flow or an annular flow. At a high refrigerant Reynolds number ($Re=13,000, 16,000$), the flow pattern was shown to be the annular flow that continuously forced oil upward, regardless of the oil flow rate. On the other hand, the churn flow was observed at a low refrigerant Reynolds number ($Re=4,000$), which resulted in unstable flow and oscillation. The oil film on the wall flowed downward, accumulated, and eventually formed plugs. The MO and high viscosity AB oil caused a larger oil amount to accumulate in the suction line tube. 2.3% to 17.6% of the oil initially charged (250 ml) to the compressor was accumulated in the suction line. Hwang and Lee recommended that the churn flow pattern be avoided because the oil transport in a vertical tube is very unstable.

The oil effect on the evaporation heat transfer in the microchannel heat exchanger was experimentally investigated by Zhao (2001). He studied various parameters such as refrigerant mass flux, saturation temperature, and vapor quality for miscible oil with CO₂. The average evaporation heat transfer coefficient was measured under various oil

circulation ratios, ranging from 0 to 7 wt.%. Increasing the vapor quality degraded the heat transfer coefficient in the presence of oil because oil acts as a thermal resistance on the wall at high vapor quality. The pressure drop increased with an increase in the oil circulation ratio because of higher CO₂/oil mixture viscosity.

Studies conducted by CEEE have focused on the oil effect on single system components only, such as the suction line or evaporator. In a vertical suction line, a minimum refrigerant flow rate that would ensure oil transport was suggested, and in this way the oil retention volume could be measured. In the evaporator, the evaporation heat transfer and pressure drop due to the presence of oil was also experimentally investigated. This research was considered as an initial step in obtaining the oil distribution in entire system components. The oil retention volume in the heat exchangers as well as the suction line at certain system conditions (i.e. refrigerant mass flow rate and oil circulation ratio) can be obtained by adapting an oil injection-extraction method into any system components.

1.3 Objectives of this Research

The literature review showed that oil return research in refrigeration systems mostly focuses on either the oil transport in a vertical tube or the oil level measurement in the compressor to predict oil logging characteristics in a system. However, these studies neither quantify the oil volume retained in the system components nor provide oil distribution information. Even though many research projects for refrigeration systems have been conducted, there is as yet no study on oil retention on a component basis, in any refrigeration system. Thus, the objective of this dissertation is to develop and use a

method to experimentally and theoretically investigate the oil retention behavior in a refrigeration system on a component by component level. A CO₂ air-conditioning system was chosen because it represents one extreme in refrigeration system design: very high pressures and refrigerant densities. Studies with medium and low-pressure systems are planned for a later thesis to eventually cover the entire range of heat pump and refrigeration systems. The tasks to be performed to achieve the objective are as follows:

- Develop an oil retention test methodology.
- Design and construct a test facility for the oil retention test.
- Investigate the oil retention volume in each cycle component of a CO₂ air-conditioning system.
- Conduct experiments with the following parameters:
 - Refrigerant mass flux
 - Oil circulation ratio
 - Evaporator inlet vapor quality
 - System components (suction line, evaporator and gas cooler)
- Investigate the effects of the presence of oil in the heat exchangers upon the pressure drop increase.
- Develop an analytical model to predict oil retention in a horizontal suction line.
- Examine various void fraction models to be used to calculate oil retention in heat exchangers.
- Verify simulation results with experimental results.

- Quantify the effect of various parameters on oil retention by using the model developed for the suction line and heat exchangers.
- Develop design guidelines in system components.

CHAPTER 2 Working Fluids

2.1 Refrigerants

2.1.1 Refrigerant Replacement Issues

In 1974, Rowland and Molina discovered that CFCs and HCFCs were destroying the stratospheric ozone layer. As a result of this discovery, the Montreal protocol was signed in 1987 to regulate the production and trade of ozone-depleting substances such as CFCs. CFCs were no longer to be sold or produced as of January 1, 1996. HCFC refrigerants were also regulated due to the ozone depletion potential (ODP) and are to be phased out by the year 2020 in the United States.

Table 2.1 Environmental Effects of Refrigerants (Hwang, 1997)

Refrigerants		Ozone Depletion Potential (ODP)	Global Warming Potential (GWP, 100 yr)
CFC	R-12	1	7100
HCFC	R-22	0.055	1500
HFCs	R-134a	0	1200
	R-407C	0	1600
	R-410A	0	2200
Natural Refrigerants	R-744 (Carbon dioxide)	0	1
	R-717 (Ammonia)	0	0
	R-290 (Propane)	0	3

R-134a has been commonly used as an alternative to R-12 in automotive air-conditioning systems. Two-potential HFC refrigerant candidates with zero ODP, R-407C

and R-410A, have emerged as alternatives to R-22. These two possible candidates show either lower performance or require new system design due to the higher vapor pressure (Hwang, 1997). Although HFCs with zero ODP seem like a logical replacement for both CFC and HCFC refrigerants, these HFC refrigerants still have high Global Warming Potential (GWP) as shown in Table 2.1. Consequently, natural refrigerants having their zero ODP, low GWP, and lack of adverse environmental effect such as carbon dioxide, ammonia, and propane have been studied. Among those natural refrigerants, CO₂ is preferable because it is non-flammable, is low cost, and has potential for reduced-size system components due to its high vapor pressure.

2.1.2 Carbon Dioxide as a Refrigerant

Increasing environmental concerns have accelerated research on refrigerants for refrigeration industries. Candidates for alternative refrigerants that have no environmental impact are under evaluation for a long term solution. CO₂ was re-investigated at the beginning of the 1990's because of environmental concerns (Lorentzen and Pettersen, 1993). CO₂ has a number of advantages, such as no need for either recycling or recovery, low cost as shown in Table 2.2, as well as zero ODP and the lowest GWP as shown in Table 2.1. CO₂ is also considered particularly for automotive systems because of the relatively higher leak rates found in automotive applications. Many researchers expect that the CO₂ will replace R-134a in the automotive air-conditioning systems in the near future.

At first glance, the thermodynamic properties of CO₂ are not nearly as good as those of the man-made refrigerants, and thus one would expect a significantly lower performance. However, the nature of the transcritical cycle with the temperature glide

results in a smaller temperature approach at the heat rejection heat exchanger outlet (Hwang, 1997 and Preissner, 2001). In addition, its transport properties are much better than those of other refrigerants. CO₂ has a much smaller surface tension and liquid viscosity, which result in higher boiling heat transfer and smaller pressure loss. These attractive characteristics might lead to expanded use of CO₂ in the future (Zhao *et al.*, 2000). So far, much research has been conducted for comparing performances with HFC refrigerants and for system optimizations; however, very few studies on CO₂ and oil issues have been published in spite of the importance of the system approach.

Table 2.2 Characteristics and Properties of Refrigerants (Hwang, 1997)

Refrigerant	R-22	R-134a	NH ₃	CO ₂
Natural Substance	No	No	Yes	Yes
Flammability	No	No	Yes	No
Toxicity	Yes	Yes	No	No
Molar mass	86.48	102.03	17.03	44.01
Approx. relative price	1	3-5	0.2	0.1

2.2 Lubricants

The essential function of a lubricant is to lubricate the moving parts of the compressor. Hydrodynamic lubrication is present in the normal modes of operation, characterized by the formation of a lubricant film between moving parts. Boundary lubrication occurs during abnormal conditions such as starting up, stopping, and overloading due to inadequate amounts of lubricants. In each of the three above cases, the mating surfaces are in contact when the lubricant film is not thick enough to keep surfaces separate (Popovic, 1999). In this section, the characteristics of MO and two synthetic oils are described.

2.2.1 Mineral Oils

Three types of MOs are used in refrigeration systems. They are naphthenic, paraffinic, and iso-paraffinic. These grades of lubricants are obtained from crude oil during the refining process. In general, the higher the degree of refining, the better the lubricating properties. Higher levels of refining also improve the stability of lubricants, which results in improved system reliability and resistance to degradation (Li and Rajewski, 2000). MOs have been traditionally used as compressor lubricants with R-12 and R-22 refrigeration systems because of good miscibility with those refrigerants. However, MOs are barely miscible with HFC refrigerants or CO₂.

2.2.2 Polyol Ester Oils

As mentioned in a previous section, environmental concerns have led the air-conditioning industry toward alternative HFC refrigerants. Due to the miscibility issue with HFC refrigerants, synthetic lubricants such as POE and PAG have been introduced as alternatives. Conventional types of POEs are manufactured using neopentyl alcohols and carboxylic acid. Most commercial products have used normal fatty acids derived from natural sources or mixtures of normal and slightly branched acid. Viscosity is increased by using higher molecular alcohols or acids (Short and Cavestri, 1992). The ester linkages in the molecules provide polarity and improved miscibility with refrigerant like HFCs, so POEs are used commercially with HFCs in all types of compressors. POEs show good miscibility characteristics with CO₂, but the viscosity reduction, caused by high solubility and instability, possibly limits their applications.

2.2.3 Polyalkylene Glycol Oils

PAGs are derived from ethylene oxide or propylene oxide. The polymerization is usually initiated with either an alcohol or water. PAGs have excellent lubricity, good low-temperature fluidity, and good compatibility with most elastomers. Major concerns are that PAGs are somewhat hygroscopic, immiscible with MO, and require additives for good chemical and thermal stability (ASHRAE Handbook, 1994). R-134a has been applied as an alternative to R-12 for automotive air-conditioners. PAGs are widely used as lubricants because of the requirement that the lubricants be soluble with R-134a. However, PAGs are considered difficult to apply to household refrigerators with hermetic compressors using R-134a due to their insulating properties (Sunami *et al.*, 1995).

2.3 Polyalkylene Glycol Oils with CO₂ Air-Conditioning Systems

To select the proper oil for CO₂ systems, several key properties should be evaluated, including solubility, miscibility, and stability. For compressors, the oil should maintain the proper viscosity and guarantee the lubricity at extremely high temperature and pressure conditions. In the two-phase region or liquid phase region, the oil must show good miscibility with the refrigerant in order to be transported by the refrigerant. The oil is required to be compatible with the materials used in the components of the system.

PAG was studied in this dissertation as a lubricant for a CO₂ air-conditioning system because the compressor manufacturer recommended PAG oil to guarantee reliability and compatibility with compressor materials. PAG that was used in this study has a viscosity of 43 cSt at 40°C, 9.2 cSt at 100°C, and a density of 996 kg/m³ at 25°C. The dielectric constant, which is measured by the level sensor to calculate the oil amount,

is around 6 at 20 °C. The following sections explain the key parameters of oil to be considered, which relationships between CO₂ and PAG in terms of mutual solubility, miscibility, viscosity, chemical stability, and lubricity.

2.3.1 Solubility

The solubility of a refrigerant/oil mixture refers to the ability of gaseous refrigerants to dissolve in a liquid lubricant (ASHRAE Handbook, 1994). Thus, this property is vital for the compressor environment, where the refrigerant exists in the vapor phase and a considerable amount of refrigerant could be dissolved in the lubricant, significantly affecting lubricant function (Popovic, 1999).

Very few studies have been conducted concerning CO₂'s solubility in oil. A solubility chart for gas CO₂ with PAG oil is shown in Figure 2.1 as was published by Hauk and Weidner (2000). At a given temperature, the CO₂ solubility in PAG oil increases with an increase of pressure. At the evaporating temperature, 10 °C, the CO₂ solubility increases up to 30 wt.%, which results in high reduction of the liquid phase viscosity. Since this chart was created for gaseous CO₂ and PAG oil when the state becomes two phase, it can not be used.

2.3.2 Miscibility

The homogeneity of a solution of substances in the liquid phase at a given pressure and temperature is known as the property of miscibility. Applying this definition to the refrigeration field, miscibility refers to the property of a liquid lubricant to form a homogenous mixture either by dissolving or by being dissolved in the liquid refrigerant. Miscibility depends on the lubricant concentration and temperature. Thus the refrigerant

oils are classified as being completely miscible, partially miscible, or immiscible in the refrigerant (ASHRAE Handbook, 1994). The completely miscible oils are mutually soluble at any temperature. This type of mixture always forms a single liquid phase under equilibrium conditions. POE oils are known as being miscible with CO₂ in all temperature and concentration conditions. The characteristic of a partially miscible solution is to exist as two distinct solutions: oil rich and refrigerant rich. Above a critical solution temperature, the refrigerant and oil mixtures in this class are completely miscible, and their behavior acts as a single phase.

Figure 2.2, based on Table 2.3, shows the CO₂ and PAG miscibility chart supplied by the oil manufacturer. PAG is known as a partially miscible oil with CO₂. In Figure 2.2, the line shows the critical solution temperature. Below the critical solution temperature, the liquid may separate into two phases: one is lubricant-rich and the other refrigerant-rich, depending on the predominant component. It seems that the CO₂ and PAG are not completely miscible in evaporator conditions. On the other hand, in the gas cooler, where temperatures are high, CO₂ and oil are possibly miscible with each other if the supercritical CO₂ exists as a liquid-like phase, which has high density.

Table 2.3 Miscibility of CO₂ and PAG (Denso Corporation, 1998)

Mass % oil	Mass % CO ₂	Temperature			Temp. of separation (°C)
		@ -20 °C	@ 20 °C	@ 40 °C	
90	10	1	1	1	-
80	20	1	1	1	-
50	50	2	1	1	11
30	70	2	1	1	20
10	90	2	2	1	26

2.3.3 Viscosity

Viscosity is defined as a resistance to flow and is a fundamental oil property. A lubricant needs to have an adequate viscosity in order to provide proper lubrication. The viscosity of oil is much greater than that of the refrigerant, and, therefore, any refrigerant, which is significantly diluted in oil, reduces the oil's viscosity. Thus, a high degree of solubility of a refrigerant in a lubricant leads to large viscosity reduction as shown in Figure 2.3, which is the viscosity chart for PAG oil with dissolved CO₂ published by Kawaguchi *et al.* (2000). As a result, an appropriate lubricant for a particular application must be carefully selected in regard to its viscosity reduction, since adequate viscosity is crucial for the lubrication of mechanical parts in compressors. For oil return, lower oil viscosity provides better oil transport in the overall system.

2.3.4 Chemical Stability

Refrigerant oil must have excellent chemical stability. Otherwise, serious problems including corrosion, plugged filters, capillary tube blockage, and reduction of system performance can occur. In the enclosed refrigeration environment, the oil must resist chemical attack by the refrigerant on all the materials encountered, including the various metals, motor insulation, and any unavoidable contaminant trapped in the system (ASHRAE Handbook, 1994). Three techniques are used to chemically evaluate materials: material tests in sealed tubes, component tests, and accelerated life and system tests. The glass sealed tube test, as described by ASHRAE Standard 97 (1989), is widely used to evaluate the long term chemical and thermal stability of refrigeration system materials. Sealed tube stability tests for CO₂ and several oils have been conducted (Li and Rajewski, 2000 and Kawaguchi *et al.*, 2000). The tubes, each containing test lubricants along with

iron, aluminum, and copper strips, were charged with CO₂. They were put into an oven controlled at 175 °C for eight weeks (Li and Rajewski, 2000). After that, the oil was analyzed for acid level, metal content and lubricant degradation. A high total acid number (TAN) and 500 ppm of dissolved iron were found in POE, while the PAG was found to have a TAN of 0.2 and 0 ppm of iron concentration. Low TAN indicates that the oil would not have been expected to cause corrosion in metals. Kawaguchi *et al.* (2000) also reported that PAG had good chemical stability with CO₂ in supercritical conditions.

2.3.5 Lubricity

The primary function of the refrigerant oil is to reduce friction and minimize wear. The oil achieves this by interposing a film between moving surfaces. The film reduces direct solid-to-solid contact or lowers the coefficient of friction. Film strength or load-carrying ability are terms often used to describe lubricant lubricity characteristics under boundary conditions. Several tests have been standardized by the American Society for Testing and Materials (ASTM) as follows: the Falex method (ASTM D 2670), the four-ball extreme-pressure method (ASTM D 2783), the Timken method (ASTM D 2782), and the Alpha LFW-1 (ASTM D 2714) (ASHRAE Handbook, 1994).

The Falex method was used by Seeton *et al.* (2000) to test lubricity of oils with CO₂. They investigated the lubricity of PAO, AB, PAG, and POE and found that PAG showed the best lubricity with CO₂. This was because PAG maintained higher mixture viscosity than other mixtures. Li and Rajewski (2000) concluded from lubricity tests using the Falex method that CO₂ did not adversely affect the load-carrying capability of the PAG compared to air. Kawaguchi *et al.* (2000) also reported that PAG showed excellent lubricity in supercritical conditions.

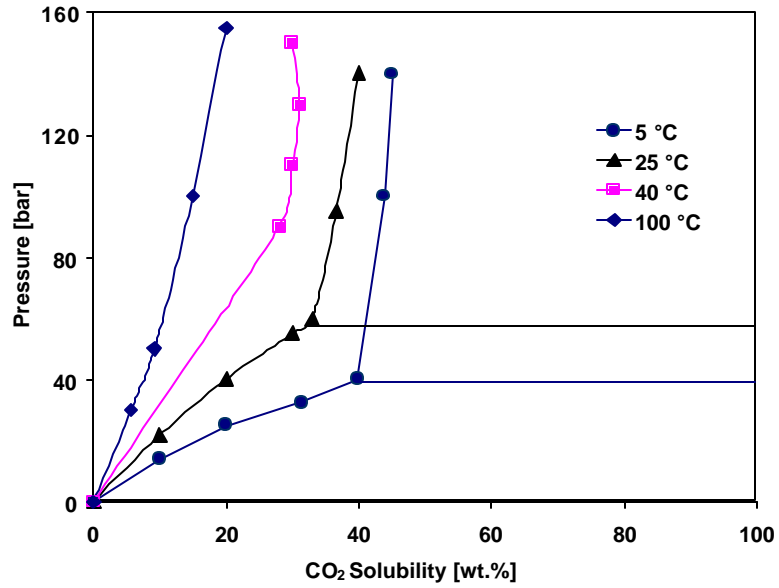


Figure 2.1 Solubility of CO₂ and PAG Oil (Hauk and Weidner, 2000)

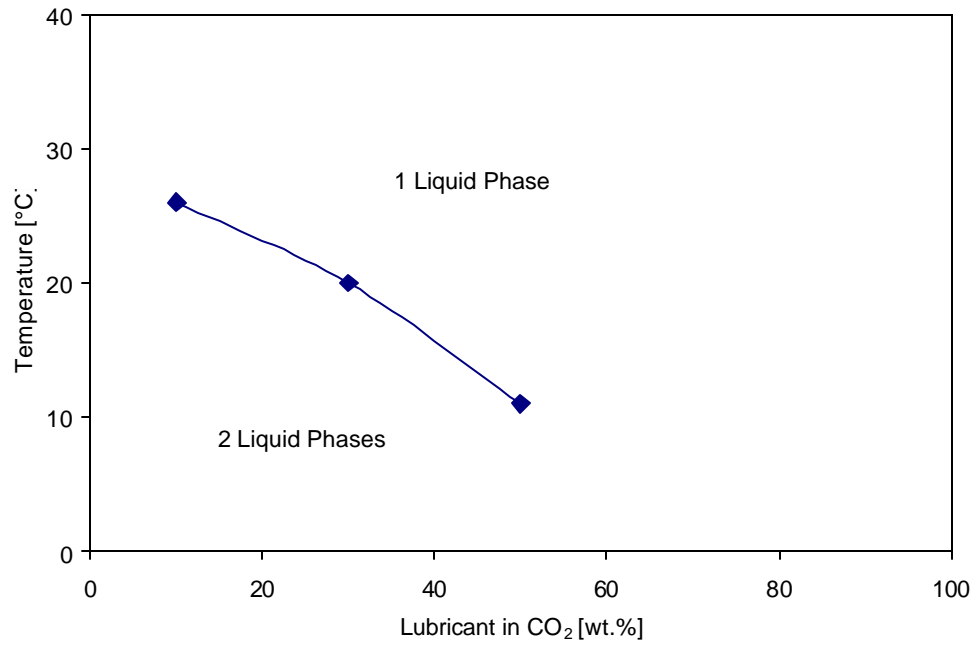


Figure 2.2 Miscibility of CO₂ and PAG Oil (Denso Corporation, 1998)

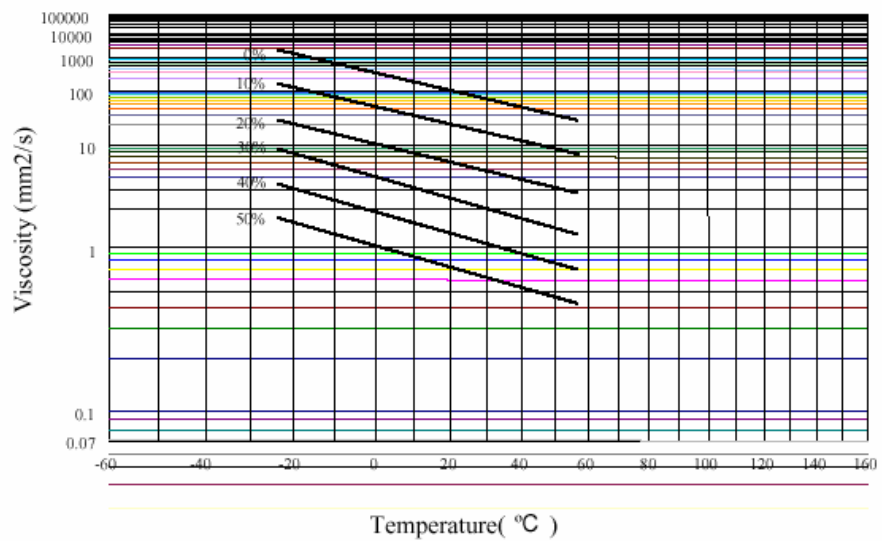


Figure 2.3 Viscosity of PAG Oil with Dissolved CO₂ (Kawaguchi *et al.*, 2000)

CHAPTER 3 Experimental Facility

3.1 Test Facility

The experimental facility was designed and constructed to investigate oil retention characteristics of each system component. The test facility for oil retention mainly consists of a refrigeration loop and an oil loop. These two loops are connected to or disconnected from each other by a three-way valve in such a way that the refrigerant flow direction can be controlled. The refrigeration loop was modified from an existing CO₂ automotive air-conditioning system. The air-conditioner was operated between two temperature conditions, indoor and outdoor. Air-side test conditions were provided by a closed air loop and an environmental chamber, which simulate the indoor and outdoor conditions, respectively. The evaporator was located in the indoor-side air loop, while the other components (i.e. compressor, gas cooler) were in the environmental chamber.

In the indoor-side air loop, as shown in Figure 3.1, the air flow rate could be adjusted using a variable speed fan. The air flow was calculated from the pressure drop across a nozzle in the loop. The air inlet and outlet temperatures were measured with a grid of nine thermocouples upstream and downstream of the evaporator. Figure 3.2 shows how the gas cooler was mounted in the outdoor-side air loop in the environmental chamber. An air-handling unit controlled the conditions in the environmental chamber in which the outdoor-side air loop was placed. The air flow rate as well as inlet and outlet air temperatures were measured in the same manner as for the evaporator.

The main functions of the oil loop are to inject oil into the system components and to extract the injected oil from the system. A number of instruments, which were linked to a data acquisition system, were used to measure and control the performance parameters.

3.1.1 Refrigeration Loop

A schematic diagram of the refrigeration loop of the CO₂ system is shown in Figure 3.3. Between each component of the system, the pressure and temperature of the refrigerant were measured to determine the state of the refrigerant. The refrigeration loop consisted of a compressor driven by an electric motor, a gas cooler, a manual expansion valve, and an evaporator.

Compressor

The open type CO₂ compressor had 6 cylinders and a displacement volume of 20.7 cm³ per revolution. Allowable running conditions were 3 to 5 MPa for the suction pressure, 7 to 15 MPa for the discharge pressure, and less than 140°C for the maximum discharge temperature. The compressor RPM was varied by an electric motor controlled by changing the inverter frequency. This procedure controlled the refrigerant mass flow rate.

Oil Separator

The oil separators were installed at the compressor discharge in order to minimize the oil flow to the test section and to supply the oil from the oil separators to the compressor suction by the pressure difference. This installation prevented potential compressor damage. The oil separators were designed to use centrifugal force to

effectively remove oil from the CO₂/oil mixture. The CO₂/oil mixture tangentially flowed into the round shape oil separator. Separated oil flowed along the wall due to its higher centrifugal force. In order to effectively minimize oil flow to other components, two oil separators were installed in series. Hwang *et al.* (2002) reported that the oil separator showed very high efficiency about 99.9% based on the ASHRAE sampling method and oil circulation ratio sensor only with one oil separator installed at the discharge line. Since two oil separators were used, the oil discharged from the compressor was effectively separated and then returned to the compressor suction.

Heat Exchangers

An evaporator and a gas cooler used in the system were based on microchannel tubes. The detail specifications of these heat exchangers are shown in Table 3.1.

Table 3.1 Specifications of Heat Exchangers

Heat Exchangers	Evaporator	Gas Cooler
Height (mm)	230	296
Length (mm)	200	638
Width (mm)	58	24
No. of Tubes	22 (2 rows)	32
No. of Port	30	21
Diameter of Port (mm)	0.55	0.7
Fin Height (mm)	9	9
Number of Fin (ea per inch)	20	14

Suction Line

In this study, the suction line is taken to mean the pipe from the evaporator outlet to the oil extractor. The suction line lay horizontally and was 3.8 m long, had an outer diameter of 0.0095 m (3/8”), a tube thickness of 0.00012 m, and a total inner tube volume

of 176 ml. The suction line was well insulated so that the temperature increase through the suction line was limited less than 1 °C.

Accumulator

An accumulator, shown in Figure 3.3, was installed in the suction line to prevent any liquid refrigerant supply to the compressor and to store excessive liquid refrigerant in some operating conditions. The internal volume of the accumulator was 250 ml. Another function of the accumulator was to supply oil to the compressor so that, initially, oil was charged in the accumulator.

Flow Visualization Section

The flow visualization section was designed to monitor flow patterns of the CO₂ /oil mixture and check the efficiency of the oil extractor or oil separators. The visualization section, shown in Figure 3.4, mainly consisted of a sight tube, a flat glass, a gasket, a body part, and two cover plates. The visualization section, 33 cm long and 7.6 cm wide, was combined with the body part and cover plate. The cushion (made of polyethylene elastomer) between the sight tube and NPT fitting was installed to fill the system with gas. 18 high-strength bolts tightened the cover plates and body part to endure such a high CO₂ system pressure. Because maximum allowable pressure of the sight tube (outer diameter: 0.0127 m, max. pressure: 4 MPa) was lower than the operating pressure, the pressure difference between inside and outside of the sight tube was minimized by connecting the pressure equalization line between the inlet tube and the outside of the sight tube as illustrated in Figure 3.4. Flat glass, which has a 20 MPa maximum operating pressure, was inserted between the body part and cover plate to observe the flow patterns

inside the sight tube. Therefore, the pressure force in the visualization section was taken by the flat glass. The gasket, made from a non-asbestos material, was inserted between the flat glass and the body part to prevent leaks from the clearance between the flat glass and cover plates. The flow visualization section was installed at the outlet of the oil separator where the compressor discharge line was located. Its function was to check the oil flow. It was also installed at the suction line for the flow pattern analysis.

3.1.2 Oil Loop

A separate oil loop was installed in the test facility to serve the following two purposes:

- Inject the oil to the test section at the desired oil circulation ratio;
- Extract the oil from the test section and measure the oil amount extracted.

The oil loop, shown in Figure 3.5, consisted of a gear pump, a mass flow meter, an oil extractor, an oil accumulator, and an oil reservoir. The test section shown in Figure 3.5 could be a suction line, an evaporator, or a gas cooler, depending upon the oil injection port. The check valves were installed ahead of the injection ports to prevent reverse flow from the refrigeration loop into the oil loop. Figure 3.6 shows the potential oil injection parts in the test setup combined with the refrigeration loop and the oil loop. While the oil injection ports were installed at the inlet and outlet of the heat exchangers, the oil extraction port was placed at the suction line in order to effectively extract the injected oil. Other injection ports were closed using their respective ball valves during the oil injection at any one specific port.

Oil Injection Pump

In order to control the oil flow rate at the desired oil circulation ratio, a gear pump driven by a variable DC motor was installed in the oil loop. The oil injection pump was connected to the oil reservoir. Basically, in order to pump oil into the system, the oil reservoir tank should maintain a certain pressure not to exceed the differential pressure limit of injection pump. If the pressure difference between injection port and oil reservoir is larger than the pump limit, magnet decoupling occurs because of the imposed excess torque limit of the pump. As a result, the pump stops its injection. The oil reservoir pressure was, therefore, equalized to the oil extractor outlet pressure by installing the pressure equalization line 1 as illustrated in Figure 3.5 to keep similar pressure between the oil injection port and oil reservoir. The specifications of the oil injection pump are shown in Table 3.2.

Table 3.2 Specifications of Gear Pump

Item	Specification
Model	220 series
Flow range	0 – 1500 ml/min (0 – 1750 rpm)
Max. pressure	10.3 MPa
Max. differential pressure	0.85 MPa
Manufacturer	Micro Pump

Oil Accumulator

As shown in Figure 3.5, an oil accumulator (2,750 ml of internal volume) was vertically positioned next to the oil extractor to measure the oil volume by the level sensor inserted into the oil accumulator. The extracted oil in the oil extractor flowed downward to the oil accumulator by gravity. The oil accumulator was connected to the

oil reservoir. After each test a valve between the oil accumulator and the oil reservoir was left open to release oil into the oil reservoir.

The pressure equalization line 2 was positioned between the oil accumulator and the low-pressure side. The purpose of the pressure equalization line is to prevent the oil accumulator from being pressurized by an increased oil volume. Without this pressure equalization line, the oil flow from the oil extractor to the oil accumulator would be disturbed due to pressurization at the oil accumulator, making it difficult to measure the flow rate of oil extraction.

Oil Extractor

The function of an oil extractor is to effectively separate oil injected at the injection port from the CO₂/oil mixture. From the literature survey (Tech Tips of Oil Separators), it was found that a commercial oil separator operates satisfactorily. However, the commercial oil separator has a maximum allowable pressure up to only 3 MPa, and could not be used as it is as an oil extractor in the CO₂ system due to its pressure limit. In order to use a commercially available oil separator in higher operating pressure systems, one was installed inside a high-pressure vessel, as shown in Figure 3.7. To minimize the pressure difference between the inside and outside of the oil separator, the oil separator outlet was exposed inside the vessel. The commercial oil separator used in this test was an AC&R Helical Oil Separator, model S-5182. Upon entering the oil separator, the refrigerant/oil mixture encounters the leading edge of a helical path. The refrigerant/oil mixture is centrifugally forced along the spiral path of the helix, which causes the heavier oil particle to spin to the perimeter, where the impingement with a screen layer occurs. The screen layer serves a dual function: an oil stripping and draining medium. Separated

oil flows downward along the boundary of the shell through a baffle and then into the oil collection area in the bottom of the separator. Virtually oil-free refrigerant gas exits through a fitting just below the lower edge of the helical path. In this experiment the efficiency of the extractor defined as the ratio of extracted oil to injected oil was measured and toward to be the range from 85 to 100%, depending on the refrigerant mass flow rate.

3.2 Measurement and Data Acquisition

The instrumentation was designed to measure system properties. There were four types of measurements necessary to obtain the data needed to calculate oil retention in CO₂ air-conditioning systems. They were temperature, pressure, mass flow rate, and oil volume.

3.2.1 Measurements

Temperature Measurements

Thermocouples were used to measure temperatures at several locations in the test facility. The data acquisition system uses hardware and software compensation to simulate the reference junction, thus eliminating the need for a physical reference junction maintained at a constant reference temperature. The voltages from the thermocouples are converted into temperature values using appropriate correlations in the data acquisition program (Hewlett Packard, 1987).

Table 3.3 Specifications of Thermocouples

Item	Specification
Thermocouple type	T-type
Alloy combination	Copper-Constantan
Temperature range	-270 to 400 °C
Accuracy	0.5 °C
Manufacturer	Omega Engineering, Inc.

The thermocouple probes were installed in-stream inlet and outlet of each cycle component. The other thermocouples were attached on the tube wall by means of aluminum adhesive tape to ensure good contact between the thermocouple junction and the tube surface. Detailed specifications are shown in Table 3.3

Pressure Measurements

System pressures were measured using Setra 280E absolute pressure transducers. The absolute pressure transducers were installed at the compressor discharge, gas cooler inlet, expansion valve inlet, evaporator inlet, and compressor suction. Differential pressure transducers were also installed between the gas cooler-inlet and, outlet and the evaporator-inlet and, outlet to measure the pressure drop across the heat exchangers. The pressure transducers had a maximum operating range of 20.7 MPa, and their output signal ranged from 0 to 5 VDC, which was arranged to be proportional to the pressure. Detailed specifications of the absolute and differential pressure transducers are shown in Table 3.4 and Table 3.5.

Table 3.4 Specifications of Absolute Pressure Transducers

Item	Specification
Model	280E
Pressure range	0-3,000 psia (0-20,684 kPa)
Accuracy	± 0.11% Full Scale
Output	0-5 VDC
Excitation	24 VDC Nominal
Manufacturer	Setra Systems, Inc.

Table 3.5 Specifications of Differential Pressure Transducers

Item	Specification	
Model	228-1	DT1400
Pressure range	0-100 psia (0-689 kPa)	0-150 psia (0-1,034 kPa)
Accuracy	± 0.2% Full Scale	
Output	0-5 VDC	
Excitation	24 VDC Nominal	
Manufacturer	Setra Systems, Inc	Stellar Technology.

Mass Flow Rate Measurements

For the oil retention test, two Coriolis mass flow meters were installed in the system to measure the oil circulation ratio, which is defined as the ratio of refrigerant mass flow rate to the total of refrigerant and oil mass flow rates. The refrigerant side mass flow meter specifications are shown in Table 3.6. The mass flow meter was installed at the gas cooler outlet.

In order to measure the amount of oil injected, an oil mass flow meter was installed just in front of the oil injection port. The density of the oil injected into the system was also measured by the oil mass flow meter. The oil mass flow meter had to be scaled down and re-calibrated in order to measure low mass flow rates because the oil

injection flow rate was relatively smaller than the capacity of the mass flow meter. By doing this calibration, the mass flow meter could measure oil injection rates up to 3 g/s, so the accuracy was increased. Specifications of the oil mass flow meter are given in Table 3.7.

Table 3.6 Specifications of Refrigerant Mass Flow Meter

Item	Specification
Sensor model	DH38 Series
Transmitter model	RFT9712
Flow range	0-115 g/s
Maximum operating pressure	35.8 MPa
Operating temperature	-240 to 117 °C
Accuracy	± 0.2% of rate
Output	4 to 20 mA
Manufacturer	Micro Motion Inc.

Table 3.7 Specifications of Oil Mass Flow Meter

Item	Specification
Sensor model	D12 series
Transmitter model	Elite Model RFT9739
Flow range	0-3 g/s
Maximum operating pressure	11.7 MPa
Operating temperature	-240 to 204 °C
Accuracy	± 0.2% of rate
Output	4 to 20 mA
Manufacturer	Micro Motion Inc.

Oil Volume Flow Rate Measurement

In order to calculate oil retention amount at each test section, it was necessary to measure the oil amount extracted from the oil extractor. A level sensor measuring the oil

level was installed at the inside of an oil accumulator to measure the oil volume rate of extracted flowing from the oil extractor by gravity.

The function of the level sensor is to measure the capacitance change by the level sensor probe depending on the dielectric constant of different materials. The dielectric constant is the ability to store an electrostatic charge using a numerical value on a scale of 1 to 100. A change in the value of the capacitance took place because of the dielectric difference between the electrode and the oil accumulator wall (Omega Handbook, 2000). The dielectric constant of CO₂ is 1, and that of PAG is 6 at 20 °C. Table 3.8 shows the specifications of the level sensor. As the level rises, the CO₂ gas is displaced by the oil, which has a different dielectric constant. A radio frequency capacitance instrument detects this change and converts it into a relay actuation or a proportional output signal, which is 0 to 20 mA. The capacitance relationship is illustrated by the following equation:

$$C = 0.255K \left(\frac{A}{D} \right) \quad (3-1)$$

where C : Capacitance [pF]
 K : Dielectric constant of material
 A : Area surrounded by oil [m²]
 D : Distance between the accumulator wall and an electrode [m]

The level sensor was calibrated by the oil mass flow meter. The oil was injected into the oil accumulator through the oil mass flow meter. At the same time, the output signal, which corresponds to the oil level in the oil accumulator, was measured by comparing the oil mass flow rate to the oil volume flow rate. Using the known oil density, the linear calibration curve was calculated.

Table 3.8 Specifications of Oil Level Sensor

Item	Specification
Sensor model	LV5200
Transmitter model	LV5900
Range	0 – 38 cm
Max. Pressure	6.89 MPa
Max. Temperature	232 °C
Linearity	± 0.5% of full scale
Output	4 to 20 mA
Manufacturer	Omega

3.2.2 Data Acquisition

Signals from system measurement devices were fed to a data acquisition system (DAS), which has hardware and software components. The hardware component consisted of a Hewlett Packard Data Acquisition Unit (HP 3497A), for collecting data and a Pentium processor personal computer for display and storage of data. The data acquisition unit has separate cards to accomplish different functions. There are mainly two types of cards: T-Couple Acquisition, which can measure temperature from T-type thermocouples, and Guarded Acquisition, which can measure the voltage output coming from various transducers or transmitters (e.g. the pressure transducers, the mass flow meters transmitters, the level sensor transmitter, etc.).

All outputs from the thermocouples, the pressure transducers, the mass flow meters, and the level sensor were connected to the DAS. All these data were displayed by LabView software, which is a graphical, user-friendly program as shown in Figure 3.8. This program converts the voltage readings into temperature, pressure, flow rate, and oil level. It displays all test status including system status and air-side cooling capacity.

While running the test, data was collected and displayed at 8 second intervals. It was also stored at the same intervals on the computer's hard drive.

3.3 Uncertainty Analysis

This section attempts to determine the magnitude of uncertainty of the oil circulation ratio and the oil retention. The systematic experimental uncertainty of measurements due to the uncertainty of individual parameters is referred to as the propagation of uncertainty (Beckwith *et al.*, 1992).

$$u_F = \sqrt{\left(\frac{\partial F}{\partial v_1} \cdot u_1\right)^2 + \left(\frac{\partial F}{\partial v_2} \cdot u_2\right)^2 + \left(\frac{\partial F}{\partial v_3} \cdot u_3\right)^2 + \dots + \left(\frac{\partial F}{\partial v_n} \cdot u_n\right)^2} \quad (3-2)$$

where u_F : uncertainty of the function
 u_n : uncertainty of the parameter
 F : function
 v_n : parameter of interest (measurement)
 n : number of variables

The oil retention volume at each test was calculated by Equation (3-3) as described in the next section, 4.1.

$$OilRetentionVolume = V_{injection} - V_{extraction} \quad (3-3)$$

$$V_{injection} = f(\mathbf{r}_o, \dot{m}_o, t) \quad (3-4)$$

$$V_{extraction} = f(V) \quad (3-5)$$

The uncertainty of the oil retention volume is estimated from two different uncertainty sources of the oil injection and oil extraction. The oil volume by injection at the test section, as shown in the Equation (3-4), is a function of oil density, oil mass flow rate, and time. The uncertainties of the oil volume by injection are found by applying Equation (3-2) to Equation (3-4).

$$u_{V_{injection}} = \sqrt{\left(u_{r_o} \cdot \frac{\partial V_{injection}}{\partial r_o}\right)^2 + \left(u_{\dot{m}_o} \cdot \frac{\partial V_{injection}}{\partial \dot{m}_o}\right)^2 + \left(u_t \cdot \frac{\partial V_{injection}}{\partial t}\right)^2} \quad (3-6)$$

On the other hand, only the level sensor caused uncertainty in the oil extraction volume, since the oil volume at the oil accumulator was directly calculated from the output signal of the level sensor. The uncertainty of the oil retention volume is calculated by using Equation (3-7).

$$u_{OilRetentionVolume} = \sqrt{(u_{V_{injection}})^2 + (u_{V_{extraction}})^2} \quad (3-7)$$

where $u_{V_{injection}}$: uncertainty of oil injection
 $u_{V_{extraction}}$: uncertainty of oil extraction

The uncertainty for the oil circulation ratio, defined by the ratio of the mass flow rate of oil to the mass flow rate of CO₂ and oil mixture, is represented by Equation (3-8).

$$u_{OCR} = \sqrt{\left(u_{\dot{m}_o} \cdot \frac{\partial OCR}{\partial \dot{m}_o}\right)^2 + \left(u_{\dot{m}_r} \cdot \frac{\partial OCR}{\partial \dot{m}_r}\right)^2} \quad (3-8)$$

The actual parameters used to calculate the Equation (3-3) are shown in Table 3.9, which also includes the associated uncertainties of these parameters.

Table 3.9 Estimates of the Uncertainty of Measured Quantities

Quantity	Actual Value of Test No. 5	Uncertainty
Time (t)	758 [sec]	± 0.15 [sec]
Oil Extraction Volume ($V_{\text{extraction}}$)	190 [ml]	± 5.3 [ml]
Oil Density (ρ_o)	1.01 [g/ml]	± 0.002 [g/ml]
Oil Mass Flow Rate (\dot{m}_o)	0.26 [g/s]	± 0.025 [g/s]
CO ₂ Mass Flow Rate (\dot{m}_r)	13.50 [g/s]	± 0.3 [g/s]

The sample results for the uncertainty of the oil circulation ratio and oil retention volume are presented in Table 3.10. For test number 5, the uncertainties of the oil circulation ratio and oil retention are shown as 9.7% and 10.9%, respectively. These large uncertainties are mainly due to the low oil mass flow rate. The uncertainties for test 5 are marked on Figure 5.1.

Table 3.10 Uncertainties for Oil Circulation Ratio and Oil Retention

Test Number in Appendix A	Uncertainty of Oil Circulating Ratio (%)	Uncertainty of Oil Retention (%)
5	9.7	10.9
15	5.5	6.0
25	5.7	7.4
45	8.3	8.8
55	5.9	6.5

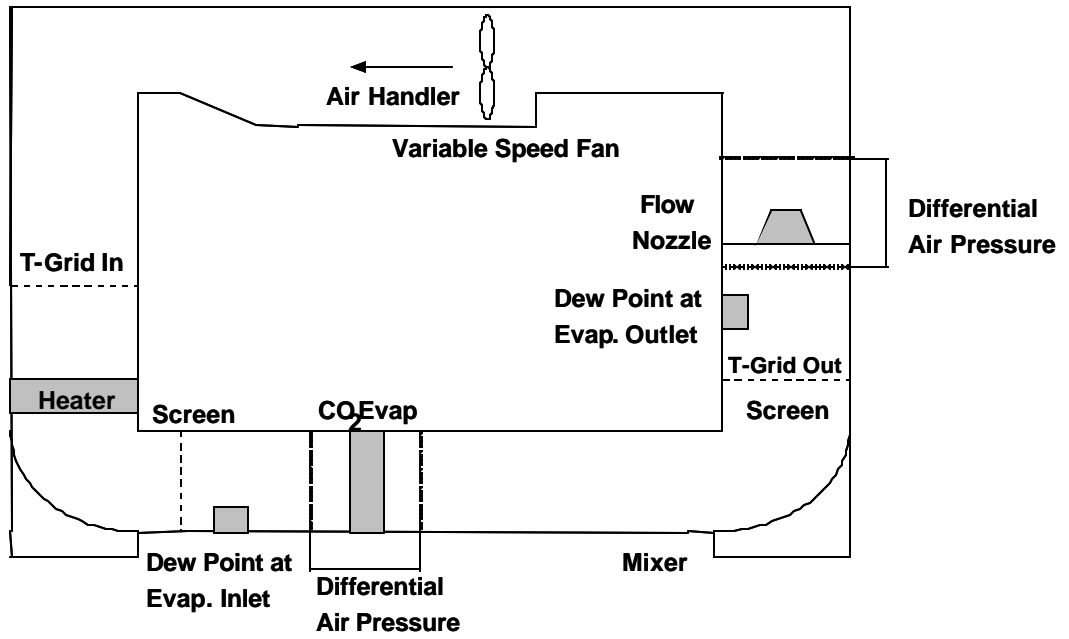


Figure 3.1 Indoor-Side Air Loop for the Evaporator

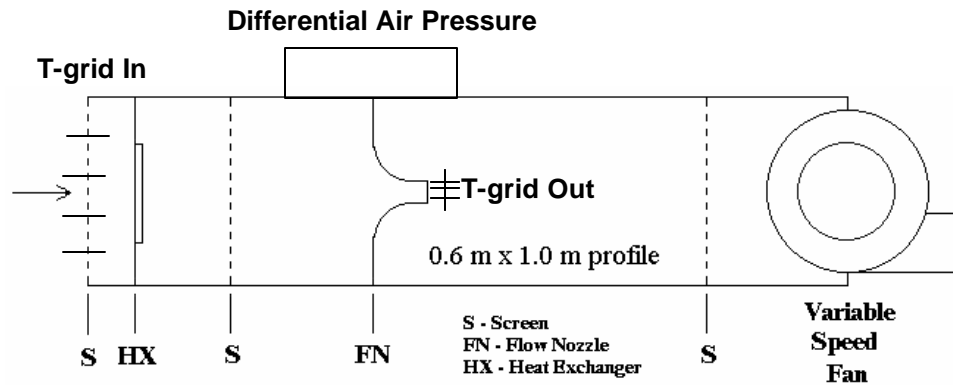


Figure 3.2 Outdoor-Side Air Loop for the Gas Cooler

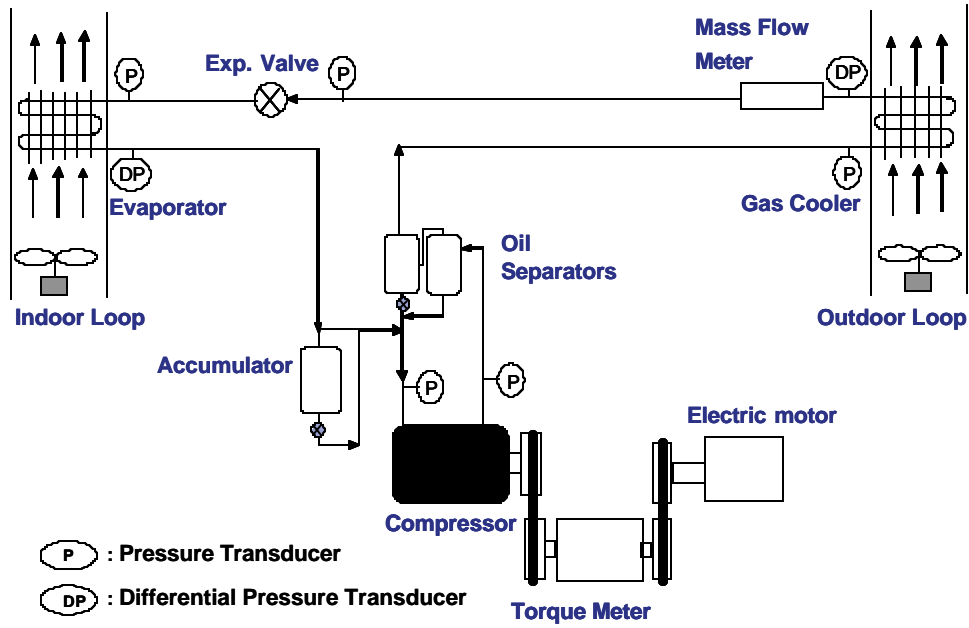


Figure 3.3 Schematic Diagram of Refrigeration Loop

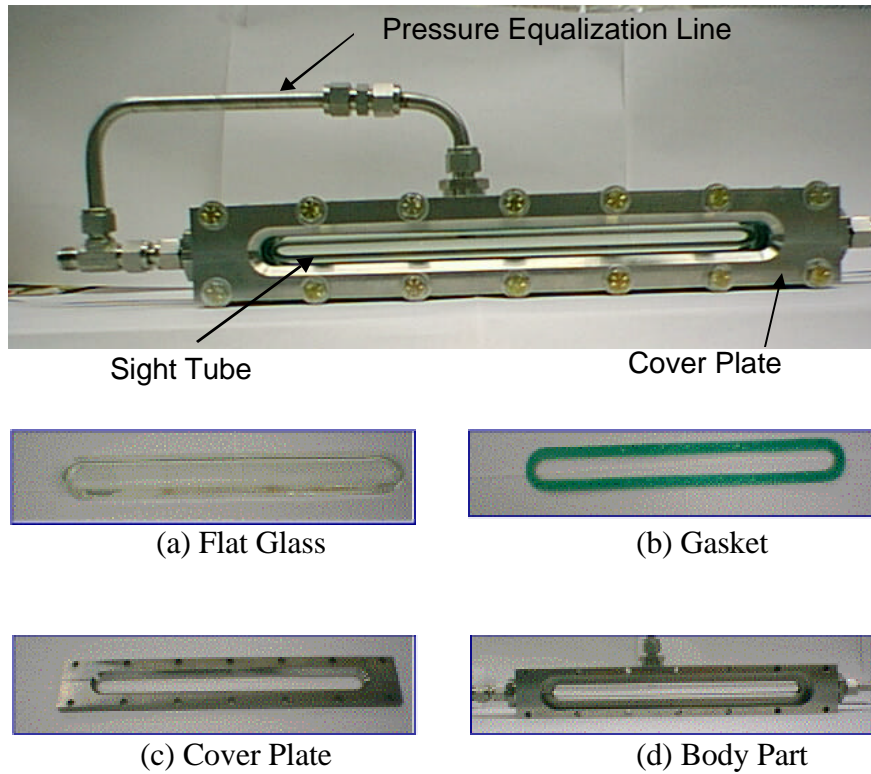


Figure 3.4 Flow Visualization Section

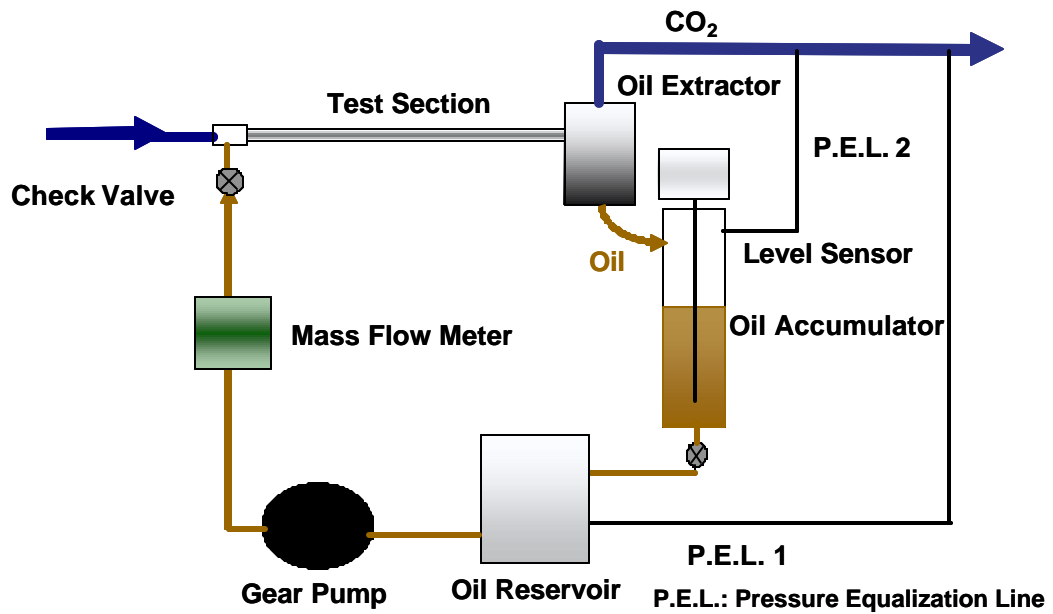


Figure 3.5 Schematic Diagram of Oil Loop

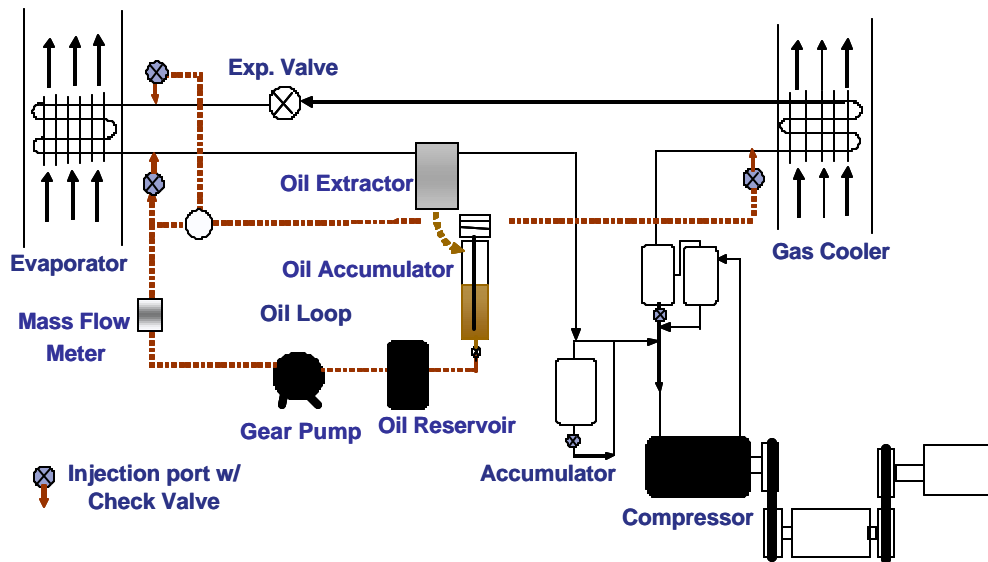
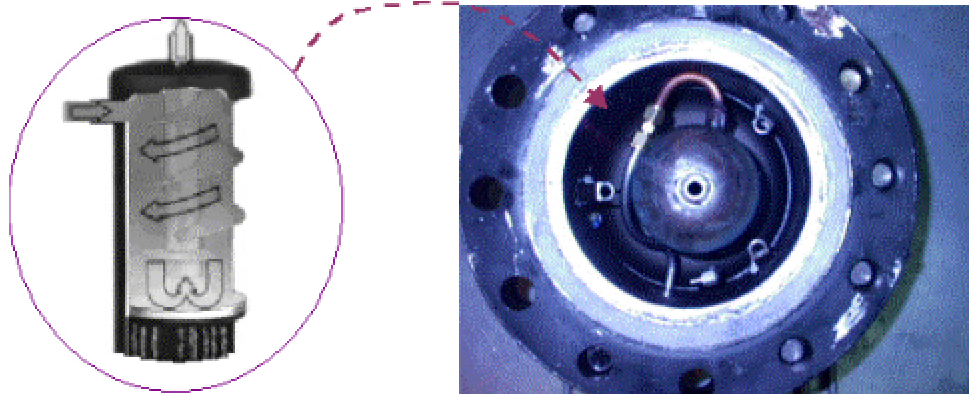


Figure 3.6 Oil Injection Ports in Refrigeration Loop



(a) Commercial Helical Oil Separator (b) Oil Extractor in High Pressure Vessel

Figure 3.7 Oil Extractor

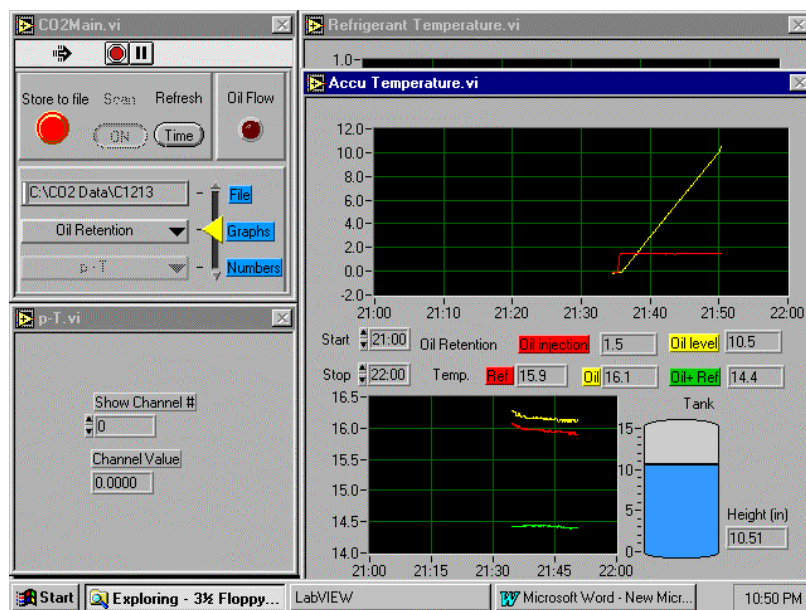


Figure 3.8 LabView Software for DAS

CHAPTER 4 Experimental Methods

4.1 Methodology of Oil Retention Measurement

In this study, an oil injection-extraction method was adopted to measure the oil retention in each cycle component. The test methodology was designed and verified by Hwang *et al.* (2000) to measure the mean oil film thickness at the vertical suction line of a freezer. The basic idea is measuring differentiated oil volume between the oil volume injected and the oil volume extracted across the test section after reaching steady state condition. As soon as oil flows into the system component, oil starts to accumulate in the component until it reaches saturation amount, which is determined by heat exchanger geometry, flow rates and thermophysical properties of refrigerant and oil. This saturation amount is referred as the oil retention volume in this dissertation. Detailed information on the methodology of oil retention is explained as follows.

At each test, oil retention volume was calculated according to Figure 4.1. In Figure 4.1, the y-axis represents the oil volume either injected at the inlet of the test section or extracted at the end of test section by the oil extractor. The x-axis represents the duration from the time of oil injection into the test section to the end of the test, which is determined by the oil volume increase rate reaching its steady state. The solid line of figure represents the oil volume injected into the system, which is obtained from the oil mass flow rate and oil density. The slope of this line shows the volumetric oil injection rate. As soon as the oil is injected into the test section, the slope of volumetric oil injection rate reaches its steady state.

A dotted line (line 1) indicates the volume of oil extracted. This line is plotted based on the measurement by the level sensor at the oil accumulator. As shown in Figure 4.1, during the first 100 seconds after oil injection began, the oil amount in the oil accumulator did not increase. This is because of the initial oil film forming in the test section between the injection port and the oil extractor. After the initial time delay, the oil film accumulation in the heat exchanger and tube reached its saturation amount. After this steady state, the increase rate of oil volume extracted at the oil accumulator became the same as that of the oil volume injected, so that two lines became parallel. The vertical distance between two lines in the figure is a measure of the oil volume that was retained in the test section.

Ideally, the two lines for oil injection and extraction should be parallel right after the initial time delay. However, because the oil extractor efficiency is less than 100% under higher refrigerant mass flux, the line labeled 1 is not parallel to the line of oil volume injected. After compensating the oil extractor efficiency, line 1 becomes line 2. Thus, these two lines become parallel to each other after an initial time delay. The oil extractor efficiency was determined by the ratio of oil amount by line 1 to the oil amount by line 2 at certain time. The oil amount lost from the oil extractor due to its efficiency was stored in the oil separator located in the compressor discharge line.

4.2 Experimental Procedures

In this study, four different refrigerant mass fluxes, 290, 352, 414, and 559 kg/m²s, based on the suction condition, were tested. These refrigerant mass fluxes were selected based on the automotive compressor idling/driving conditions. However, since the

pressure drop across the oil extractor was found to be too high at driving conditions (1,800 RPM), the compressor RPM was reduced to 600 RPM for idling and 1,450 RPM for driving.

The oil circulation ratio, which is defined as the ratio of the mass flow rate of the oil to that of the refrigerant/oil mixture, was varied from 1 to 7 wt.% by changing the oil mass flow rate while fixing the refrigerant mass flow rate. An injection port was installed at the inlet and outlet of the evaporator and at the inlet of the gas cooler. The oil retention volume in the suction line, evaporator, and gas cooler was obtained by choosing different oil injection ports.

In the test runs, the evaporator inlet pressure was kept at 4 MPa, which is a typical condition of automotive air-conditioning systems. The temperatures selected to simulate indoor and outdoor operations were 27°C and 36.1°C, respectively, while the humidity was fixed around 40% RH in all tests. The pressure drop across the heat exchangers was measured to investigate the effect of oil retention on the pressure drop. To examine the effect of the inlet vapor quality at the evaporator on the oil retention, a suction line heat exchanger (SLHX) was installed for the refrigerant mass flux at 290 kg/m²s. A series of tests was conducted to determine the oil retention amount at each cycle component.

In order to remove the oil remaining in the system from the preceding test, the system was flushed with higher refrigerant flow rate after each test. During this process, oil level at the oil accumulator was also monitored to check whether any further oil extraction occurs or not. It is determined that the system is free of oil when the monitored oil level does not change. However, in spite of the flushing procedure, it is possible that small amount of oil might still remain in system component as a thin oil film on the walls

of tubes or heat exchangers. Thus, the oil retention volume measured in current experiment possibly includes the residual oil amount from the proceeding test. However, after each component test, the residual oil at system components was purged with high pressure nitrogen gas, and it was found that only few grams of oil, which was less than 1% of oil volume charge initially, was collected. Therefore, this residual oil amount due to preceding test was so small that the effect was negligible. The test procedure was as follows:

1. The refrigerant mass flow rate was set to desired values by adjusting the compressor RPM, an expansion valve opening, and the charge amount.
2. The evaporator inlet pressure was fixed to 4 MPa by adjusting the expansion valve opening. For all tests, the evaporator inlet pressure was kept constant for a fair comparison of the oil retention in the evaporator.
3. When the refrigeration cycle reached its steady state and the oil level in the oil accumulator was saturated, the oil injection was started.
4. The oil injection mass flow rate was adjusted to the desired value by adjusting the variable speed gear pump.
5. The ball valve, which was installed at the oil injection port, was opened, and oil was injected into the system through the check valve. The oil was injected until the oil volume increase rate in the oil accumulator reached its steady state.
6. After stopping the oil injection, the refrigeration system was kept running until the extracted oil reached its steady state. This means that most of injected oil was removed from all the system components by the refrigerant flow.

7. Tests were repeated for various refrigerant mass flow rates, oil circulation ratios, and injection ports.

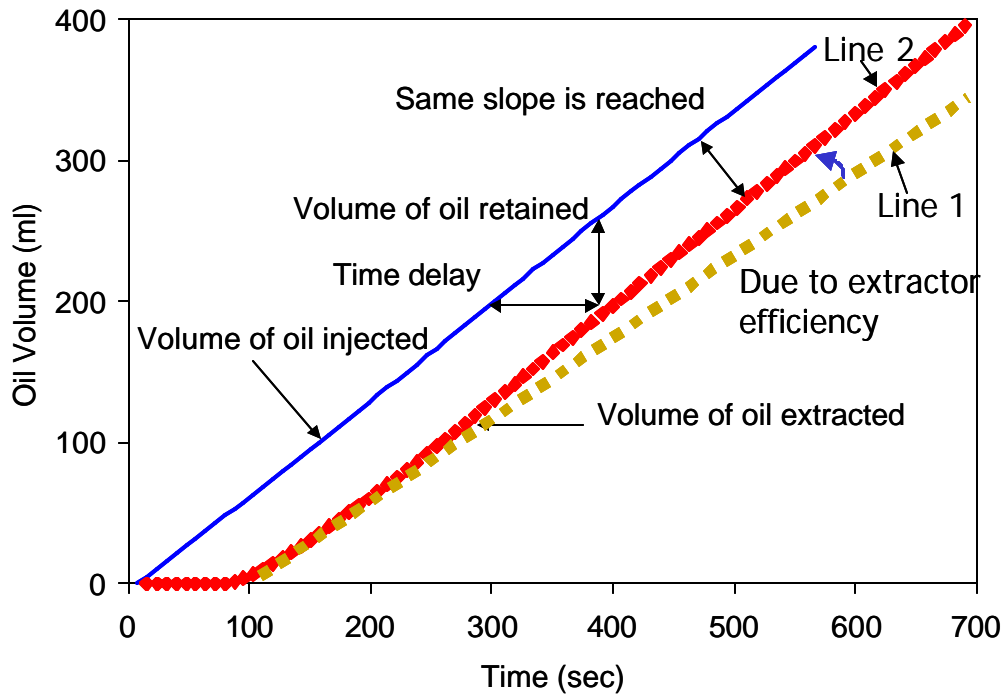


Figure 4.1 Oil Retention Characteristics

CHAPTER 5 Experimental Results

5.1 Oil Retention

In general, most oil stays either in the compressor shell or in the discharge oil separator, which is a larger container for oil storage during operations. However, a certain amount of oil discharged with refrigerant from the compressor is retained in cycle components, so the performance or reliability of system can be affected by oil retention. Since the thermal conditions of each component at given refrigerant flow rate and the geometry of each component are different, the oil retention amount for each system component can also be different.

In this chapter, the experimental test results of the oil retention and pressure drop are described, which were obtained by using the oil injection-extraction method at various refrigerant mass fluxes and oil circulation ratios for the different system components, including the suction line, the evaporator, and the gas cooler. First, the test results for oil retention in the suction line and evaporator are discussed, and the effects of the refrigerant mass flux and inlet vapor quality are presented. Then, oil retention at the gas cooler is described. Second, based on the oil retention results for each component, an oil distribution chart for CO₂ air-conditioning systems is suggested. All test conditions and results of the oil retention obtained during the current experiments are summarized in Appendix A.

5.1.1 Oil Retention in the Suction Line & Evaporator

To investigate oil retention characteristics of the suction line and evaporator, oil was injected twice at the evaporator inlet and outlet. While the evaporator inlet pressure was kept at 4 MPa for all tests, the oil flow rate was varied to obtain the desired oil circulation ratio. The oil retention volume ratio indicated on the y-axis in Figure 5.1 through Figure 5.10 is defined as the ratio of the oil retention volume obtained by current experiments to the oil volume charged initially in the accumulator. The amount of oil volume charged initially was 250 ml, which is typical oil charge amount for the automotive air conditioning systems. Thus, the oil retention volume ratio represents oil distribution at each cycle component based on the fixed oil amount charged initially. Oil circulation ratio indicated on the x-axis in Figure 5.1 through Figure 5.12 is defined as the ratio of refrigerant mass flow rate to the total mass flow rate of refrigerant and oil mixture. Oil circulation ratio was varied up to 7 wt.% based on the typical oil circulation ratio of air conditioning systems, which is less than 5 wt.%.

In all figures, data are presented at fixed mass flux. Since, at given refrigerant mass flow rate, the mass flux is different at each system component due to difference inner cross sectional area, mass flux at the suction line is used in figures for the oil retention volume ratio and mass flux of each heat exchanger is used in figures for pressure drop penalty factor.

The symbols (\blacklozenge), (\uparrow) in Figure 5.1 through Figure 5.4 represent the oil retention volume ratio at given conditions when the oil is injected at the evaporator outlet and the evaporator inlet, respectively. The lower curves with diamond symbols in figures show the oil retention volume ratio from the evaporator outlet to the oil extractor. This denotes

the oil retention volume ratio of the suction line. The upper curves with square symbols represent the oil retention volume ratio from the evaporator inlet to the oil extractor, which means the oil retention volume ratio of the evaporator as well as the suction line. Thus, the oil retention volume ratio in the evaporator can be determined by the differences between the two curves. The test results, detailed in Appendix A and corresponding to test numbers 1 through 17 and 35 through 39, depending on injection port, are plotted in Figure 5.1. Figure 5.1 shows oil retention volume ratio versus oil circulation ratio up to 7 wt.% in the suction line and the evaporator for the mass flux $290 \text{ kg/m}^2\text{s}$. The uncertainty of test number 5 is shown as overlapping with the lower curve of Figure 5.1. The oil retention volume ratio in the suction line increases up to 0.15 at 5.2 wt.% of the oil circulation ratio, at the same time the oil retention volume ratio in both evaporator and suction line increases from 0.18 to 0.28 at the oil circulation ratio 1.4 to 6.0 wt.%. As the oil circulation ratio increases, the oil retention volume ratio in the suction line also increases. The oil retention volume ratio in the evaporator, which is the difference between the two curves of figure, slightly increases with an increase of the oil circulation ratio. Figure 5.2 through Figure 5.4 also show the oil retention volume ratio under three different mass fluxes, $352 \text{ kg/m}^2\text{s}$, $414 \text{ kg/m}^2\text{s}$, and $559 \text{ kg/m}^2\text{s}$, respectively. These results show similar trends indicating that the oil retention volume ratio of the suction line and evaporator increases with an increase of the oil circulation ratio.

The lower curves with diamond symbols in Figure 5.1 through Figure 5.4, which are the measured value of oil retention volume ratios in the suction line, have a tendency to bend toward around 0 or minimal oil retention volume ratio when the oil circulation ratio is close to 0 wt.%. On the other hand, the upper curves with square symbols, which

are the oil retention volume ratios both in the evaporator and suction line, do not show a similar tendency and seem to result in certain oil retention volume ratio from 0.06 to 0.1 at around 0 wt.% of the oil circulation ratio. This indicates that the evaporator has the minimum oil retention volume. As soon as the circulating oil enters the evaporator, it is retained either in the microchannel tubes or headers of the evaporator. Then, as shown Figure 5.5, the oil retention volume ratio in the evaporator reaches minimum retention values of around 0.02 to 0.08, depending on the mass flux. Since the evaporator can retain a certain amount of oil even at a small oil circulation ratio, it is assumed that the evaporator can be free from the oil only at 0 wt.% of oil circulation ratio.

Figure 5.1 through Figure 5.4 indicate that the oil retention volume ratio of the suction line is not affected by the mass flux. It should be noted that the temperature at the evaporator outlet was varied from 9°C to 17°C even though the evaporator inlet temperature was kept constant for all tests. For a higher mass flux, 559 kg/m²s, the suction temperature was around 9°C due to less superheating at the evaporator outlet. On the other hand, the suction temperature for the lower mass flux, 290 kg/m²s, was around 17°C. The difference in the suction temperature was caused by the difference of inlet vapor quality at the evaporator. When the refrigerant temperature decreased, the oil becomes more viscous and the oil film becomes thicker. Relatively high oil viscosity due to the lower temperature caused more oil retention even for the higher mass flux, 559 kg/m²s. The measured oil volume ratio for the mass flux, 559 kg/m²s, in the suction line shows amounts similar to the value for the mass flux, 414 kg/m²s.

5.1.2 The Effects of Refrigerant Flow Rate

The effects of refrigerant flow rate on oil retention were investigated with respect to the oil circulation ratio. The values of oil retention volume ratio in the evaporator, as shown in Figure 5.5, are not directly measured from the experiment but are calculated from the difference between the two curves as shown in Figure 5.1 to Figure 5.4.

In the case of mass flux, $290 \text{ kg/m}^2\text{s}$, represented by the top curve with diamond symbols of Figure 5.5, the oil retention volume ratio in the evaporator increases from 0.09 to 0.11 as the oil circulation ratio increases from 1 to 5 wt.%. For the mass flux of $414 \text{ kg/m}^2\text{s}$, the oil retention volume ratio in the evaporator was increased from 0.03 to 0.07, which is less than that of the mass flux of $290 \text{ kg/m}^2\text{s}$. As the mass flux increases, the oil retention in the evaporator decreases due to higher viscous forces of the CO_2 gas. When the mass flux was further increased to $559 \text{ kg/m}^2\text{s}$, the oil retention volume ratio was similar to the result for the mass flux, $414 \text{ kg/m}^2\text{s}$. This means that a minimum oil retention volume may exist in the evaporator against the increase of mass flux based on the mass flux range of current experiment.

It should be noted that the inlet vapor quality of the evaporator in this study was varied from 0.5 to 0.8 depending on the mass flux. The inlet vapor quality of the evaporator was kept in 0.8 and 0.5 for the mass flux, $290 \text{ kg/m}^2\text{s}$ and $559 \text{ kg/m}^2\text{s}$, respectively. The oil retention in the evaporator is for the most part caused by the increase in the local liquid viscosity and surface tension forces in the oil rich film. Such oil retention generally occurs in the high quality and superheated region of the evaporator (Zurcher *et al.*, 1998). For mass flux of $290 \text{ kg/m}^2\text{s}$, a relatively larger oil retention volume ratio was resulted in the evaporator since the lower mass flux causes a lower

viscous force, and the high quality and superheated region are dominant in the microchannel tubes of the evaporator. The effect of vapor quality on oil retention in the evaporator is discussed in the next section.

The oil retention is also affected by the geometry of the evaporator. In the evaporator, oil can be retained not only in the horizontal microchannel tubes, but also in vertical headers of the evaporator. Some oil might be retained at the outlet header, since the CO₂ gas should carry the oil film vertically upward. However, it is possible that oil cannot be carried by CO₂ gas when the CO₂ gas velocity at the lower part of the outlet header is not enough to exert sufficient shear force on the oil. For a low mass flux, 290 kg/m²s, more oil can be retained both in the outlet header due to low a shear force to carry the oil to vertical upward and also in the microchannel because of the reasons mentioned above. Even though the header's effect on the oil retention in the evaporator was not investigated directly during the current experiment, the oil retention with consideration of header in the evaporator can be estimated by means of a simulation. This simulation result is discussed in section 7.2.2.

5.1.3 The Effect of Inlet Vapor Quality

As described in the previous section, oil retention usually occurs increasingly in the high quality and superheated region of the evaporator. At the same mass flux, higher inlet vapor quality results in more superheated area at the evaporator, which causes different oil retention effect. To verify this statement, the oil retention volume ratio of the evaporator was measured by varying inlet vapor quality. The result of the evaporator inlet vapor quality effect on oil retention can be seen in Figure 5.6. The mass flux is fixed at 290 kg/m²s while the inlet vapor quality has the value shown for the two curves, 0.7 and

0.8. The larger oil retention volume ratio was observed for the higher inlet vapor quality, 0.8, than for the inlet vapor quality, 0.7. This is because a greater portion of the evaporator is occupied by a high vapor quality and superheated vapor in the case of the higher inlet vapor quality, 0.8. Basically, oil retention in the evaporator increases at the end of the evaporation process where either the vapor quality is high or vapor is superheated because the local liquid viscosity increases by the increase of oil concentration in the liquid film. To minimize this type of oil retention in the evaporator, maintaining a high refrigerant flow rate and a low inlet vapor quality in the evaporator is recommended. The simulation result for the effect of inlet vapor quality and degree of superheating in the evaporator is also discussed in detail in the sections 7.3.2 and 7.3.3.

5.1.4 Oil Retention in the Gas Cooler

The oil retention volume ratio at the gas cooler was measured by means of injecting oil at the gas cooler inlet. Figures 5.7 and 5.8 show the oil retention volume ratios for two different oil injection ports versus oil circulation ratios. The difference between the two lines means the oil retention volume ratio in the gas cooler and in the tube between the gas cooler outlet and the evaporator inlet. The oil retention volume ratio in the heat exchangers for the refrigerant mass fluxes, 290 kg/m²s and 414 kg/m²s, are shown in Figure 5.9. The oil retention volume ratio in the gas cooler was about 0.05 at 5 wt.% of oil circulation ratio and mass flux 290 kg/m²s.

The oil retention volume ratio in the gas cooler was quite small compared to the 0.11 measured in the evaporator at 5 wt.% of oil circulation ratio. This can be explained by the different properties of oil and CO₂ between in the evaporator and gas cooler, which are summarized in Table 5.1. The mean temperature of the superheated region in

the evaporator was chosen in Table 5.1 because the superheated region is responsible for the oil retention in the evaporator. On the other hand, the temperatures of both the inlet and outlet in the gas cooler are indicated in the table, and properties corresponding to the temperature and pressure are also shown. Lower oil kinetic viscosity is one of the reasons for less oil retention in the gas cooler. Oil kinetic viscosity in the gas cooler is much less than that in the evaporator due to the high temperature during gas cooling process. The lower oil viscosity provides better oil transport in the gas cooler, which results in less oil retention volume ratio. Surface tension of the oil is another parameter for less oil retention in the gas cooler. Since surface tension helps the liquid adhere to tube walls, the lower surface tension due to high temperature and pressure conditions in the gas cooler, causes the oil to be more easily transported by supercritical CO₂.

Table 5.1 Properties of Oil and CO₂ in Heat Exchangers (G=290 kg/m²s)

Component	Temperature (°C)	Pressure (MPa)	Oil Kinetic Viscosity (cSt)	Oil Surface Tension (N/m)
Evaporator	10*	4	159.9	0.030
Gas Cooler	80 to 36**	8	11.4 to 52.2	0.023 to 0.027

* : the mean temperature at superheated region in the evaporator

** : the temperatures of inlet and outlet of the gas cooler

Moreover, the mass flux in the gas cooler is 57% higher than that in the evaporator. As a result of the combined effects of the parameters described above, less oil is retained in the gas cooler. The oil retention at the three system components is shown in Table 5.2. The dimensionless oil film thickness, d/D , in Table 5.2 is defined as the mean oil film thickness (δ) relative to the inside diameter of the tube (D). To determine dimensionless oil film thickness, the internal tube volume was calculated. Then, the

dimensionless oil film thickness was calculated from the amount oil retained in the system component to the total internal tube volume.

Due to the higher refrigerant mass flux at the suction line than evaporator, as shown in Table 5.2, the dimensionless oil film thickness of the suction line is less than that for the evaporator. However, since the internal volume of the suction line is larger than that of the evaporator, the oil retention volume ratio for the suction line is larger than that for the evaporator in spite of lower dimensionless oil film thickness ratio.

Table 5.2 Summary of Test Condition (MFR_{ref}=14g/s, OCR=5 wt.%)

Component	Refrigerant mass flux (kg/m ² s)	d/D	Internal volume (ml)	Oil retention volume ratio
Suction line	290	0.06	176	0.16
Evaporator	70	0.09	80	0.11
Gas Cooler	110	0.02	165	0.05

5.1.5 Oil Distribution in CO₂ Air-Conditioning Systems

From previous sections, oil retention volume ratio at each system component such as suction line, evaporator, and gas cooler was obtained for various mass fluxes and oil circulation ratios. Based on those results, oil distribution of a CO₂ air-conditioning system for the steady state condition was obtained. Figure 5.10 shows the oil distribution in a CO₂ air-conditioning system for two different oil circulation ratios and two different refrigerant mass fluxes. For the mass flux of 290 kg/m²s, 9 to 11% of the total oil volume was retained in the evaporator under 1 to 5 wt.% oil circulation ratios. On the other hand, only 2 to 5% of the total oil volume was retained in the gas cooler for the same conditions. In the suction line, a relatively higher oil volume was retained compared to oil volume retained in gas cooler. 7 to 16% and 5 to 14% of the total oil volume were retained in the

suction line for the mass fluxes of $290 \text{ kg/m}^2\text{s}$ and $414 \text{ kg/m}^2\text{s}$, respectively. As a result, 32% of the total oil volume was retained in the evaporator, the gas cooler, and the suction line for the mass flux $290 \text{ kg/m}^2\text{s}$ at 5 wt.% of oil circulation ratio.

It is to be expected that the oil, which is retained in neither the heat exchangers nor the suction line, would stay in either the compressor shell for the hermetic compressor case or in the oil separator located in the compressor discharge line. For an air-conditioning system with an oil separator at the compressor discharge line, the oil retention would be expected to be less than 20% for the lower mass flux based on the above result because the oil circulation ratio is less than 1 wt.%. Moreover, the oil retention volume in the system can be minimized by reducing the size of the suction line or by having a low inlet vapor quality in the evaporator. From the oil distribution chart shown in Figure 5.10, the questions of the amount of oil in the system and the location of the discharged oil from the compressor are answered.

5.2 Pressure Drop

The oil flows along the pipe, generates waves at the liquid-gas interface, and thereby increases the interface roughness. Due to the presence of oil in the system components, the pressure drop increases. The pressure drop penalty factor (PDPF), defined as the ratio of the pressure drop with the presence of the oil to the pressure drop without oil, is now introduced. The pressure drop through the heat exchangers was measured by a differential pressure transducer for both cases with and without oil injection.

The PDPF of the evaporator was measured with respect to two different mass fluxes, 70 and 135 kg/m²s, during oil retention test. As shown in Figure 5.11, for the refrigerant mass flux of 135 kg/m²s at the evaporator, the PDPF increased up to 40% at 5 wt.% oil circulation ratio as compared to at 0 wt.% of oil circulation ratio. The PDPF of the lower mass flux, 70 kg/m²s at the evaporator, was 78% higher than that of the mass flux of 135 kg/m²s at oil circulation ratio 4 wt.% because of the larger oil retention in the evaporator. Basically, the gas refrigerant/oil mixture flow in the tube can be divided into two different flow regimes: high-speed gas refrigerant flow at the core and viscous flow of liquid oil film along the wall. Interfacial shear stress depends upon the difference between the refrigerant gas velocity and liquid oil film velocity. These velocities vary due to the oil amount retained in the tube. Thus, the pressure drop, which is a function of the interfacial friction factor, is affected by the oil retention in the tube.

The effect of oil on pressure drop was found to be most significant at high vapor qualities where the local oil mass fractions were the highest. This is because the local liquid viscosity of the refrigerant/oil mixtures at the high vapor quality region increases close to that of pure oil during the evaporation process. Since the PDPF is the function of liquid viscosity, PDPF is higher at the lower mass flux, 70 kg/m²s, due to the relatively larger area being high vapor quality and superheated region in the evaporator.

The effect of vapor quality on the PDPF due to the presence of the oil was also investigated by Zurcher *et al.* (1998). They reported that the PDPF at the mass flux of 100 kg/m²s and high quality region, 0.8, was around 2 in the 9 mm outer diameter smooth tube. On the other hand, at the same mass flux, the PDPF was only 1.3 at vapor quality, 0.5. They concluded that the influence of oil on the pressure drop was more severe at

high vapor qualities. The PDPF due to the oil in the microchannel evaporator was also investigated by Zhao (2001). He reported that PDPF at the mass flux of $100 \text{ kg/m}^2\text{s}$ and lower vapor quality region of 0.1 with 5 wt.% of oil circulation ratio is less than 2. As the vapor quality increases at the fixed refrigerant mass flux, PDPF due to the presence of the oil increases. The PDPF of current study at mass flux, $70 \text{ kg/m}^2\text{s}$, is around 2.7 at 4.5 wt.% of oil circulation ratio, which is higher than that of previous studies mentioned above. This is because inlet vapor quality is so high that high quality and superheated region is dominant in the evaporator. Thus, the pressure drop caused by oil retention is more significant in the high vapor quality region in the evaporator.

PDPF was measured in the gas cooler while oil was injected in gas cooler inlet with respect to various oil circulation ratios. The PDPF of the evaporator and the gas cooler for the refrigerant mass flux of $290 \text{ kg/m}^2\text{s}$ at the suction line, for various oil circulation ratios up to 8.5 wt.%, is shown in Figure 5.12. The PDPF of the evaporator-side is higher than that of the gas cooler-side because of higher oil retention in the evaporator.

Based on the measurements made in the current study, the PDPF increases with the increase of vapor quality and decrease of mass flux at the evaporator. The higher PDPF caused by higher vapor quality and lower refrigerant mass flux results in higher oil retention in the evaporator. Similar to the PDPF, several studies have also reported that the heat transfer coefficient is degraded due to the presence of the oil in the heat exchanger (Nidegger *et al.*, 1997, Tatara and Payvar, 2000, and Zhao *et al.*, 2002). Therefore, the high oil retention in the evaporator degrades the heat transfer coefficient and increases pressure drop, and then causes system performance degradation.

5.3 Conclusions

In this chapter, the experimental test results for various refrigerant mass fluxes and oil circulation ratios measured by using the oil injection-extraction method for the different system components including the suction line, the evaporator, and the gas cooler are discussed. The conclusions from experimental results are as follows.

- As the oil circulation ratio increases, the oil retention volume ratio in the heat exchanger and suction line also increases.
- For a refrigerant mass flux of $290 \text{ kg/m}^2\text{s}$ at the suction line, the oil retention volume ratio in the evaporator is around 0.09 to 0.11 for 1 to 5 wt.% oil circulation ratio.
- For a higher refrigerant mass flux of $559 \text{ kg/m}^2\text{s}$, oil retention volume ratio in the evaporator for 1 to 5 wt.% oil circulation ratio is 0.04 to 0.06.
- The oil retention volume ratio in the gas cooler is less than 0.05.
- The oil retention in the gas cooler is quite small because of high CO_2 density, low oil viscosity, and low oil surface tension.
- Higher inlet vapor quality results in higher oil retention in the evaporator.
- 16% and 10% of the total amount of oil charged initially is retained in heat exchangers at 5 wt.% of oil circulation ratio for refrigerant mass flux of $290 \text{ kg/m}^2\text{s}$ and $414 \text{ kg/m}^2\text{s}$, respectively.
- For high refrigerant mass flux, less oil volume is retained in the heat exchangers, which results in a lower pressure drop penalty factor.
- The effect of oil on pressure drop was found to be most profound at high vapor qualities where the local oil mass fractions were the highest.

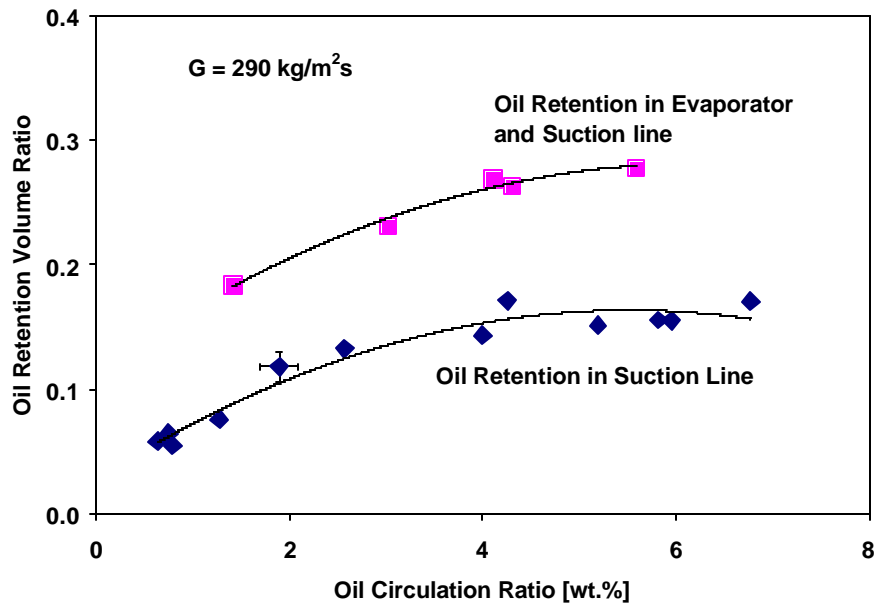


Figure 5.1 Oil Retention in Evaporator and Suction Line ($G = 290 \text{ kg/m}^2\text{s}$)

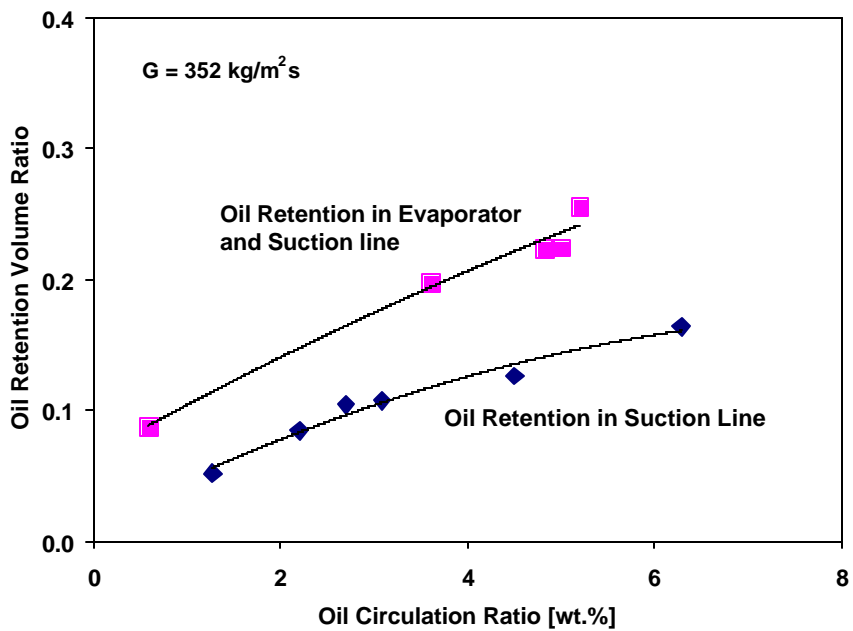


Figure 5.2 Oil Retention in Evaporator and Suction Line ($G = 352 \text{ kg/m}^2\text{s}$)

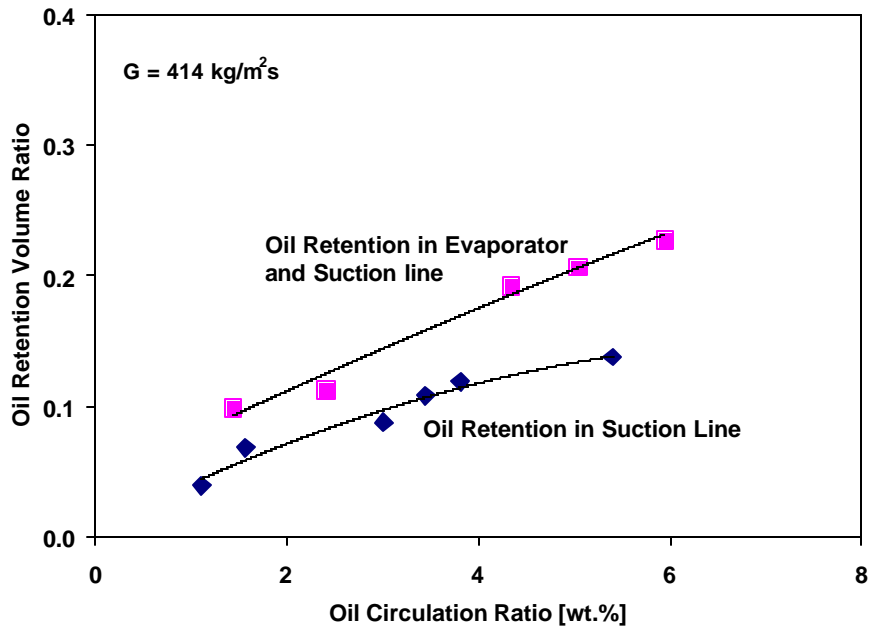


Figure 5.3 Oil Retention in Evaporator and Suction Line ($G = 414 \text{ kg/m}^2\text{s}$)

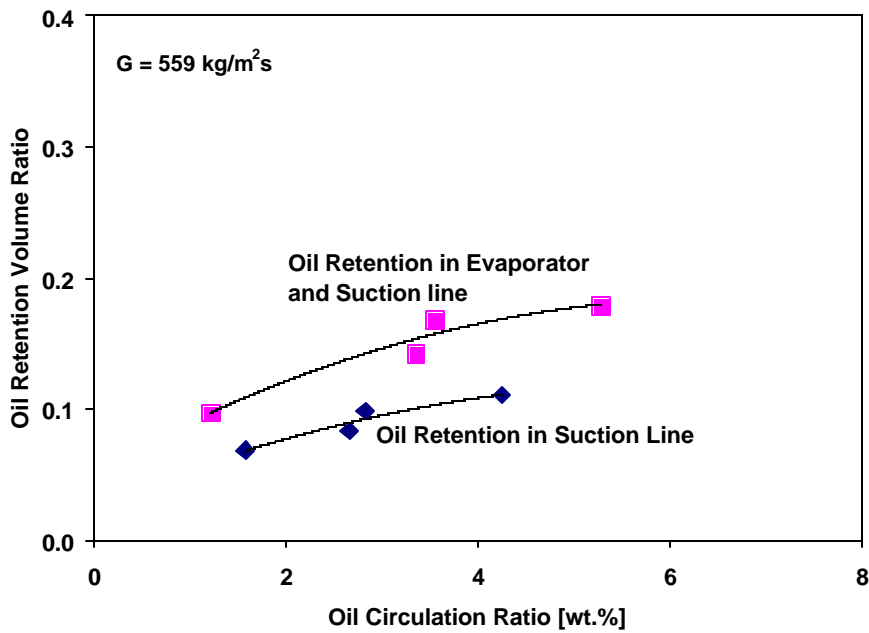


Figure 5.4 Oil Retention in Evaporator and Suction Line ($G = 559 \text{ kg/m}^2\text{s}$)

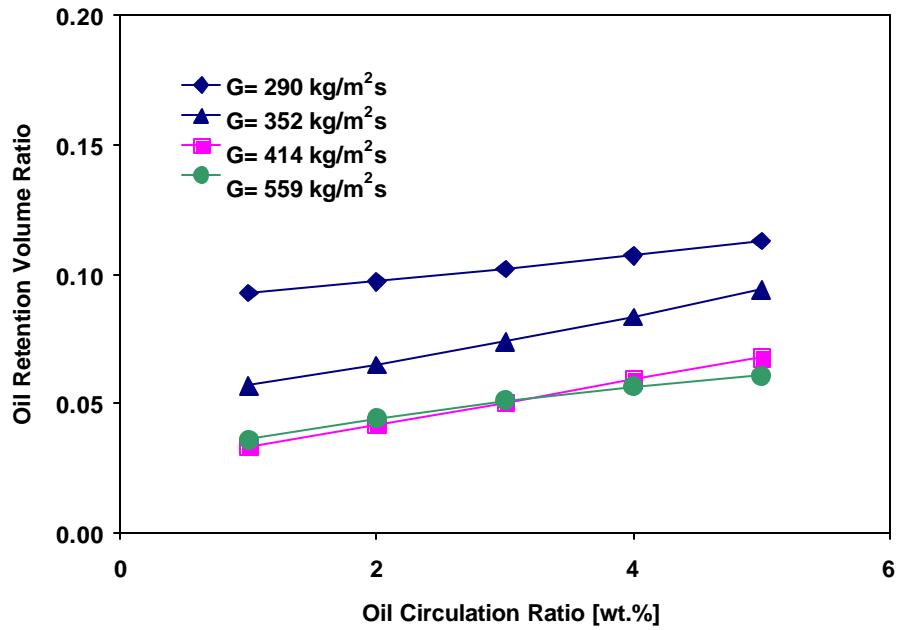


Figure 5.5 Effect of Refrigerant Mass Flux on Oil Retention in Evaporator

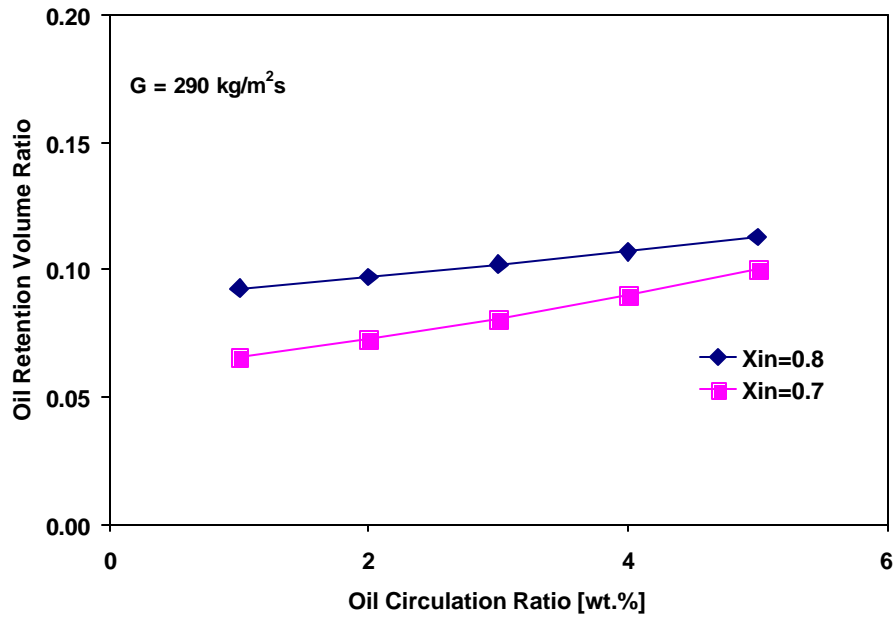


Figure 5.6 Effect of Evaporator Inlet Vapor Quality on Oil Retention

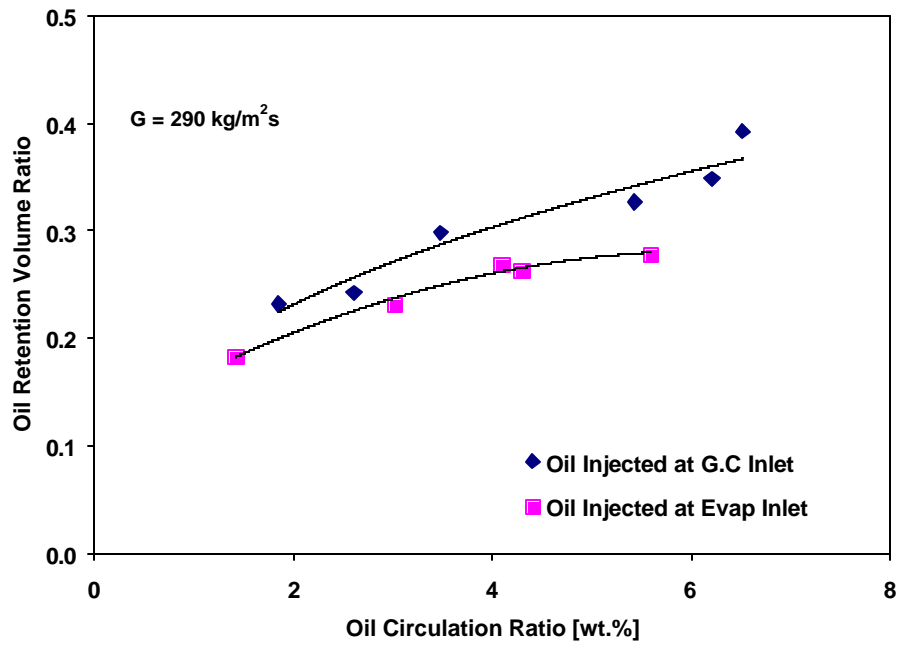


Figure 5.7 Oil Retention in Gas Cooler ($G = 290 \text{ kg/m}^2\text{s}$)

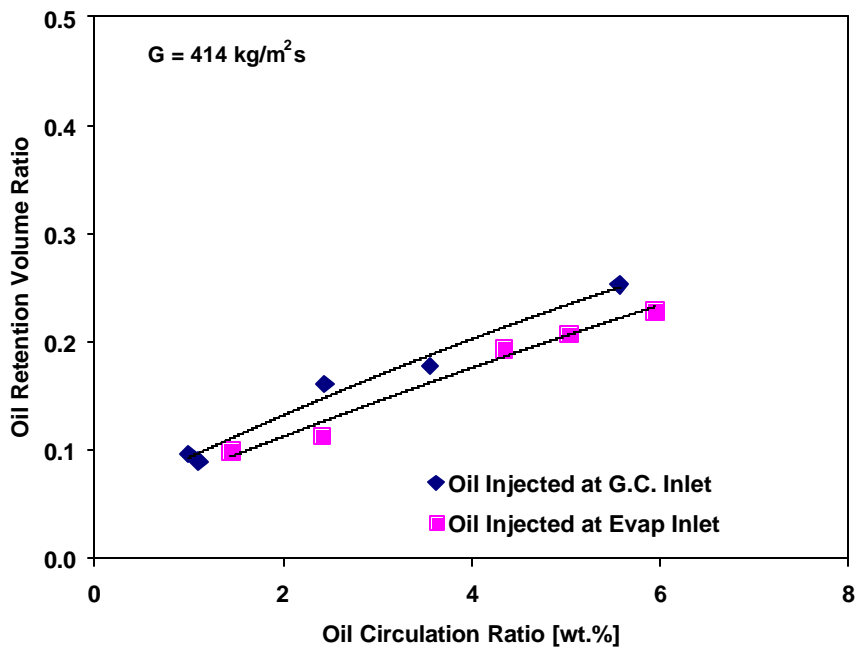


Figure 5.8 Oil Retention in Gas Cooler ($G = 414 \text{ kg/m}^2\text{s}$)

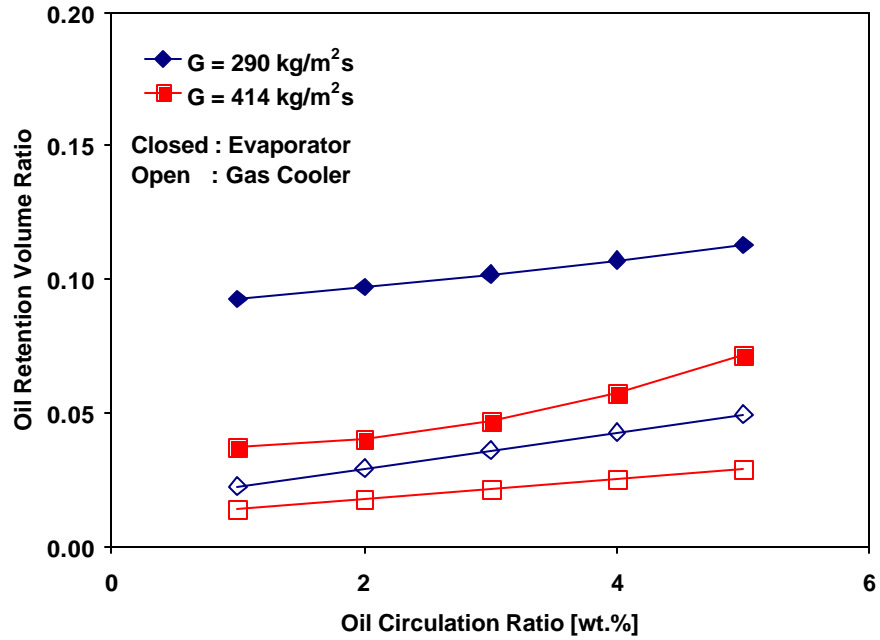


Figure 5.9 Oil Retention in Heat Exchangers

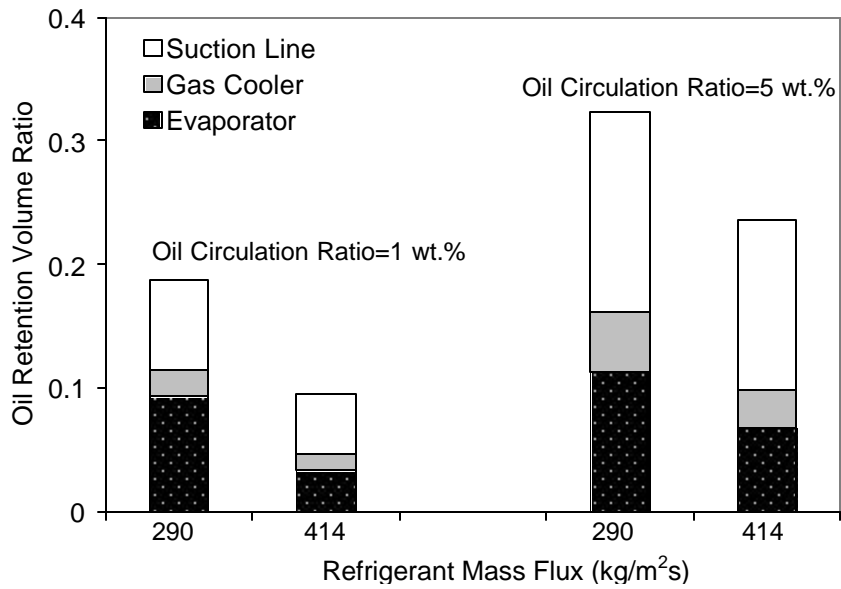


Figure 5.10 Oil Distribution in CO₂ Air-Conditioning Systems

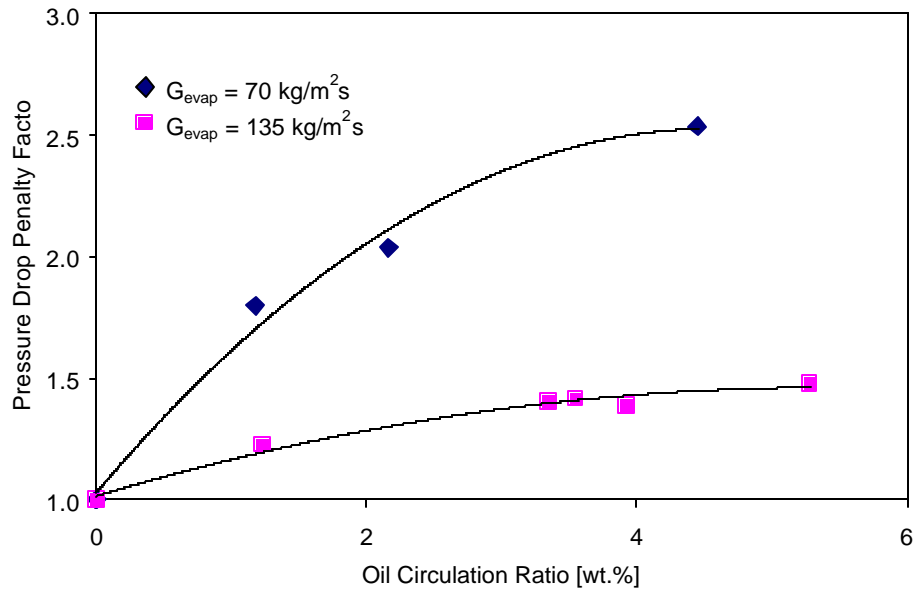


Figure 5.11 Pressure Drop Penalty Factor in Evaporator

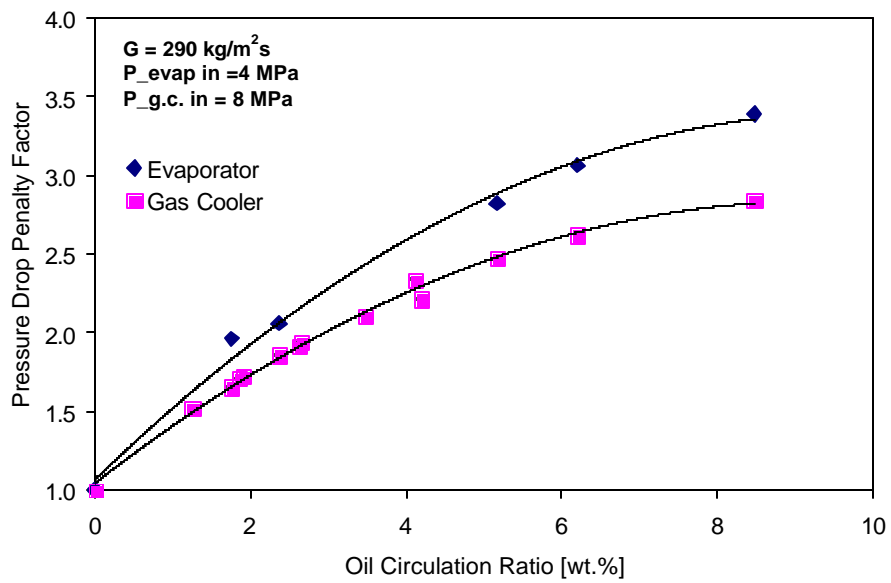


Figure 5.12 Pressure Drop Penalty Factor in Heat Exchangers

CHAPTER 6 Modeling of Oil Retention in the Suction Line

6.1 Introduction

Since the experimental results described in CHAPTER 5 were obtained under limited test conditions, an oil retention model for each cycle component was developed to generalize the oil retention in various conditions. This chapter describes details of the oil retention modeling of the suction line in a CO₂ air-conditioning system. The flow patterns of the CO₂/oil mixture in the suction line were studied, and then modeling corresponding to the flow patterns is described in detail. The simulation results of the oil retention at the suction line are achieved by the analytical model and then compared with experimental results.

6.2 Modeling of Oil Retention in the Suction Line

This section describes the analytical model developed to predict oil retention in the suction line. In order to estimate the oil retention, the flow pattern should be identified first. However, since the flow pattern map for CO₂/oil mixture is not available yet, the flow pattern of CO₂/oil mixture is instead based on the existing two-phase flow pattern maps. The Navier-Stokes equations with appropriate assumptions were solved to predict the oil film thickness in a circular tube. From the oil film thickness, the oil retention in the suction line was calculated for a range of conditions.

6.2.1 Flow Patterns in the Suction Line

Since most flow pattern maps are based on air-water two-phase flow, a correction factor or property consideration to compensate for different properties from air-water is required in order to apply the CO₂/oil mixture flow to the air-water flow pattern maps. Baker's flow pattern map (1954) for horizontal flow is shown in Figure 6.1. Basically, the x- and y-axis represent corrected liquid mass flux (G_l) and vapor mass flux (G_g), respectively, by using the correction factors λ and β , which allow the use of other fluid mixtures. The correction factors λ and β are given by the Equation (6-1):

$$I = \left[\left(\frac{\rho_g}{\rho_a} \right) \left(\frac{\rho_l}{\rho_w} \right) \right]^{1/2}, \quad Y = \left[\left(\frac{\mu_l}{\mu_w} \right) \left(\frac{\rho_w}{\rho_l} \right)^2 \right]^{1/3} \left(\frac{S_w}{S} \right) \quad (6-1)$$

where ρ_g, ρ_l : gas and liquid density [kg/m³]
 ρ_a, ρ_w : air and water density [kg/m³]
 μ, μ_w : liquid and water viscosity [kg/m-s]
 S, S_w : liquid and water surface tension [N/m]

The subscripts a and w refer to the values of properties for air and water at atmospheric pressure and temperature. For instance, the correction factors λ and β are 1 for the air-water two-phase flow in a horizontal pipe. In the case of 4.2 wt.% of oil circulation ratio at refrigerant mass flux 290 kg/m²s, the correction factors λ and β for the two-phase flow of the gas CO₂ and liquid oil mixture in the suction line are 11.4 and 9.2, respectively. From the Figure 6.1, the flow pattern of CO₂/oil mixture in the suction line is assumed to be an annular flow. In annular flow, oil flows in a film along the tube wall, with a high velocity CO₂ stream in the core of the tube.

Taitel and Dukler (1976) proposed a flow pattern map for two-phase flow in a horizontal or a slightly inclined round tube as shown in Figure 6.2. The map was originally developed to predict flow pattern transitions from the stratified wavy flow to annular flow. The flow pattern transitions shown in Figure 6.2 are presented in terms of Martinelli's parameter, X , and the parameter F_{TD} , which are defined as

$$X = \left[\frac{(dP/dz)_l}{(dP/dz)_g} \right]^{1/2}, \quad F_{TD} = \left[\frac{\mathbf{r}_g j_g^2}{(\mathbf{r}_l - \mathbf{r}_g) D g \cos \mathbf{q}} \right]^{0.5} \quad (6-2)$$

where $(dP/dz)_l$: frictional pressure gradient for the liquid
 $(dP/dz)_g$: frictional pressure gradient for the gas
 j_g : superficial gas flux [m/s]
 D : tube diameter [m]
 g : gravitational acceleration [m/s²]

The flow pattern of the CO₂/oil mixture in the suction line corresponds an annular flow in the flow pattern map by Taitel and Dukler (1976).

Moreover, the flow pattern of CO₂/oil mixture was observed through the flow visualization section installed in the suction line. As shown in Figure 6.3, thicker oil film flows on the wall while high velocity of CO₂ gas flows in the core of tube. The oil film thickness was varied depending on the oil circulation ratio at fixed refrigerant mass flux. Therefore, it was concluded that the flow pattern of CO₂/oil mixture in the suction line is annular flow.

Based on the annular flow pattern, an analytical model to estimate oil retention was developed for CO₂/oil mixture in the suction line as next.

6.2.2 Analytical Model

To predict the oil retention in the suction line, the same approach used by Mehendale (1998) was used. First, the oil film thickness was obtained from the governing equations based on the following assumptions.

- Axisymmetric flow.
- Steady state, adiabatic and fully developed flow.
- The oil film has CO₂ dissolved in it. Since the oil properties are not the same as those of the pure oil, properties of oil with CO₂ solution are estimated based on the solubility of CO₂ in oil. This varies depending on the temperature and pressure conditions of a suction line.
- The oil film uniformly covers the inside tube along the tube length and flows in an annular flow pattern.

The oil retention volume ratio in the suction line is calculated by the integration of oil film thickness with respect to the cross sectional area (tube outer diameter: 9.5×10^{-3} m, thickness: 1.2×10^{-4} m) as well as the entire length (3.8 m) of the suction line tube, as shown in Equation (6-3).

$$OilRetentionVolumeRatio = L \cdot A \cdot \left[1 - \left(1 - \frac{d}{R} \right)^2 \right] \cdot \frac{1}{V_{ini}} \quad (6-3)$$

where L : total suction line length [m]
 A : tube inner cross sectional area [m²]
 R : tube inner radius [m]
 d : oil film thickness [m]
 V_{ini} : oil volume charged initially [m³] (0.25×10^{-3} m³)

6.2.3 Oil Film Analysis

The governing equations for the oil film with the consideration of above assumptions are described as follows.

The continuity equation:

$$\frac{d}{dr}(ru_r) = 0 \quad (6-4)$$

Z-directional momentum equation:

$$\frac{m_l}{r} \frac{d}{dr} \left(r \frac{du}{dr} \right) = \frac{dP}{dz} \quad (6-5)$$

Integrating the above equation with respect to r ,

$$m_l r \frac{du}{dr} = \frac{dP}{dz} \cdot \frac{r^2}{2} + C_1 \quad (6-6)$$

where C_1 is a constant of integration. The above equation becomes Equation (6-7) by imposing the shear stress term for a Newtonian fluid.

$$-t \cdot r = \frac{dP}{dz} \cdot \frac{r^2}{2} + C_1 \quad (6-7)$$

where $t = -m \frac{du}{dr}$

Using boundary condition $t = t_i$ at $r = R - d$,

$$-t_i(R - d) = \frac{dP}{dz} \cdot \frac{1}{2}(R - d)^2 + C_1 \quad (6-8)$$

Eliminating C_1 between Equation (6-7) and (6-8) leads to Equation (6-9):

$$\mathbf{t} = \mathbf{t}_i \frac{(R-d)}{r} - \frac{1}{2} \cdot \frac{dP}{dz} \left(\frac{r^2 - (R-d)^2}{r} \right) \quad (6-9)$$

If the shear stress term is expressed by the velocity gradient, Equation (6-9) becomes

$$-\mathbf{m}_l \frac{du}{dr} = \mathbf{t}_i \frac{(R-d)}{r} - \frac{1}{2} \cdot \frac{dP}{dz} \left(\frac{r^2 - (R-d)^2}{r} \right) \quad (6-10)$$

Integrating Equation (6-10) with respect to r and using a no-slip boundary condition for the oil film at the wall $u(r=R)=0$ show, respectively,

$$-\mathbf{m}_l u = \mathbf{t}_i \ln r \cdot (R-d) - \frac{1}{2} \cdot \frac{dP}{dz} \left(\frac{r^2}{2} - (R-d)^2 \cdot \ln r \right) + C_2 \quad (6-11)$$

$$0 = \mathbf{t}_i \ln R \cdot (R-d) - \frac{1}{2} \cdot \frac{dP}{dz} \left(\frac{R^2}{2} - (R-d)^2 \cdot \ln R \right) + C_2 \quad (6-12)$$

Eliminating C_2 between (6-11) and (6-12) yields the velocity profile u as follows:

$$u = \frac{1}{\mathbf{m}_l} \left[\left(\mathbf{t}_i \cdot (R-d) + \frac{(R-d)^2}{2} \cdot \frac{dP}{dz} \right) \cdot \ln \frac{R}{r} - \frac{1}{4} \frac{dP}{dz} (R^2 - r^2) \right] \quad (6-13)$$

The oil mass flow rate can be obtained by integrating the velocity profile over the cross sectional area:

$$\dot{m}_o = \frac{2pr_l}{m_f} \left(t_i(R-d) + \frac{(R-d)^2}{2} \frac{dP}{dz} \right) \left(\frac{R^2 - (R-d)^2}{4} - \frac{(R-d)^2}{2} \ln \frac{R}{R-d} \right) - \frac{pr_l}{8m_f} \frac{dP}{dz} (R^2 - (R-d)^2)^2 \quad (6-14)$$

For the given fluid properties and the tube diameter, Equation (6-14) contains three unknown quantities, which are

- 1 oil film thickness (d)
- 2 pressure gradient ($\frac{dP}{dz}$)
- 3 interfacial shear stress (t_i)

Since the only known value in Equation (6-14) is the oil mass flow rate (\dot{m}_o) for the certain oil circulation ratio at given refrigerant mass flow rate, the interfacial shear stress and the pressure gradient should be correlated to obtain oil film thickness as described next.

6.2.4 CO₂ Core Analysis

Figure 6.4 shows the force balance of the annular flow. It is assumed that the oil film thickness, δ , uniformly covers the inside tube wall while CO₂ gas flows through the core. When the force balance applied to the CO₂ core is drawn,

$$\frac{dP}{dz} + \frac{t_i p D_c}{A_c} = 0 \quad (6-15)$$

where D_c : vapor core diameter [m]
 A_c : vapor core cross sectional area [m²]

If the void fraction, α , is used,

$$\mathbf{a} = \frac{A_c}{A} = \left(\frac{D_c}{D}\right)^2 \quad (6-16)$$

Equation (6-15) yields:

$$\frac{dP}{dz} + \frac{4\mathbf{t}_i}{D\sqrt{\mathbf{a}}} = 0 \quad (6-17)$$

Thus, the pressure gradient of the CO₂ core is a function of the oil film thickness, which is replaced by the void fraction (a), and the interfacial shear stress. The interfacial shear stress can be calculated by using the empirical interfacial friction factor described in the next section.

6.2.5 Interfacial Friction Factor

The interfacial shear stress exerted on the liquid film by the gas is given by the following equation:

$$\mathbf{t}_i = \frac{1}{2} f_i \mathbf{r}_g (u_g - u_i)^2 \quad (6-18)$$

where f_i : interfacial friction factor
 u_g : gas core velocity [m/s]
 u_i : interface velocity [m/s]

However, because the CO₂ gas velocity is much larger than the oil film surface velocity, the interfacial shear stress can be approximated as

$$\mathbf{t}_i = \frac{1}{2} f_i \mathbf{r}_g u_g^2 \quad (6-19)$$

The interfacial friction factor, f_i , in Equation (6-19) is the most important parameter in estimating the oil film thickness and has been empirically correlated by several researchers as summarized below. For the vertical upward flow with thin films and gas core, Wallis (1969) proposed an interfacial friction factor, which is a function of liquid film thickness, for the vertical upward flow.

$$f_i = 0.005 \left(1 + 300 \frac{d}{D} \right) \quad (6-20)$$

The correlation by Wallis was modified by Fore *et al.* (2000) for a better fit for the thin liquid film thickness. Two nominal system pressures, 340 to 1,700 kPa, and two nominal temperatures, 38 to 93 °C, with nitrogen and water as working fluids were used. The test section, 5.08×101.6 mm rectangular duct, was placed in a vertical upward position.

$$f_i = 0.005 \left(1 + 300 \left(\frac{d}{D} - 0.0015 \right) \right) \quad (6-21)$$

However, since the above correlations are limited to thin liquid film, Fukano and Furukawa (1998) suggested an empirical correlation for the interfacial friction factor considering the change in the fluid viscosity, which is also applicable to thicker liquid film. The experiment was conducted with water and aqueous glycerol solutions with different liquid viscosities, and air in the vertical upward tube, 26 mm of inner diameter, at atmospheric pressure at a temperature of 27 to 29 °C.

$$f_i = 1.7 \left(12 + \frac{n_l}{n_w} \right)^{-1.33} \left(1 + 12 \frac{d}{D} \right)^8 \quad (6-22)$$

where \mathbf{n}_l : kinetic viscosity of aqueous glycerol solution [m^2/s]
 \mathbf{n}_w : kinetic viscosity of water [m^2/s]

Most interfacial friction factors mentioned above are expressed as a function of liquid film thickness and ignore the influence of gas velocity or the gas Reynolds number. The following interfacial friction factors are empirically correlated in terms of the gas Reynolds number. Newton *et al.* (1999) suggested the interfacial friction factor for the horizontal tube, 50 mm of inner diameter, based on their experimental results. Their experiments were conducted with air and three different liquids, distilled water, kerosene, and Propar-22, which is a light machine oil. They proposed two different friction factors depending on the interface roughness.

$$f_i = 6.5 \times 10^{-4} Re_g^{0.3} \text{ for a smooth interface}$$

$$f_i = 0.003 Re_g^{0.2} \text{ for a wavy interface} \quad (6-23)$$

where $3,500 < Re_g < 12,000$

Wongwises and Kongkiatwanitch (2001) proposed a new, empirically correlated interfacial friction factor with air and water. According to their dimensional analysis of fully developed single-phase turbulent flow in vertical pipes with 29 mm of inner diameter, the friction factor can be expressed as a function of the gas Reynolds number and a dimensionless liquid film thickness:

$$f_i = 17.172 \cdot Re_g^{-0.768} \left(\frac{d}{D} \right)^{-0.253} \quad (6-24)$$

Since the friction factors described above are generally obtained from studies for either air-water flow or in vertical flow, it is not appropriate to use them in the current simulation, which models CO₂/oil flow in a horizontal tube. Therefore, in this study, a new empirical correlation for the friction factor of CO₂ and oil flow is proposed, based on experimental results in the suction line as follows.

First, the relationship between the CO₂ Reynolds number and friction factor were examined. As the refrigerant gas velocity increases, the interfacial shear stress increases because of a higher interfacial drag force. A plot of the data on a logarithmic scale, as shown in Figure 6.5, indicates that t_i increases in proportion to $u_g^{2.29}$. If we use the definition of the friction factor of the interfacial shear stress, the interfacial friction factor is found from Equation (6-25),

$$f_i = C u_g^{0.29} \quad (6-25)$$

where C is a dimensional constant to be determined from the experimental data.

Figure 6.6 shows the variation of the interfacial friction factor with respect to the CO₂ gas Reynolds number. In Figure 6.6, both Blasius's correlation for the turbulent flow in a smooth tube and Newton's correlation for a wavy interface are compared with the current correlated interfacial friction factor. Because of the higher roughness caused by an oil film wave, the interfacial friction factor of the current study is higher than that of the Blasius's correlation. On the other hand, the Newton's interfacial friction factor agrees with the current friction factor obtained by experiments. As the gas CO₂ Reynolds number increases, the friction factor increases slightly due to the increase of the relative roughness of the interface.

Figure 6.7 shows the relation between interfacial friction factor and dimensionless oil film thickness, δ/D . Based on the figure, as the CO₂ flow rate increases at a fixed oil flow rate, the oil film thickness decreases due to the higher drag force exerted by CO₂ gas. Thus, the friction factor increases with a reduction of the dimensionless film thickness at fixed oil flow rate. This result matches well with the results for horizontal flow from Wallis (1969).

According to the above analysis of CO₂ and oil flow in the suction line, the interfacial friction factor should be expressed as a function of the CO₂ gas Reynolds number as well as the dimensionless oil film thickness. By using curve fit software, an empirical interfacial friction factor based on the experimental results was developed as shown in Equation (6-26),

$$f_i = 9.287 \times 10^{-5} Re_g^{0.2976} \left(\frac{d}{D} \right)^{-0.6515} \quad (6-26)$$

which was obtained in the range $1.6 \times 10^5 < Re_g < 3.5 \times 10^5$ of CO₂ gas. The gas Reynolds number in this equation is based on the gas core area due to the reduction in flow caused by the growth of the oil film.

$$Re_g = \frac{G \cdot D_H}{\mu_g} \quad (6-27)$$

where G : CO₂ gas mass flux [kg/m²s]
 D_H : hydraulic diameter [m]
 μ_g : CO₂ dynamic viscosity in gas phase [kg/m-s]

A comparison of interfacial friction factors obtained from the experiments with this new proposed empirical correlation is shown in Figure 6.8, which shows that the

interfacial friction factor is correlated well with experimental data within 25% error bounds. The agreement of these data is better with this new correlation, Equation (6-26), than with other correlations.

6.2.6 Oil Retention Volume

The oil film thickness for the suction line can be calculated by solving Equations (6-14), (6-17), and (6-19) with the empirically correlated friction factor from Equation (6-26). From the obtained oil film thickness at given flow rates and properties, the oil retention volume ratio in the suction line can be calculated with Equation (6-3).

6.3 Verification of Model

The oil retention calculations in the suction line of CO₂ air-conditioning systems were discussed in section 6.2. This section includes a validation of the analytical model using experimental data.

The oil retention volume ratio in the suction line was calculated with two different interfacial friction factors; one is proposed by Wallis (1969) which is the function of dimensionless oil film thickness only, and the other is the new empirical correlation developed in the current study. It is a function of both the gas Reynolds number and a dimensionless oil film thickness.

As shown in Figure 6.9, the oil retention simulation using the interfacial friction factor proposed by Wallis (1969) predicts a lower value when the oil retention volume ratio is larger. Wallis's friction factor was originally based on a thin liquid film for the vertical upward flow, whose dimensionless oil film thickness, δ/D , is less than 0.04. Thus,

Wallis's correlation is expected not to fit with current experimental results, whose dimensionless oil film thickness is higher than 0.08. A comparison between the oil retention simulation and experimental results using a new empirically correlated friction factor, Equation (6-26), is shown in (b) of Figure 6.9. It can be seen that almost all the simulation results are bounded by $\pm 20\%$ from experimental results. This implies that the analytical model developed for the suction line can predict the oil retention in the suction line of CO₂ systems within 20% error. In the next sections, the several parameters affecting the oil retention in the suction line are discussed.

6.4 Parametric Study

6.4.1 The Effects of CO₂ Solubility

The properties of a CO₂/oil mixture in the system change significantly depending on the CO₂ solubility in the oil. The solubility is the amount of refrigerant that can be dissolved in oil by weight percentage. This solubility varies depending on the temperature and pressure. Thus, solubility is one of the important parameters in determining oil retention.

The effect of solubility on oil retention in the suction line for different refrigerant mass fluxes was investigated. In the simulation, pressure was set to 4 MPa, which was the suction condition of the current experiment, and the temperature was set to 5 K superheating at the suction pressure. As shown in the Figure 6.10, the oil retention volume ratio decreases with an increase of solubility. This is because the CO₂/oil mixture's viscosity decreases as the CO₂'s solubility increases. As more CO₂ is dissolved in the oil, the lower CO₂/oil mixture viscosity can be expected. On the other hand, the

CO₂/oil mixture viscosity increases as the solubility decreases, which results in a thicker oil film and higher oil retention in the suction line.

6.4.2 The Effects of Tube Diameter

The effects of the suction tube diameter on oil retention were studied. The oil retention volume ratio for different suction tube diameter was calculated by varying oil circulation ratio. In order to distinguish tube diameter effects only, oil retention volume ratio was calculated at fixed refrigerant mass flow rates, 15 and 25 g/s, instead of using mass flux, which already includes tube diameter effects. The pressure and temperature of the suction line was kept constant at 4 MPa and 5 K superheating while the suction line tube diameter was changed from ¼" to ½" tubing. Normally, a larger diameter suction line tube has the advantage of reduced refrigerant pressure drop. However, as shown in Figure 6.11 on the matter of oil retention in a suction line, a larger diameter tube results in higher oil retention even in the case of higher refrigerant mass flow rate. For example, the oil retention volume ratio dramatically increases up to 0.35 at a refrigerant mass flow rate of 15 g/s and an oil circulation ratio of 5 wt.%. This is because the refrigerant velocity in the larger tube, which is the driving force to transport the oil film, is quite slower than in the smaller tube. However, the oil retention volume ratio for the ¼" tube in the suction line is less than 0.04 even at a higher oil circulation ratio of 5 wt.%. Therefore, it can be said that the effect of refrigerant mass flow rate on oil retention is not significant in the case of a small diameter tube.

For the design of a suction line, the tube size should be carefully considered while balancing the effects of refrigerant pressure drop and oil retention. If a larger amount of

oil is retained in the suction line because of a larger diameter tube, the oil amount in the compressor shell in a hermetic compressor may not be sufficient for proper lubrication.

6.4.3 The Effects of Suction Line Superheating

The effect of superheating of the suction line on oil retention was investigated. As shown in Figure 6.12, the higher superheating at the suction line for the given pressure of 4 MPa shows lower oil retention than the lower superheating, shown as the solid lines. This is because the oil viscosity and CO₂ density decrease as the superheating increases, which results in less oil retention.

If summarize observations discussed above, a lower oil retention volume ratio in the suction line is achieved using a smaller tube diameter, increasing superheating, and using oil which has a high CO₂ solubility in oil. The higher refrigerant flow rate assures lower oil retention in the suction line in all cases.

6.5 Conclusions

Based on the flow pattern in the suction line by using existing two-phase flow pattern maps and observed flow pattern, an analytical model for the annular flow pattern to estimate oil retention volume was developed. According to the analysis of CO₂ and oil flow in the suction line, the interfacial friction factor can be expressed as a function of the CO₂ gas Reynolds number and of dimensionless oil film thickness. An empirical interfacial friction factor based on the experimental results was also developed. The simulation results at the suction line were compared with the experimental results.

Parametric studies were also conducted. The following conclusions were obtained from the modeling of oil retention in the suction line:

- Most simulation results are bounded by $\pm 20\%$ compared to experimental results.
- The oil retention decreases with an increase in solubility because the CO₂/oil mixture viscosity reduces as the CO₂ solubility increases. To minimize oil retention in the suction line, it is recommended to use oil that has high CO₂ solubility.
- A small diameter suction tube results in lower oil retention in the suction line. For the design of the suction line, the tube size should be carefully considered while balancing the refrigerant pressure drop and oil retention.
- Higher superheating at the suction line shows smaller oil retention than lower superheating.

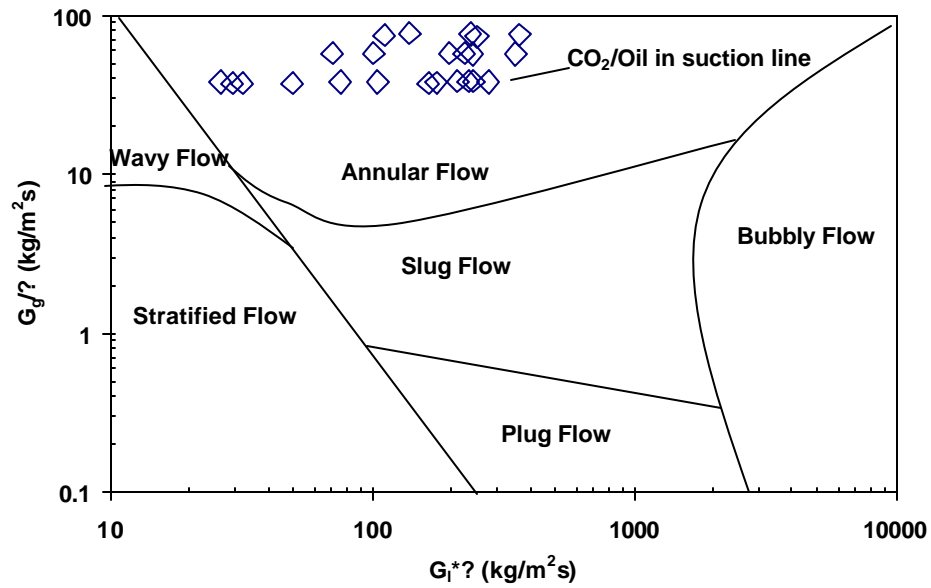


Figure 6.1 Baker's Flow Pattern Map For Horizontal Flow (1954)

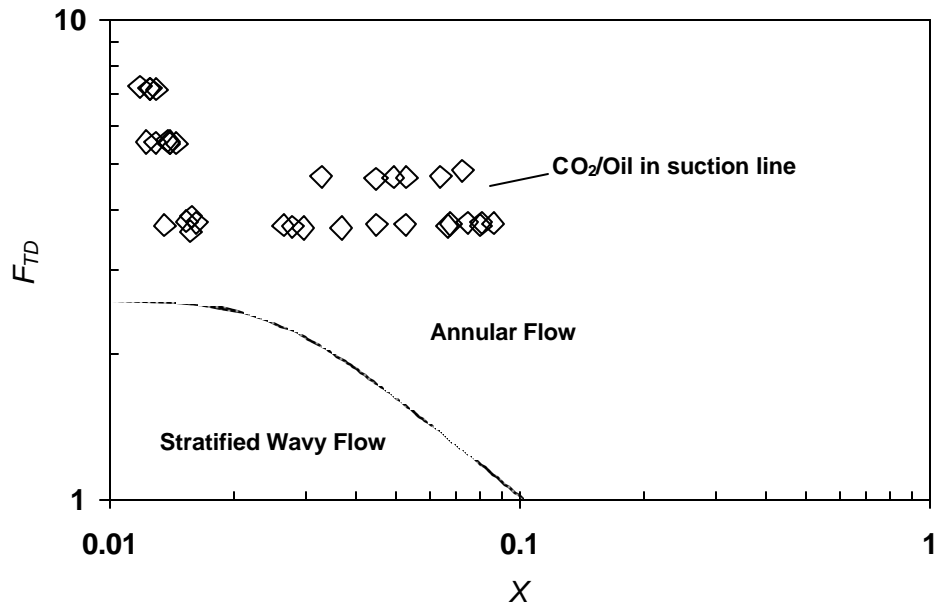


Figure 6.2 Flow Pattern Map (Taitel and Dukler, 1976)

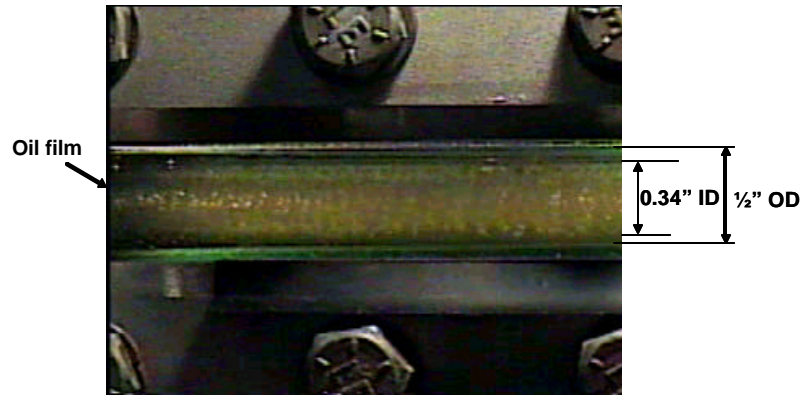


Figure 6.3 Visualized CO₂/Oil Flow in Suction Line

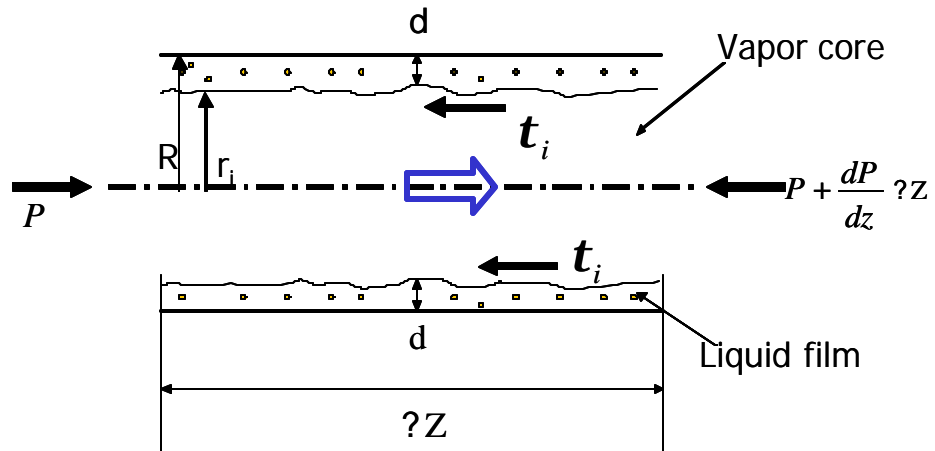


Figure 6.4 Force Balance of Annular Flow

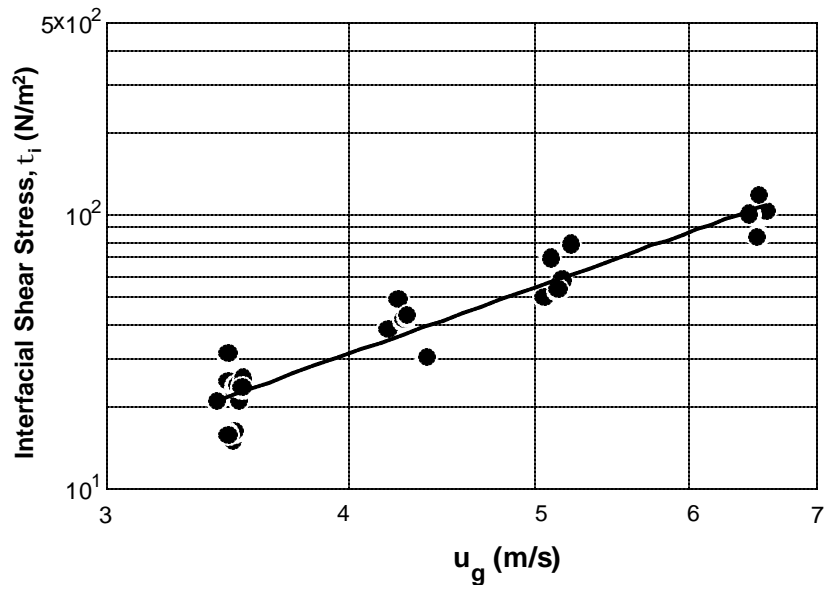


Figure 6.5 Interfacial Shear Stress vs. Refrigerant Gas Velocity

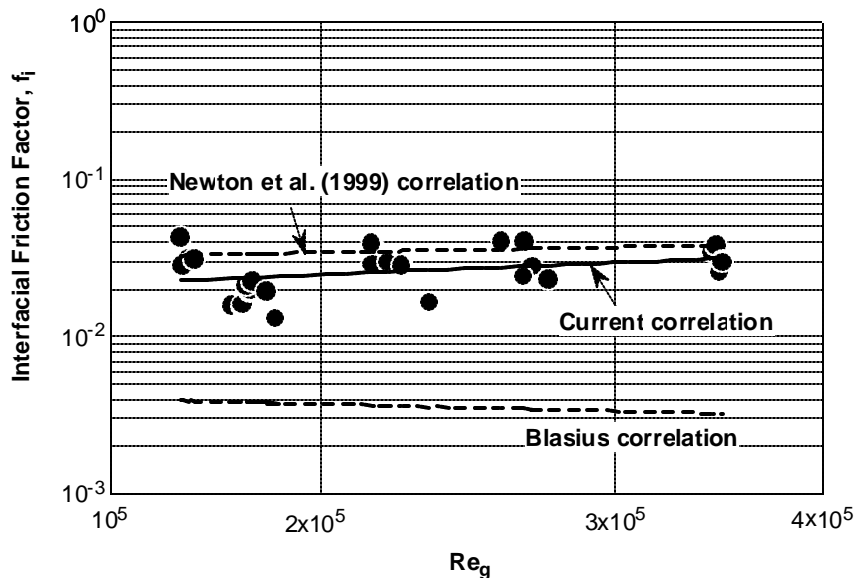


Figure 6.6 Interfacial Friction Factor vs. Reynolds Number

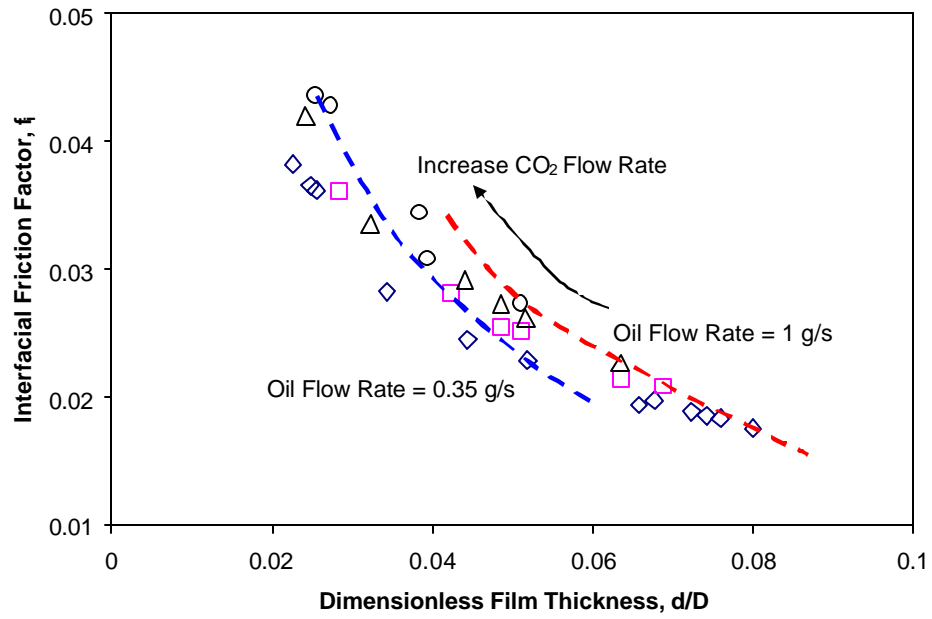


Figure 6.7 Interfacial Friction Factor vs. Dimensionless Oil Film Thickness

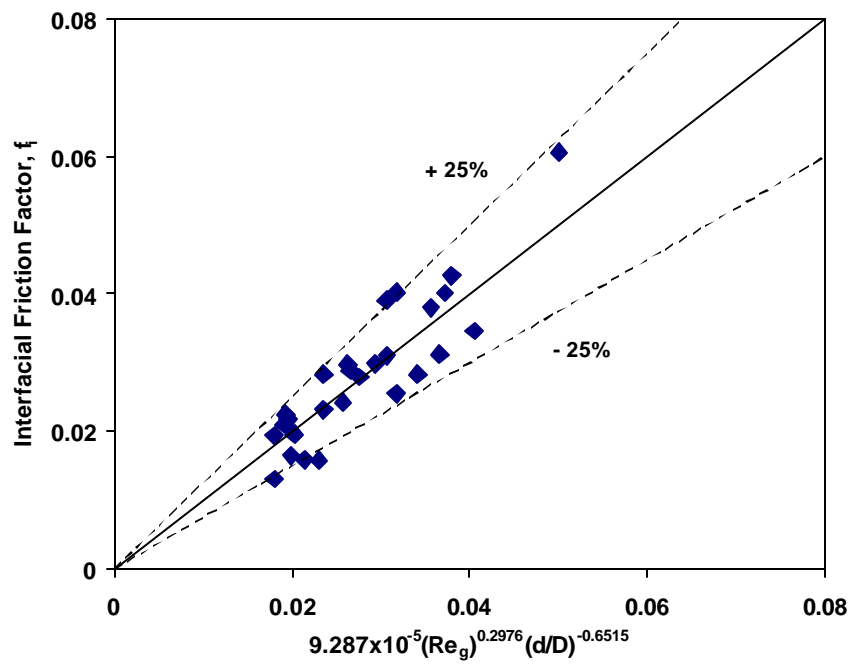
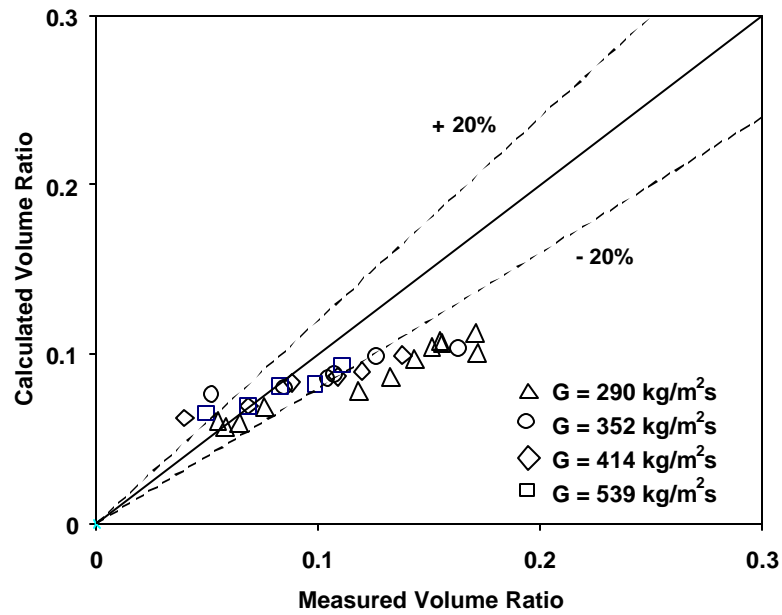
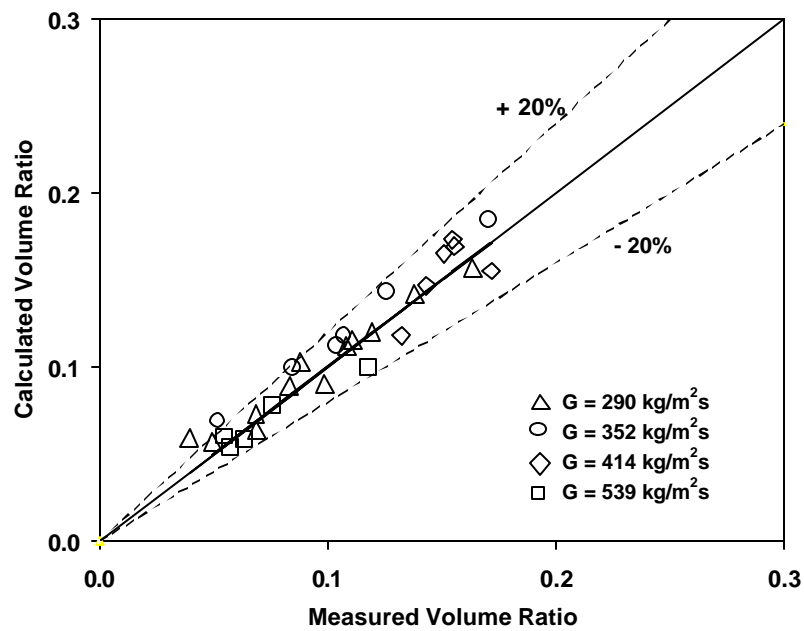


Figure 6.8 Interfacial Friction Factor with New Correlation



(a) Using Wallis's Interfacial Friction Factor



(b) Using Empirically Correlated Interfacial Friction Factor

Figure 6.9 Comparisons of Oil Retention Volume Ratios between Measured and Calculated Values

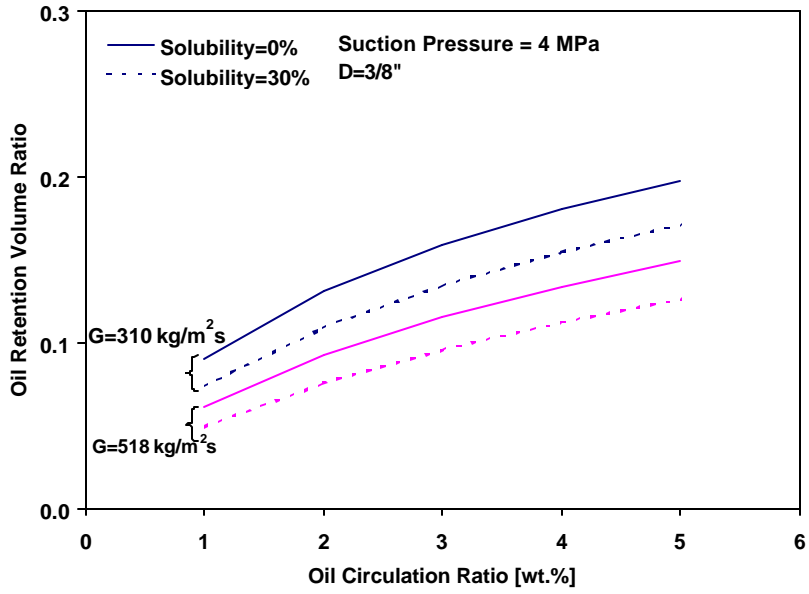


Figure 6.10 Effects of CO₂ Solubility in Suction Line

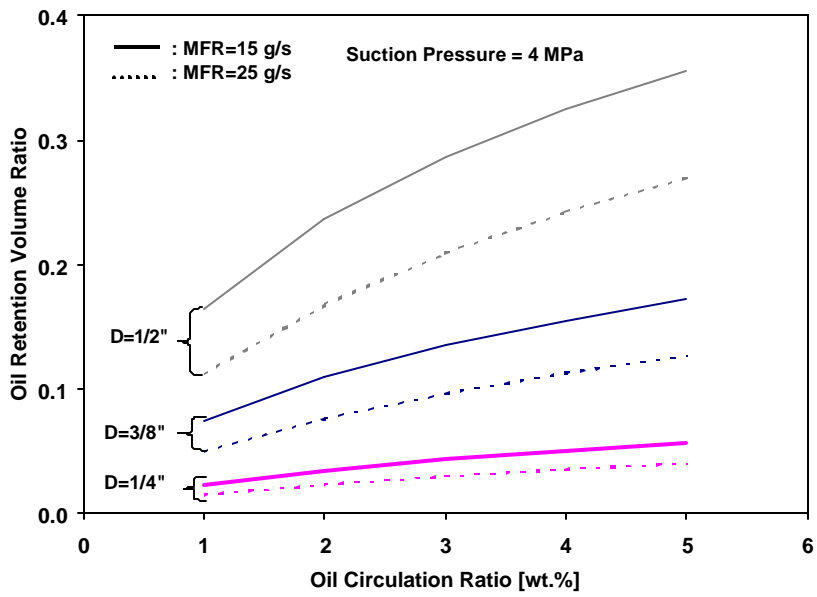


Figure 6.11 Effects of Tube Diameter in Suction Line

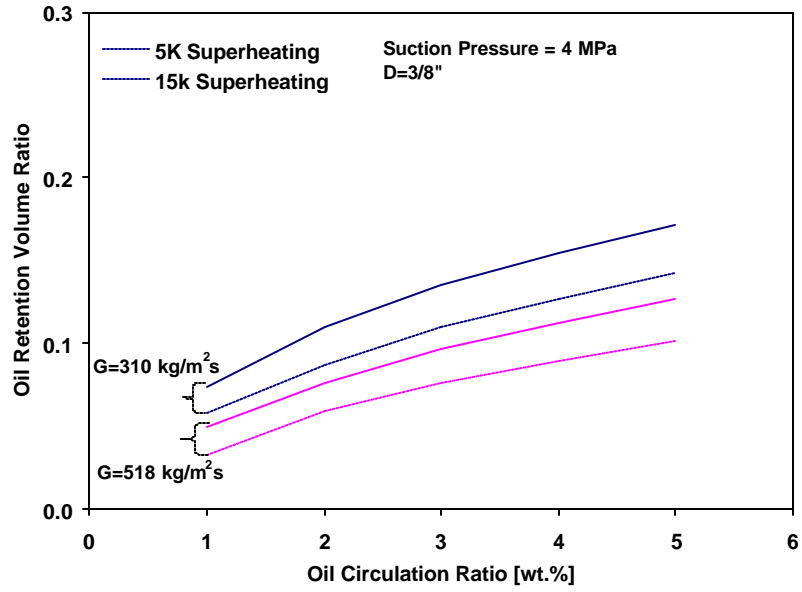


Figure 6.12 Effects of Superheating of the Suction Line

CHAPTER 7 Modeling of Oil Retention in Heat Exchangers

7.1 Introduction

Characteristics of the oil retention in heat exchangers are expected to be quite different from those in the suction line because of phase or temperature changes, so that other approach is required to estimate the oil retention in heat exchangers. In this chapter, modeling of oil retention in heat exchanger is discussed in detail. First, the flow pattern of a CO₂/oil mixture in heat exchangers is discussed, and various void fraction models are described, which were used in estimating the oil retention in heat exchangers. Then, modeling of the oil retention at the microchannel tube and header is presented. The way the model was validated using experimental results is described. Finally, parametric studies are discussed with the validated model to investigate the influence of different variables on oil retention.

7.2 Modeling of Oil Retention

7.2.1 Flow Patterns in Heat Exchangers

The flow patterns of the CO₂/oil mixture in heat exchangers are significantly different from those in the suction line because the internal port diameters of the microchannels used in the evaporator and gas cooler are only 0.55 mm and 0.7 mm, respectively. Although microchannel heat exchangers have been widely used in

automotive products, there are only a few published papers that are about the flow patterns in small diameter tubes. They are summarized below.

Fukano and Kariyasaki (1993) conducted flow visualization experiments for small diameter tubes. Air and water were injected at the mixer, located in front of the test section, which had inner diameters of either 1, 2.4, or 4.9 mm. The major difference of the flow patterns in a small diameter tube compared to the patterns in a large tube was that no stratified and wavy flow was observed. The slug and churn flow patterns occurred over their test range. Fukano and Kariyasaki reported that the flow patterns in the small diameter tubes were not severely affected by the flow direction, and that small bubbles did not exist in liquid slugs and liquid films.

Triplett *et al.* (1999) suggested a flow pattern map of air-water flowing in 1.1 and 1.49 mm hydraulic diameter tubes for both circular and semi-triangular microchannels. They concluded that surface tension was dominant in a microchannel and that gas-liquid stratified flow did not occur in a microchannel. Triplett *et al.*'s experiment results were in accord with those of Fukano and Kariyasaki (1993). However, Triplett *et al.* demonstrated that a flow pattern map showed poor agreement with that for a larger diameter tube, 12.7 mm, because separated flow was not observed in the microchannel.

Yang and Shieh (2001) conducted a flow visualization experiment for air-water and R-134a in a 1 mm microchannel. The microchannel tended to keep bubbles retaining their circular shapes. It also tended to keep a liquid holdup between the tube walls in a way that retarded the transition from slug flow to annular flow. They concluded that, in small tubes, in addition to the buoyant force and turbulent fluctuations, the surface tension force was also an important parameter for flow pattern determination.

Another flow pattern study in the microchannel was accomplished by Nino *et al.* (2002). Flow patterns and void fraction for multi-port microchannel tubes, which were 1.54 mm and 1.02 mm in diameter, were investigated. By using a trapping method for two-phase fluid, they measured the void fraction of R-134a and R-410A in ranges of mass fluxes from 100 to 300 kg/m²s. When the quality and mass flux increased, their observations showed that the refrigerant distribution became uniform in all channels with an annular flow regime.

Two-phase flow patterns for CO₂ in microchannel were observed by Pettersen (2003). Compared to small diameter observations with air/water at low pressure, the transition from intermittent into annular flow occurred at a much lower superficial vapor velocity for CO₂ because the kinetic energy of the vapor flow is higher at a given velocity due to the higher vapor density of CO₂. At a mass flux of 100 kg/m²s, the flow regime changed from intermittent to annular flow as the vapor quality was increased. He reported that flow, in annular flow observations, was quite unstable and flow pattern transition lines are uncertain due to limited number of data points.

Although flow visualization in the microchannel was not conducted in this study, the flow patterns were assumed to be predictable based on other research. Figure 7.1 shows flow pattern maps for a small hydraulic diameter tube. These maps were developed by Yang and Shieh (2001) and Pettersen (2003), and the flow pattern of CO₂/oil mixture discussed in this thesis is plotted on the dotted area at the lower edge of the map. Based on flow pattern map by Yang and Shieh (2001), intermittent flow such as a plug or slug flow pattern was to be expected in the evaporator due to the combined effect of low refrigerant velocity and the more dominant surface tension in small

hydraulic diameter tube. An intermittent flow is a series of individual large bubbles that form and carry liquid film or slug. On the other hand, flow pattern in the microchannel is expected to be intermittent to annular flow with the increase of gas velocity based on the flow pattern map by Pettersen (2003). Although they do not give exact answer for what kind of flow pattern for CO₂/oil mixture is expected in microchannel, the flow pattern of the CO₂/oil mixture is expected to be an intermittent flow or annular flow with unstable flow. Since it is not simple to analytically calculate the oil retention in the microchannel tube, using a void fraction model can be an alternative method to predict the oil retention in heat exchangers. The detailed discussion of several void fraction models to predict oil retention in heat exchangers is presented in section 7.2.4.

7.2.2 Oil Retention in the Header

The evaporator used in the current experiment and simulation consists of horizontal microchannel tubes and vertical headers, as shown in Figure 7.2. Since the oil can be retained both in microchannel tubes and headers, the header effect should be accounted for calculating the oil retention in the evaporator. In order to calculate the oil retention in the header of the evaporator, it was assumed that the refrigerant and oil flows are uniformly distributed for each microchannel tube. As a result, both flow rates linearly decrease at the inlet header and increase at the outlet header in the direction of flow. The oil volume retained in the inlet header of the evaporator is ignored because the oil is mixed with a large amount of liquid CO₂ and also because the CO₂/oil mixture flows vertically downward. On the other hand, in the outlet header, an oil return problem might occur because the oil film must overcome gravity in order to be carried by the superheated refrigerant.

It is noted that for the vertical upward flow at the outlet header the refrigerant flow rate is taken to be quite small at the lower part of the outlet header because of the assumption that the refrigerant and oil flows are uniformly distributed. This means that the refrigerant velocity may not high enough to carry the oil film vertically upward in the header. To determine whether the oil transport is sufficient or failed, the critical refrigerant mass flow rate was introduced (Mehendale, 1998). The critical refrigerant mass flow rate for the vertical upward flow is defined as the minimum flow rate to carry the oil film vertically upward. Whenever the refrigerant mass flow rate is lower than the critical refrigerant mass flow rate, the net pressure force is insufficient to balance the weight of the fluids, and the oil immediately adjacent to the wall is presumed to start flowing in a downward direction.

In order to calculate the oil retention in the outlet header, the header was divided into 22 segments, the same number of microchannel tubes previously described in Table 3.1. The temperature and pressure are assumed to be kept constant. The refrigerant and oil flow rates at each segment are determined by the summation of the flow rate from the microchannel and from the previous segment, as shown in Figure 7.3. The local critical refrigerant mass flow rate was calculated at each segment and was compared to the refrigerant mass flow rate. If the local refrigerant mass flow rate was less than the critical refrigerant mass flow rate, it was then assumed that the oil film failed to be transported by the refrigerant and was trapped in that segment. For the segment where the oil was not carried vertically upward, it was assumed that oil filled an entire segment. Otherwise, under the given flow rates and properties, the oil film thickness was calculated from the

annular flow model with the consideration of gravity. Then, total oil retention in the outlet header was calculated by integrating the oil amount for each segment.

The gas cooler consists of horizontal microchannel tubes with vertical inlet and outlet headers as shown in Figure 7.4. However, similar to the procedure used in the simulation for the inlet header of the evaporator, the header effect was ignored in the gas cooler simulation because the CO₂/oil mixture flows vertically downward in both inlet and outlet headers resulting in vertical downward flow of the CO₂/oil mixture. Therefore, oil is supposed to be retained only in the microchannel tubes.

7.2.3 Oil Retention in Microchannel Tubes

For the oil retention simulation in the microchannel, the microchannel was divided into segments such that all segments had the same refrigerant side heat transfer rate. Figure 7.5 shows the oil retention modeling at each segment in the evaporator and gas cooler. The oil retention volume ratio was calculated from the liquid fraction, $(1 - \mathbf{a})$, the length of the corresponding segment, and oil volume charged initially, as shown in Equation (7-1). The oil fraction parameter, F_i , is defined as the ratio of the mass flow rate of the oil to the mass flow rate of the liquid phase, as shown in Equation (7-1). For two-phase CO₂ with the oil region in the evaporator, the oil fraction parameter, F_i , increases as the vapor quality (x_g) increases. This results in a small liquid CO₂ flow rate at a fixed oil flow rate. In both evaporator, where the superheated CO₂ with oil region exists, and gas cooler, the oil fraction parameter, F_i , can be 1.

$$OilRetentionVolumeRatio = \left(\sum_{i=1}^n A \cdot L_i \cdot (1 - \mathbf{a}_i) \cdot F_i \right) \cdot \frac{1}{V_{ini}}$$

where
$$F_i = \frac{\dot{m}_{o,i}}{\dot{m}_{o,i} + \dot{m}_{r,i}} \quad (7-1)$$

- L : length of segment [m]
 A : microchannel cross sectional area [m²]
 a : void fraction
 n : number of segments
 V_{ini} : oil volume charged initially [m³]

In order to calculate the oil retention in the microchannel, several assumptions were made as follows:

- The heat transfer rate (\dot{Q}_i) at each segment is the same.
- The length of each segment (L_i) is determined depending on the heat transfer area.
- For the evaporator, the liquid phase of CO₂ and oil are homogeneously mixed and act as a single phase. Therefore, the liquid properties for CO₂/oil mixture are calculated based on the mixing rule. This assumption is reasonable in that separated flow is hardly ever observed in the microchannel, based on literature reviews (Fukano and Kariyasaki, 1993 and Triplett *et al.*, 1999).
- The vapor quality at each segment of the evaporator increases linearly in the direction of flow.
- The temperature at each segment of the gas cooler decreases linearly in the direction of flow.

From the above assumptions, the length of each segment, L_i , was calculated based on the following equations (7-2) and (7-3).

$$\dot{Q} = \sum_{i=1}^n (UA)_i T_{LMTD,i}$$

$$\dot{Q} = \dot{m}_r \Delta h \quad (7-2)$$

$$\left(\frac{1}{UA} \right)_i = \left(\frac{1}{HTC_r A_r} + \frac{1}{HTC_a A_a} + R \dots \right) \frac{1}{L_i} \quad (7-3)$$

where

- \dot{Q} : heat transfer rate [kW]
- A_r, A_a : refrigerant or air side heat transfer area for unit length [m²/m]
- U : overall heat transfer coefficient [kW/m²K]
- HTC_r, HTC_a : refrigerant or air side heat transfer coefficient [kW/m²K]
- L_i : length of segment [m]
- R : thermal resistance for conduction or fouling per unit length [m/(kW/K)]
- T_{LMTD} : log mean temperature difference [K]

The total heat transfer rate is calculated by the summation of heat transfer rates at each segment. This summation is the multiplication of the UA value and log mean temperature difference (T_{LMTD}) as shown in the Equation (7-3). The evaporation heat transfer coefficient of CO₂ was estimated from the test results for the microchannel shown by Zhao *et al.* (2001). On the other hand, the heat transfer coefficient of the gas cooler was calculated by using the Gnielinski's (1976) correlation. As a result, the length of each segment in the microchannel of heat exchanger was obtained from Equation (7-3). Oil and CO₂ properties at the corresponding segment were calculated based on the temperature and pressure or vapor quality.

In the oil retention model for the evaporator, the vapor quality effect should be considered. After the end of evaporation, the temperature starts to increase. As a result,

the evaporator can be expected to have two major sections, one consisting of a two-phase CO₂ with oil region and another region of superheated CO₂ with oil. In the superheated region of the evaporator, the oil retention was calculated by the oil fraction (1- α) at each segment as is discussed in section 7.2.4. For this region, the temperature glide was considered. The oil retention in the gas cooler was calculated in the same way as for the superheated region at the evaporator. The total oil retention in the gas cooler was obtained by the summation of the oil retention at each segment. The oil retentions in the microchannel tubes of the evaporator and the gas cooler are explained in detail in the next sections.

7.2.4 Void Fraction Models

Void fraction, a , is defined as the ratio of the area occupied by vapor phase to the inner cross sectional area of the tube. It has been used to determine the refrigerant charge amount in air-conditioning systems. A void fraction model can be also used to estimate oil retention volume since the liquid fraction including the oil is simply obtained as 1- a . Therefore, the oil retention volume in heat exchangers is calculated by various void fraction models. The void fraction is generally represented as the function of mass quality, x , as shown in Equation (7-4) and various properties.

$$x = \frac{\dot{m}_{r,g}}{\dot{m}_{r,g} + \dot{m}_{r,l} + \dot{m}_o} \quad (7-4)$$

where $\dot{m}_{r,g}$: gas CO₂ mass flow rate [kg/s]

$\dot{m}_{r,l}$: liquid CO₂ mass flow rate [kg/s]

\dot{m}_o : oil mass flow rate [kg/s]

The various void fraction models by Coddington (2002), Casciaro (2001), Rice (1987), and Butterworth (1975) are summarized and classified into categories in the next paragraphs.

Slip Ratio Correlated Model

The slip ratio correlated void fraction assumes that there is a velocity difference between the two phases. The slip ratio, S , is defined as the velocity ratio of vapor velocity to liquid velocity:

$$\mathbf{a} = \frac{1}{1 + S \left(\frac{1-x}{x} \right) \left(\frac{\mathbf{r}_g}{\mathbf{r}_l} \right)} \quad (7-5)$$

where x : mass quality
 S : slip ratio

Zivi (1964) developed the slip ratio as a function of density ratio of the two phases such as $S = \left(\frac{\mathbf{r}_g}{\mathbf{r}_l} \right)^{-1/3}$. This relation was developed for annular flow under the assumption of zero liquid entrainment. However, viscosity effects on the void fraction are not accounted for in Zivi's model.

Homogeneous Model

A homogeneous model for two-phase flow gives the void fraction in Equation (7-6). The void fraction by the homogeneous model is obtained simply by assuming no slip between two phases, as the two-phase is assumed to be a homogeneous mixture.

Therefore, the velocity slip between two phases is 1, which means the liquid and vapor phases travel together at a common velocity.

$$\mathbf{a} = \frac{1}{1 + \left(\frac{1-x}{x} \right) \left(\frac{\mathbf{r}_g}{\mathbf{r}_l} \right)} \quad (7-6)$$

Martinelli's Parameter Correlated Model

Martinelli's parameter, X_{tt} , (Lockhart and Martinelli, 1949) in Equation (7-7) gives a measure of the degree to which the two-phase mixture behaves as a liquid rather than as a gas. Martinelli's empirical void fraction as a function of Martinelli's parameter is represented in Equation (7-8).

$$X_{tt} = \left(\frac{1-x}{x} \right)^{0.9} \left(\frac{\mathbf{r}_g}{\mathbf{r}_l} \right)^{0.5} \left(\frac{\mathbf{m}_l}{\mathbf{m}_g} \right)^{0.1} \quad (7-7)$$

$$\mathbf{a} = \left(1 + X_{tt}^{0.8} \right)^{-0.378} \quad (7-8)$$

Mass Flux Dependent Model

Premoli *et al.* (1971) developed an empirical correlation of the void fraction by using slip ratio in terms of the Reynolds number and Weber number as seen in the following expressions.

The slip ratio, S , is calculated by

$$S = 1 + B_1 \left[\frac{y}{1 + yB_2} - yB_2 \right]^{1/2} \quad (7-9)$$

where

$$y = \frac{\mathbf{b}}{1 - \mathbf{b}} \quad (7-10)$$

and β is the gas to total volume flow ratio given by

$$\mathbf{b} = \frac{1}{1 + \left(\frac{x}{1-x} \right) \left(\frac{\mathbf{r}_l}{\mathbf{r}_g} \right)} \quad (7-11)$$

The parameters B_1 and B_2 are given by

$$B_1 = 1.578 \cdot Re_l^{-0.19} \left(\frac{\mathbf{r}_l}{\mathbf{r}_g} \right)^{0.22}$$

$$B_2 = 0.0273 \cdot We Re_l^{-0.51} \left(\frac{\mathbf{r}_l}{\mathbf{r}_g} \right)^{-0.08} \quad (7-12)$$

where

$$Re_l = \frac{D \cdot G}{\mathbf{m}_f}$$

$$We = \frac{D \cdot G^2}{\mathbf{s} \cdot \mathbf{r}_l} \quad (7-13)$$

Another empirical correlation for the void fraction that considers the effect of mass flux was developed by Hughmark (1962). Although the void fraction model was developed for vertical upward flow with air-liquid mixtures near atmospheric pressure, Hughmark reported that the correlation was found to be applicable for horizontal flow, for high pressure, and for other flow regimes. The void fraction is given by a correction factor, K_H , to the homogeneous model as follows:

$$\mathbf{a} = \frac{K_H}{1 + \left(\frac{1-x}{x} \right) \left(\frac{\mathbf{r}_g}{\mathbf{r}_l} \right)} \quad (7-14)$$

where $K_H = f(z)$.

“z” is dependent on the Reynolds number, the Froude number, and the liquid volume fraction.

$$z = Re_a^{1/6} Fr^{1/8} y_l^{-1/4} \quad (7-15)$$

where

$$Re_a = \frac{G \cdot D}{\mathbf{m}_f + \mathbf{a}(\mathbf{m}_g - \mathbf{m}_l)} \quad (7-16)$$

$$Fr = \frac{1}{gD} \left(\frac{G \cdot x}{\mathbf{b} \mathbf{r}_g} \right)^2 \quad (7-17)$$

$$y_L = 1 - \mathbf{b} \quad (7-18)$$

Although the void fraction models described above were originally developed for an air-water mixture or vapor-liquid of the refrigerant, in the current study, such void fraction correlations were used in the oil retention volume ratio estimation. In this paper, the simulation results by using those five void fraction correlations were compared with experimental results for the evaporator and the gas cooler.

7.2.5 Sensitivity to Number of Segments

The sensitivity to the number of segments in the evaporator and gas cooler was investigated by conducting calculations with varying numbers of segments from 10 to 100. In these calculations, Hughmark's (1962) and Premoli's (1971) void fraction models for the evaporator and gas cooler, respectively, were used because simulation result by using those two void fraction models shows better agreement with experimental result. The detailed discussion for the comparison result is presented in section 7.3.2 and 7.4.2 for the evaporator and gas cooler, respectively. The result of sensitivity on the number of segments is shown in Figure 7.6. The oil retention in the evaporator was not so sensitive to the number of segments; thus, the number of segments was set to be at 20 when the changes in oil retention were less than 0.1%. On the other hand, the oil retention in the gas cooler was very sensitive to the number of segments because of the fast changes of the properties during the gas cooling process. The number of segments for the gas cooler was then set to be 60 when the changes in the oil retention were less than 0.5%.

7.3 Simulation Results for the Evaporator

For the evaporator, oil can be retained in the header as well as in the microchannel tubes as mentioned in section 7.2. In the present section, oil retentions in the microchannel and header were investigated based on the given experiment condition. Then, several void fraction models were tested with experimental results. With the best of the void fraction models, various parameters affecting oil retention in the evaporator were examined.

7.3.1 Oil Retention in the Evaporator

During the evaporating process, vapor quality increases which results in property changes for oil and CO₂. The oil retention distribution in the microchannel evaporator is affected by their property changes. The oil retention volume ratio in the microchannel of the evaporator is shown in Figure 7.7. The oil retention volume ratio of primary y-axis in left hand side was calculated with respect to dimensionless length of the evaporator. The secondary y-axis in right hand side shows vapor quality and liquid CO₂ fraction out of liquid phase. The refrigerant mass flux of the evaporator was 135 kg/m²s and the oil circulation ratio was 5 wt.% with inlet vapor quality, 0.49. Vapor quality increased with the progress of evaporation until it ended in the 18th segment, and then the vapor was superheated in the last two segments shown as a blank area in Figure 7.7. Within the dimensionless length of 0.6, the oil fraction in the total liquid phase consisting of liquid CO₂ and oil was less than 0.25, so the local liquid viscosity, mostly governed by viscosity of the liquid CO₂, was relatively low. This explains the smaller oil retention in the two-phase region. With further evaporation, the oil retention significantly increased due to the fact that the local liquid viscosity was almost the same as that of the pure oil. When the two-phase evaporation process was over, the oil retention reached its maximum. Therefore, it is concluded that most of the oil is retained at the end part of the evaporator. As the portion of the superheated and high vapor quality area increases, the oil retention in the evaporator increases.

7.3.2 Verification of Model

As mentioned in previous section 7.2.2, some amount of oil can be retained in the vertical header of the evaporator. The simulation result for oil retention volume ratio in

the evaporator header with respect to the oil circulation ratio is shown in Figure 7.8. The oil retention volume ratio in the header was about constant regardless of the oil circulation ratio. If the refrigerant gas velocity was not enough to carry an oil film in the lower part of header due to the low refrigerant flow rate, the oil failed to be carried and then began to be trapped in the lower part of the header. However, the relatively higher refrigerant flow rate at the upper part of the outlet header kept carrying the oil in a thin film. As mentioned in section 7.2.2, the critical refrigerant mass flow rate plays an important role in understanding oil retention behavior in the vertical outlet header. As shown in (a) of Figure 7.8, the oil retention volume ratio in the outlet header of the evaporator is 0.03 and 0.04 corresponding to refrigerant mass flux of the evaporator, 125 and 70 kg/m²s, respectively. For example, as can be seen in (b) of the Figure 7.8, 73% to 94% of total oil retained in the outlet header accumulated in the lower part at the refrigerant mass flux, 75 kg/m²s. This means that the oil retention in the upper part of outlet header was negligible compared to the oil retention in the lower part of outlet header. To reduce the oil retention at the header, the smaller size header is recommended. In this way, the oil film can be carried by the high velocity refrigerant in the vertical upward flow.

Experimental oil retention volume ratio and five sets of calculated oil retention volume ratio from void fraction models, which were discussed in section 7.2.4, are compared. Since the experimental result was obtained when the oil was injected at the evaporator inlet, it includes the oil retention volume ratio at the evaporator and the suction line. Thus, the calculated oil retention volume ratio includes three parts: the suction line, evaporator outlet header, and microchannel tubes. The oil retention volume

ratio in the suction line is calculated by using the analytical model as described in section 6.2 while the oil retention volume ratio in the microchannel tubes is calculated using various void fraction models.

For the comparison of these void fraction models, the criteria used are the average deviation ($s_{average}$) and the standard deviation ($s_{standard}$), which is a measure of the scatter of errors defined in Equation (7-19). The results of these deviations of the various void fraction models are summarized in Table 7.1.

Two void fraction models, one by Hughmark (1962) and the other by Premoli *et al.* (1971), which are dependent on the flow rate of CO₂, predict well the oil retention volume ratio in the evaporator. The standard deviations of oil retention volume ratio using the Hughmark's (1962) and Premoli *et al.*'s (1971) void fraction models are 11% and 14%, respectively, which are the smallest values of all void fraction models. Among void fraction models, the Hughmark's (1962) model shows the best agreement with the experimental results. This result can be also seen from Figure 7.9. Most of the simulated results are within $\pm 20\%$ of the experimental results.

The other void fraction models are independent of the refrigerant flow rate and under-predict the oil retention volume ratio for the high oil retention region, where a lower refrigerant flow rate is to be expected. On the other hand, at lower oil retention regions, these void fraction models show good agreement with experimental results. It seems that those void fraction models that are independent on the gas flow rate can be applied only to higher flow rates. By adapting the Hughmark's (1962) void fraction model, parametric studies affecting the oil retention at the microchannel tubes of the evaporator were examined as seen in the next section, starting at 7.3.3.

Table 7.1 Average and Standard Deviations of Oil Retention in the Evaporator

Void Fraction Model	Average Deviation (%)	Standard Deviation (%)
Hughmark (1962)	5	11
Premoli <i>et al.</i> (1971)	10	14
Lockhart-Martinelli (1949)	21	24
Zivi (1963)	23	27
Homogeneous	25	28

$$e_{error} = \left(\frac{ORVR_{exp} - ORVR_{cal}}{ORVR_{cal}} \right) \times 100$$

$$s_{average} = \frac{1}{n} \sum e_{error}$$

$$s_{standard} = \sqrt{\frac{\sum e_{error}^2}{n}} \quad (7-2)$$

where $ORVR$: Oil Retention Volume Ratio
 n : number of samples

7.3.3 The Effects of Superheating in the Evaporator Outlet

The effects of superheating at the evaporator outlet on the oil retention are shown in Figure 7.10. The inlet vapor quality is assumed to be constant, 0.5, in both cases shown in the same figure. Superheating at the evaporator outlet is shown for two temperatures of 5 K and 15 K. For higher superheating at the evaporator outlet, since the evaporation process then ends faster than for the other case, the remaining part of the evaporator occupied by the oil and vapor CO₂, the so-called superheated region, is relatively large. Oil tends to be retained more in the superheated region because the local liquid film

viscosity is higher than in the region where the evaporation process still occurs. As a result, more oil is retained with an increase of the superheating region in the evaporator.

7.3.4 The Effects of Inlet Vapor Quality of the Evaporator

The effects of inlet vapor quality at the evaporator on the oil retention were investigated. The oil retention volume ratio in the microchannel tubes of the evaporator was calculated for two different inlet vapor qualities, 0.4 and 0.65, while the evaporator pressure and superheating at the evaporator outlet were kept at 4 MPa and 0 K, respectively. As shown in Figure 7.11, lower inlet vapor quality results in low oil retention volume ratio. This is because a larger amount of liquid CO₂, which is mixed with oil and reduces the oil viscosity more than for the other case, exists at the lower inlet vapor quality. In the case of the higher inlet vapor quality, 0.65, the higher quality region is dominant, so more oil is retained due to the higher liquid phase viscosity. Therefore, keeping a lower inlet vapor quality is the key to minimize the oil retention in the evaporator.

Based on both the results of the superheating effect and the inlet vapor quality effect upon the oil retention in the microchannel tubes, the worst case of the oil retention in the evaporator is when inlet vapor quality is high and the vapor is largely superheated at the evaporator outlet. Thus, less superheating at the outlet of evaporator and lower vapor inlet quality are preferable in order to minimize oil retention in the evaporator.

7.4 Simulation Results for the Gas Cooler

In this section, oil retention in the microchannel tubes of the gas cooler is investigated. Then, several void fraction models are tested with experimental results similar to the procedure already discussed for the evaporator modeling. Parametric studies on oil retention in the gas cooler are discussed in this section.

7.4.1 Oil Retention in the Gas Cooler

The flow characteristics in the gas cooler are different from those in the evaporator because CO₂ phase change does not occur in the gas cooler but does occur in the evaporator. Instead of phase change, a much larger temperature change occurs in the gas cooler than in the evaporator. Properties of oil and refrigerant varied significantly while undergoing the gas cooling process and are responsible for the oil retention in the gas cooler.

Refrigerant temperature and oil retention distributions with respect to dimensionless length of the gas cooler are shown in Figure 7.12. Each data point in Figure 7.12 represents the mean refrigerant temperature and oil retention volume ratio corresponding to each segment. Since the specific heat of CO₂ considerably increases as the critical point is approached where the gas cooler outlet is located, the refrigerant temperature decreases by only 2.5 K at the dimensionless length between 0.6 and 1. On the other hand, during the first half of the gas cooler calculations the refrigerant temperature significantly decreases by 46 K. From this temperature distribution in the gas cooler calculations, relatively higher oil viscosity is to be expected at the second half of the gas cooler.

Oil retention distribution in the gas cooler side is also shown in the same figure. Total oil retention volume ratio for refrigerant mass flux, $157 \text{ kg/m}^2\text{s}$ at the gas cooler, at 1 wt.% of oil circulation ratio is 0.01, which is the summation of oil retention volume ratios for the first and second half of the gas cooler, 0.004 and 0.006, respectively. The reason more oil retention occurs in the second half of the gas cooler can also be explained making use of Figure 7.13.

The oil retention volume ratio is calculated by using the Equation (7-1). The oil fraction, $(1-\alpha)$, is obtained from the void fraction model by using the refrigerant and oil properties as well as flow rates at each segment. As shown in Figure 7.13, the solid line showing the oil fraction slightly increases until about segment position of 50, and then increases very rapidly till the end. This sharp increase is caused by parameters such as the refrigerant density and oil viscosity.

Normally, the higher gas density in two-phase flow results in a thicker liquid film at a given refrigerant flow rate because the velocity of the vapor flow decreases. The refrigerant density increases by three times from the inlet to the outlet of the gas cooler. Major increase of the refrigerant density occurs at the second half of the gas cooler, especially at last few segments. The oil viscosity is another factor determining the oil fraction in the gas cooler. Generally, higher oil viscosity results in a higher oil fraction. The oil viscosity increases from inlet to outlet of the gas cooler because of the large temperature drop during the gas cooling process. Because of these reasons, the oil fraction is significantly increased at the end of the gas cooler.

The length of the segment, the dotted line in Figure 7.13, is determined by the heat transfer rate. Since, in the modeling of the gas cooler, the heat transfer rate of each

segment is assumed to be constant, the length of the segment until segment position 40 is very short due to the higher log mean temperature difference between the refrigerant and air temperature. As the refrigerant temperature approaches the air inlet temperature at the end of gas cooler, the length of segment becomes longer. The length of the segment dramatically increases after the segment position of 50. Therefore, the combination effects of the oil fraction and length of segment result in higher oil retention close to the end of the gas cooling.

7.4.2 Verification of Model

In a manner similar to the evaporator modeling, various void fraction models were used to calculate the oil retention in the gas cooler, and then simulation results were compared to experimental results. The oil retention volume ratio in the gas cooler was experimentally obtained by injecting oil at the gas cooler inlet and extracting it at the oil extractor located in the suction line. Since the experimental oil retention volume ratio includes the oil volume retained in the suction line, evaporator, and gas cooler, the oil retention volume ratio in the simulation was also separately calculated for the suction line, evaporator and gas cooler. The oil retention volume ratio in the suction line and in the evaporator was calculated by using the analytical model discussed in section 6.2, and the Hughmark's (1969) void fraction, respectively.

The experimental oil retention volume ratio for the gas cooler was compared with calculated oil retention volume ratio by using five sets of void fraction models. The average and standard deviations of oil retention volume ratio in the gas cooler are summarized in the Table 7.2. Except the Hughmark's void fraction model, standard deviations of simulation results by using other void fraction models were bounded 18 to

21%. This is because the velocity slip between oil and supercritical CO₂ decreases due to higher CO₂ density. Among those void fraction models, the Premoli *et al.* (1971) model shows the best agreement. This result can be shown in Figure 7.14. Simulation results using Premoli's void fraction model are bounded by nearly $\pm 20\%$ using experimental results. Therefore, by using the Premoli *et al.* (1971) void fraction model, parametric studies for the gas cooler were further investigated.

Table 7.2 Average and Standard Deviations of Oil Retention in the Gas cooler

Void Fraction Model	Average Deviation (%)	Standard Deviation (%)
Premoli <i>et al.</i> (1971)	15	18
Hughmark (1962)	32	38
Lockhart-Martinelli (1949)	17	19
Zivi (1963)	18	20
Homogeneous	19	21

Figure 7.15 shows a comparison of the oil retention volume ratio between measured and calculated in the suction line, evaporator, and gas cooler. In this graph, the best void fraction models, Hughmark's (1962) and Premoli's *et al.* (1971), were used to estimate the oil retention in the evaporator and gas cooler, respectively. Most calculated oil retention volume ratio results are bounded by $\pm 20\%$ from experimental results.

7.4.3 The Effects of Approach Temperature

The approach temperature is defined as the difference between the refrigerant temperature at the gas outlet and air inlet temperature. The approach temperature affects the oil retention volume ratio in the gas cooler. As shown in Figure 7.16, the calculated oil retention volume at 1 K of the approach temperature is larger than that at 6 K. This is

because the low temperature at the gas cooler outlet results in higher oil viscosity and higher CO₂ density.

7.4.4 The Effects of Gas Cooling Pressure

The gas cooling pressure effect on the oil retention volume ratio in the gas cooler is shown in Figure 7.17 for two different conditions; one is for 9.0 MPa and 100 °C at the gas cooler inlet, and the other is for 7.6 MPa and 80 °C at the gas cooler inlet. The approach temperature was kept at 5 K in all cases. As mentioned in section 7.4.1, the oil retention volume ratio at the first half of the gas cooler is minimal compared to the oil retention volume ratio in the second half. The conditions of the gas cooler outlet, such as the oil viscosity and CO₂ density, are important factors of the oil retention in the gas cooler.

Even though the higher refrigerant temperature, 100 °C with 9.0 MPa, at the inlet of the gas cooler, results in low oil viscosity, high oil retention occurs at the gas cooler. This is because the higher gas cooling pressure, 9.0 MPa, results in the higher CO₂ density, which is twice higher than the CO₂ density at 7.6 MPa for the same temperature at the end of the gas cooler. In this case, as a result of the higher CO₂ density, more oil is retained at the gas cooler due to the low CO₂ velocity. Therefore, higher gas cooling pressure is not recommended with regard to the oil retention in the gas cooler.

7.5 Conclusions

In the case of the heat exchangers, i.e. evaporators and gas coolers, void fraction models were used to estimate oil retention. Due to the property changes, the heat

exchangers were divided into several segments that had the same heat transfer rate. Then, the oil retention in the heat exchangers was obtained using the oil fraction and the length of corresponding segments. The number of segments was set at 20 and 60 for the evaporator and gas cooler, respectively, based on a sensitivity study of the number of segments. In the evaporator, the high quality and superheated region were responsible for the oil retention due to the higher liquid film viscosity. In the gas cooler, most of the oil was retained at the second half of the gas cooler because of the higher oil viscosity and CO₂ density.

- The void fraction models, Hughmark (1962) and Premoli *et al.* (1971), show good agreement with experimental results for oil retention at the evaporator and the gas cooler, respectively.
- Simulation results at the evaporator and the gas cooler are bounded by \pm 20% of experimental results.
- A small size of outlet header in the evaporator is recommended to enhance the high refrigerant velocity in order to carry an oil film vertically upward.
- Higher superheating at the evaporator outlet results in higher oil retention. Oil tends to be retained more in the superheated region because of the higher local liquid film viscosity.
- Low inlet vapor quality is preferable to reduce the oil retention in the evaporator because the larger amount of liquid CO₂ mixed with oil reduces the oil viscosity than the other case.
- A low approach temperature at the end of the gas cooler results in more oil retention because of the oil viscosity and CO₂ density.

- High gas cooling pressure causes high oil retention in the gas cooler due to higher CO₂ density.

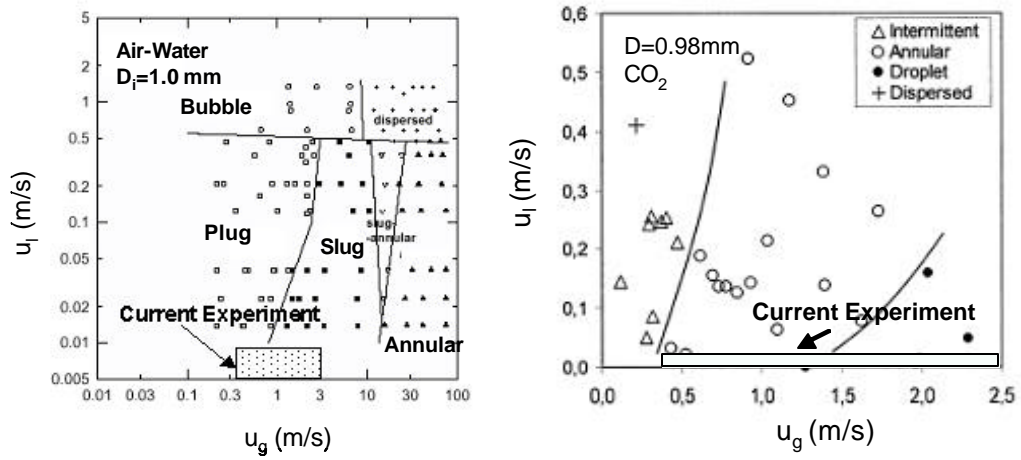


Figure 7.1 Flow Pattern Map for Two -Phase Flow in Microchannel

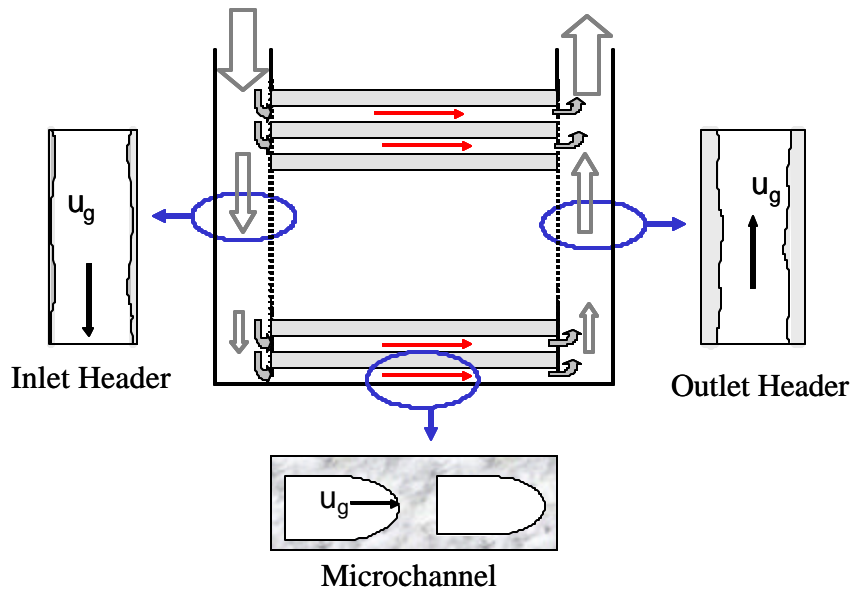


Figure 7.2 CO₂/Oil Mixture Flows in the Evaporator

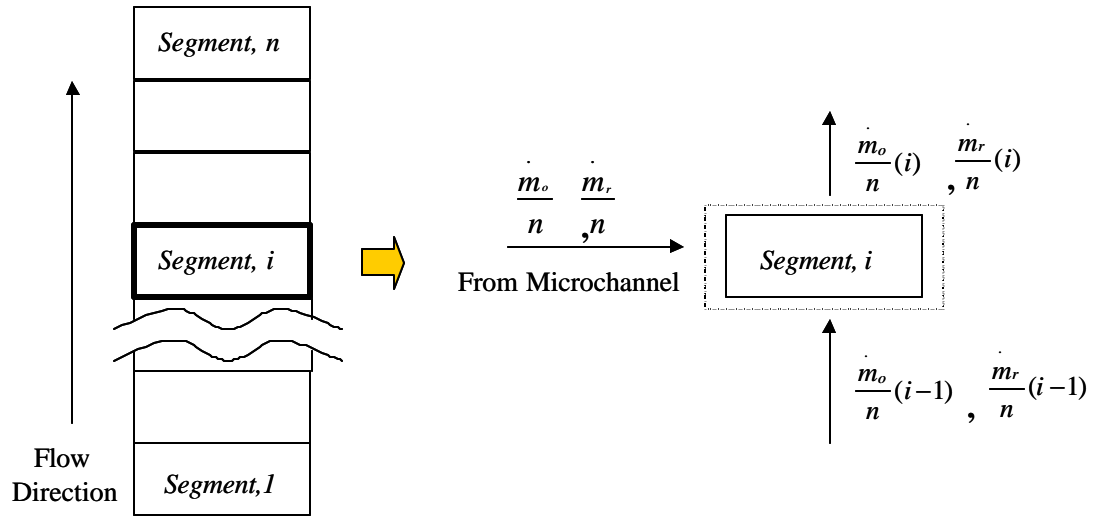


Figure 7.3 Modeling of Oil Retention in Outlet Header of the Evaporator

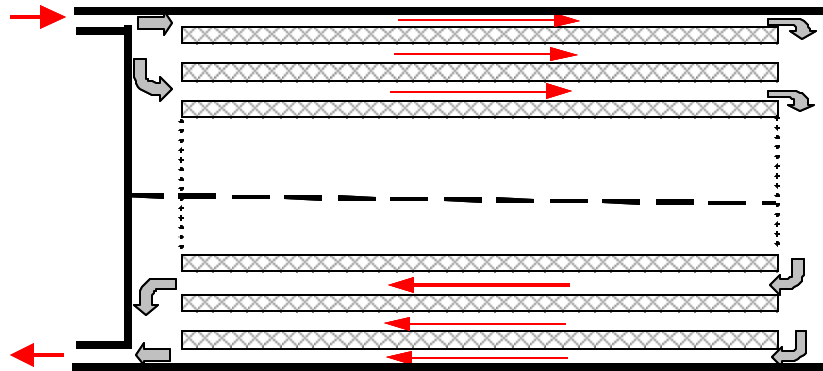


Figure 7.4 CO₂/Oil Mixture Flows in the Gas Cooler

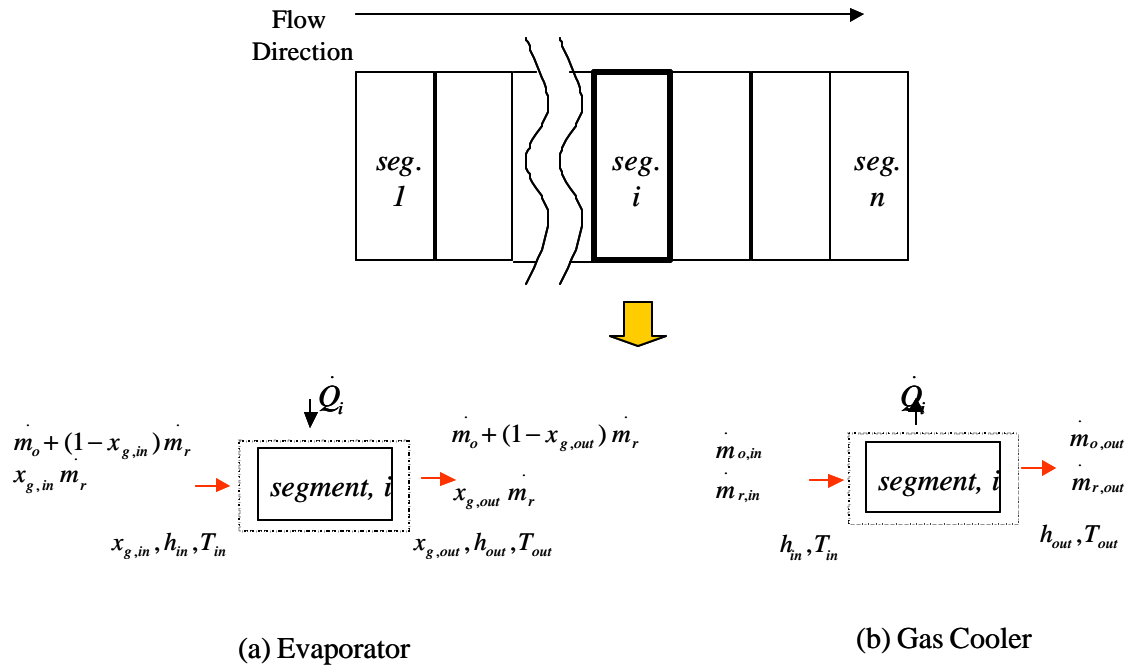


Figure 7.5 Modeling of Oil Retention in a Microchannel of Heat Exchangers

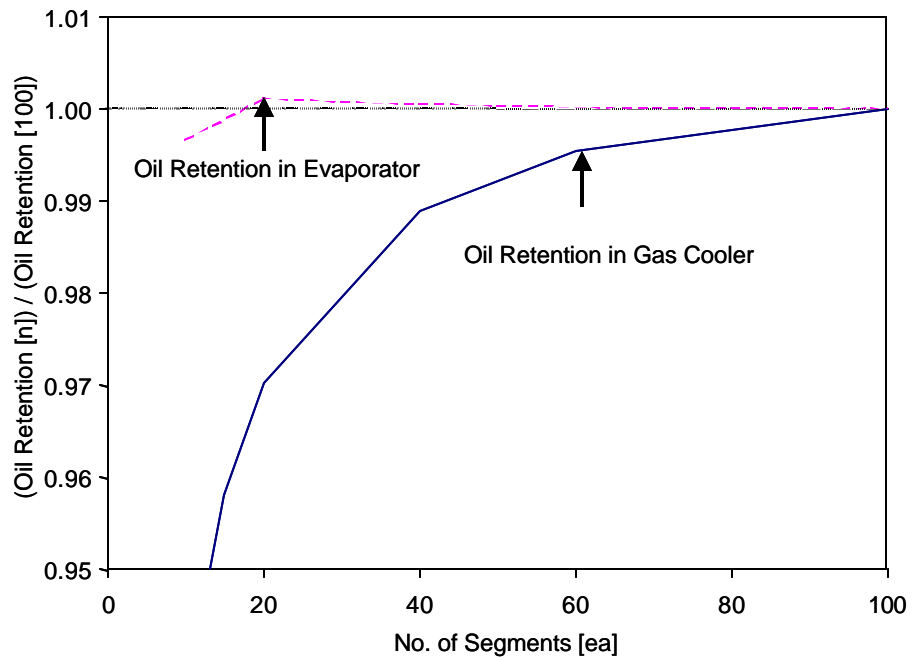


Figure 7.6 Sensitivity to Number of Segments to Oil Retention

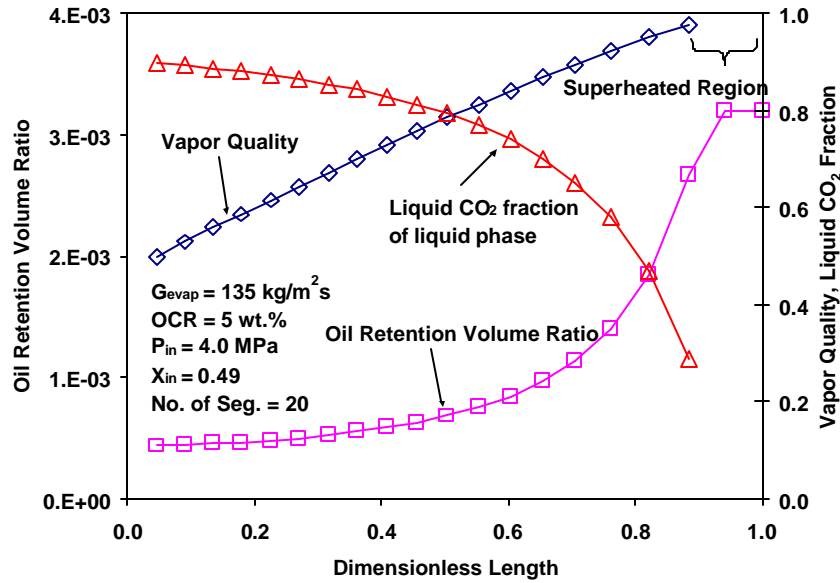


Figure 7.7 Calculated Oil Retention Volume Ratio and Vapor Quality in the Evaporator

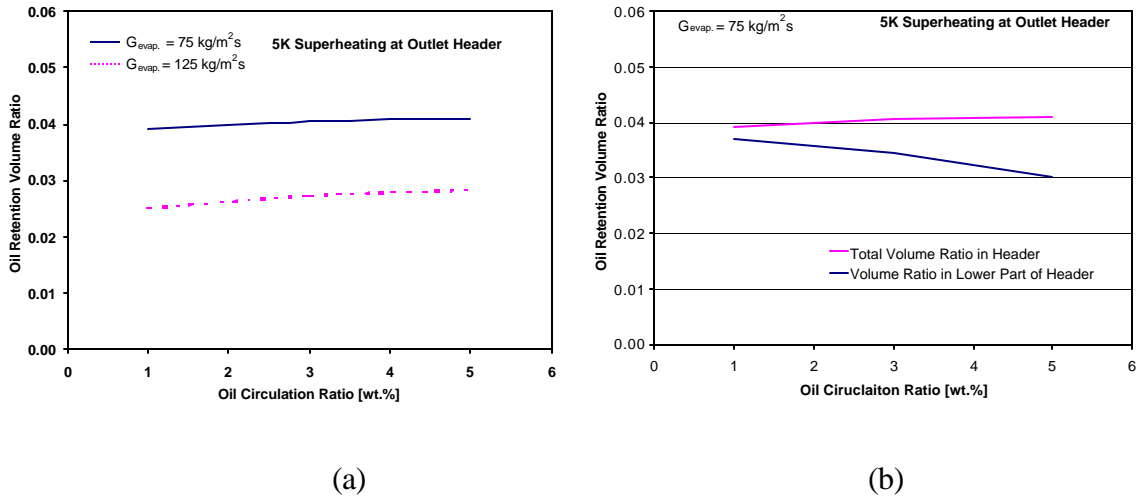
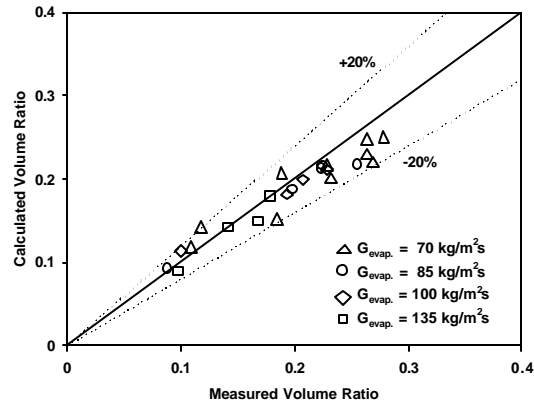
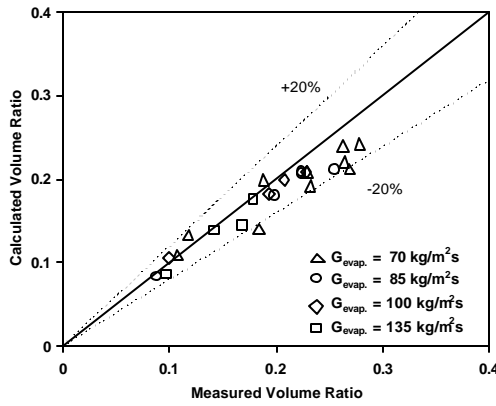


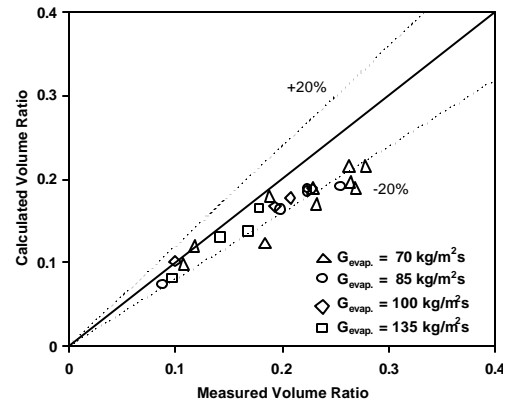
Figure 7.8 Calculated Oil Retention Volume Ratio in the Evaporator Header



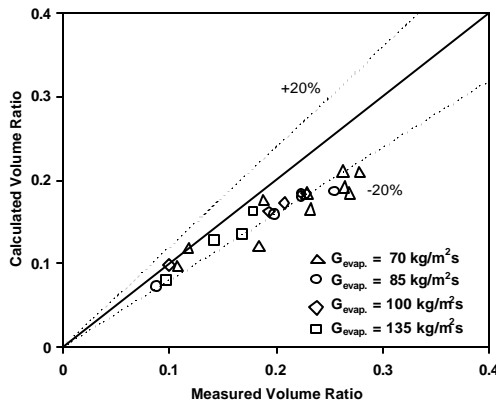
(a)



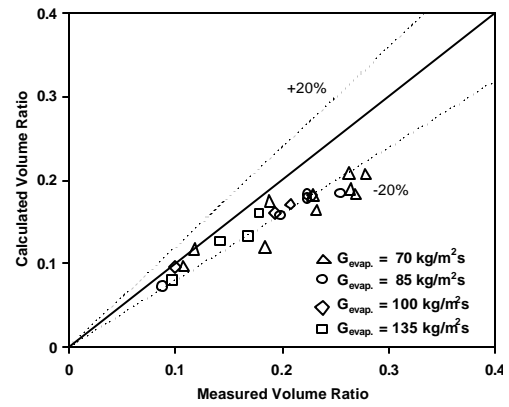
(b)



(c)



(d)



(e)

Figure 7.9 Volume Ratios in the Evaporator using Various Void Fraction Models

(a) Hughmark (1962)

(b) Premoli *et al.* (1971)

(c) Lockhart-Martinelli (1949)

(d) Zivi (1963)

(e) Homogeneous

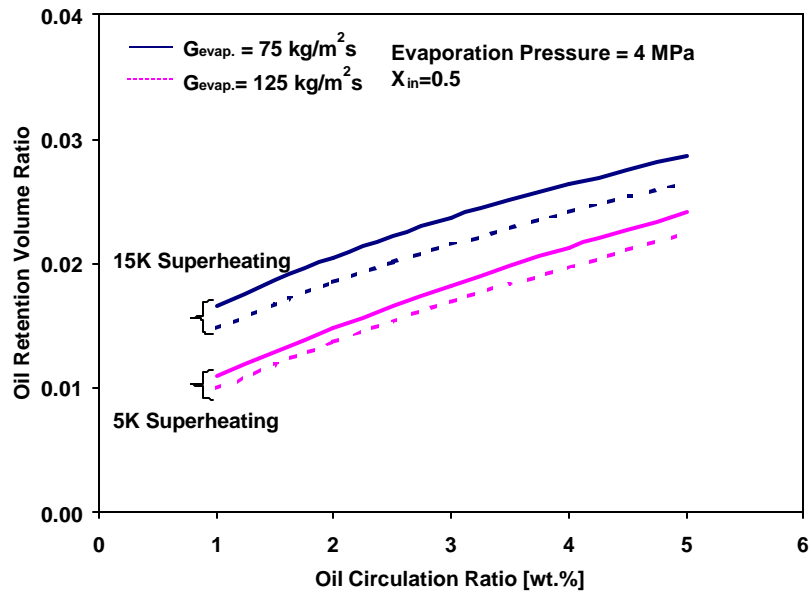


Figure 7.10 Effects of Superheating in the Evaporator Outlet

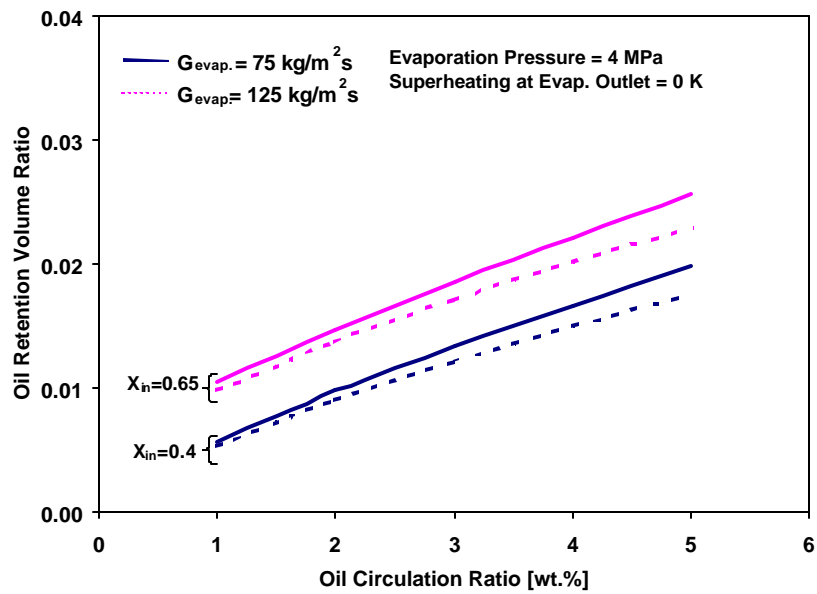


Figure 7.11 Effects of Vapor Inlet Quality in the Evaporator

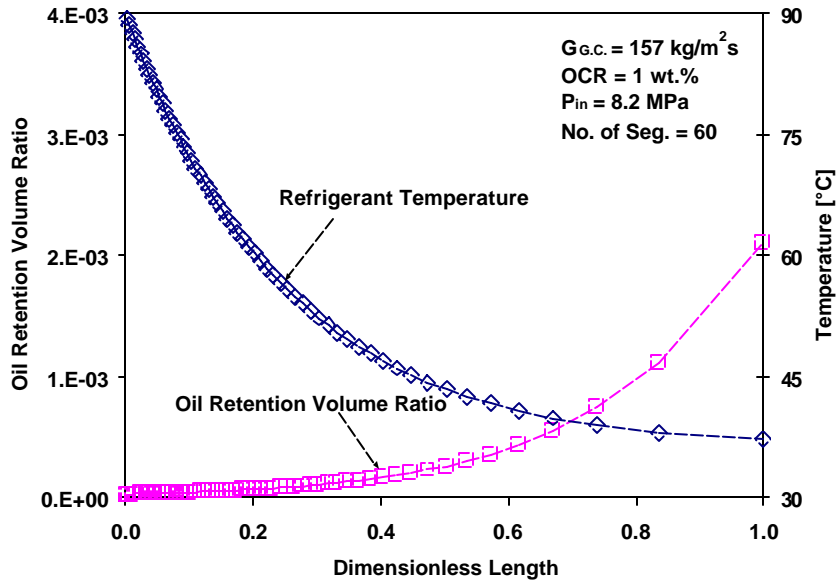


Figure 7.12 Calculated Oil Retention Volume Ratio and Temperature in the Gas Cooler

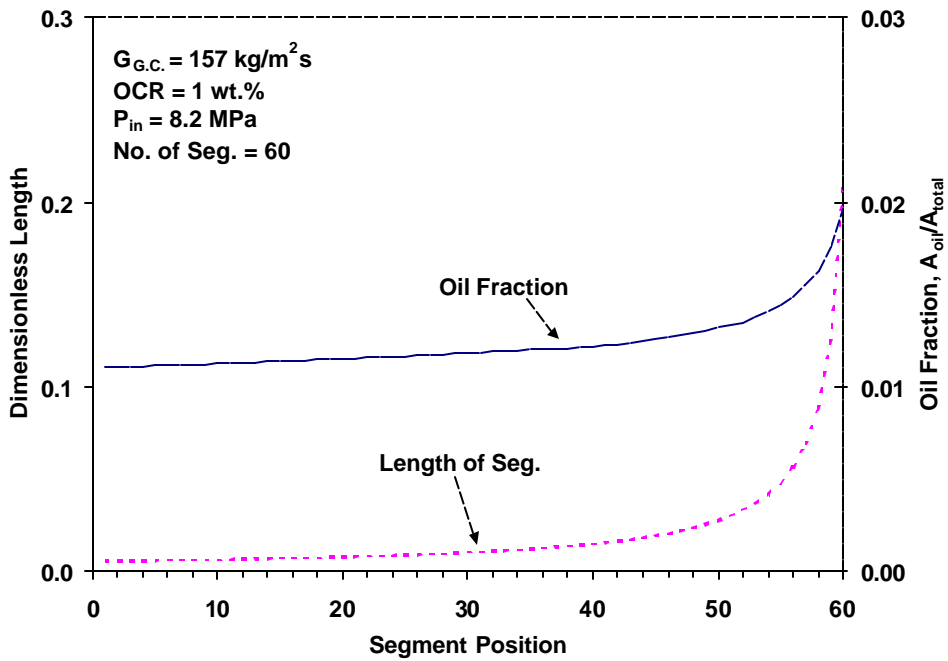
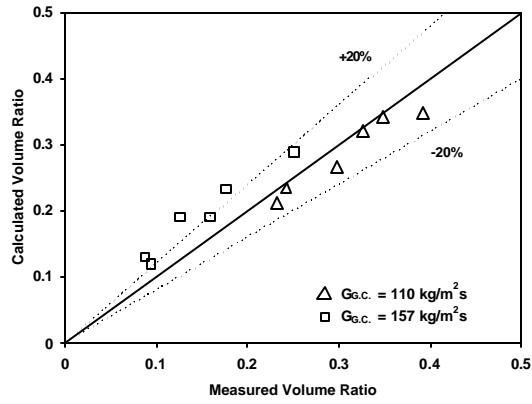
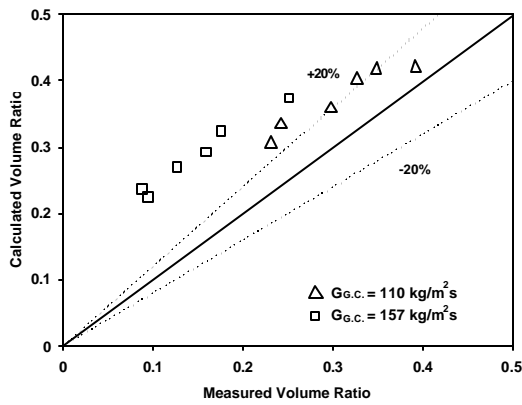


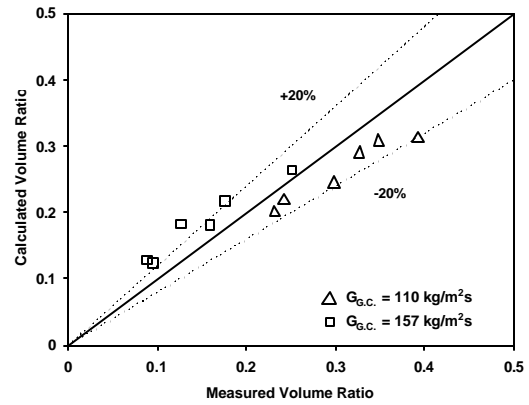
Figure 7.13 Calculated Length of Segment and Oil Fraction in the Gas Cooler



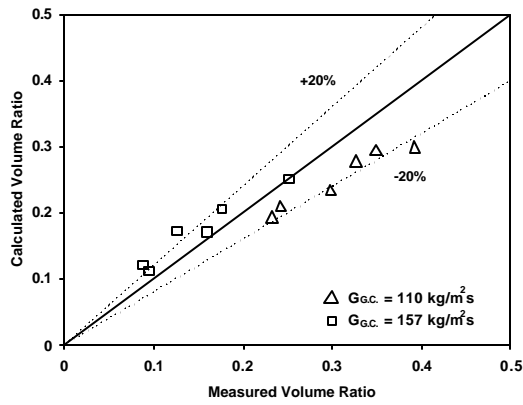
(a)



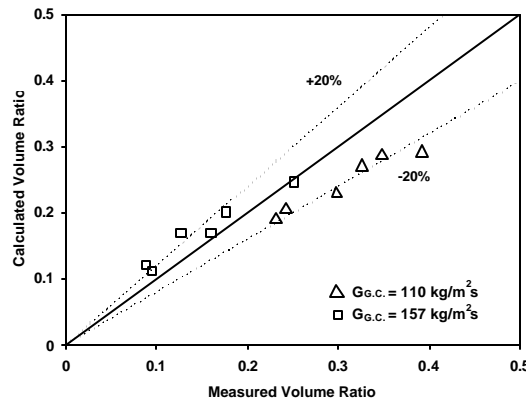
(b)



(c)



(d)



(e)

Figure 7.14 Volume Ratio in the Gas Cooler using Various Void Fraction Models

(a) Premoli *et al.* (1971)

(b) Hughmark (1962)

(c) Lockhart-Martinelli (1949)

(d) Zivi (1963)

(e) Homogeneous

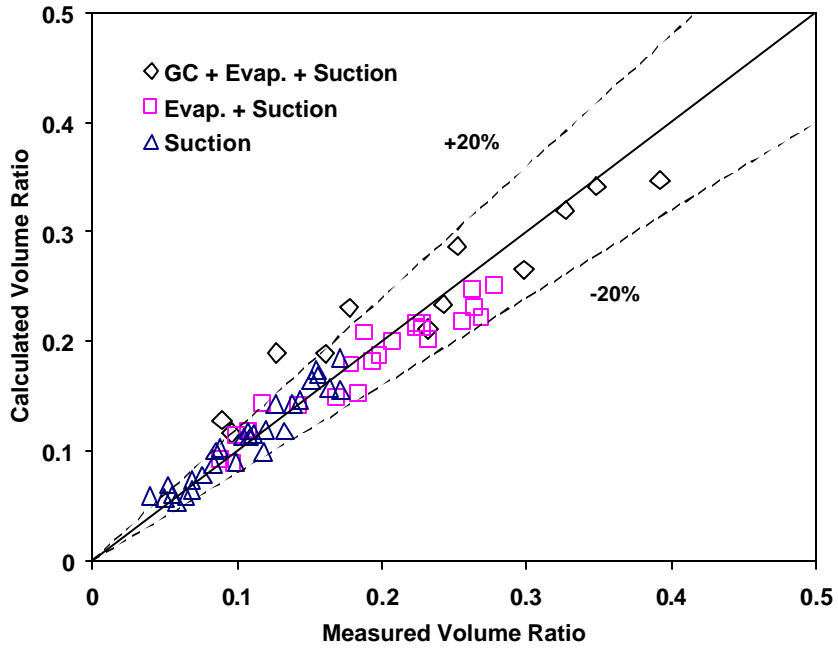


Figure 7.15 Calculated and Measured Oil Retention Volume Ratio in System

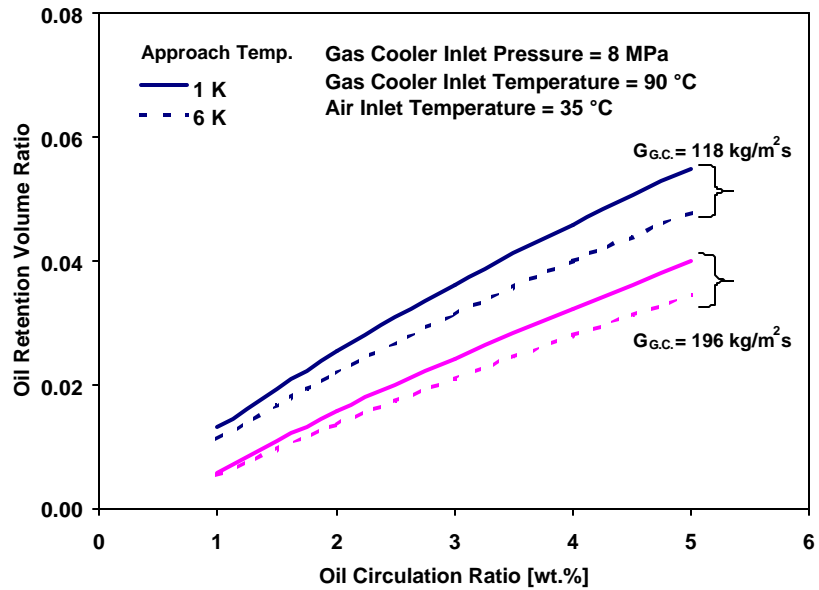


Figure 7.16 Effects of Approach Temperature in the Gas Cooler

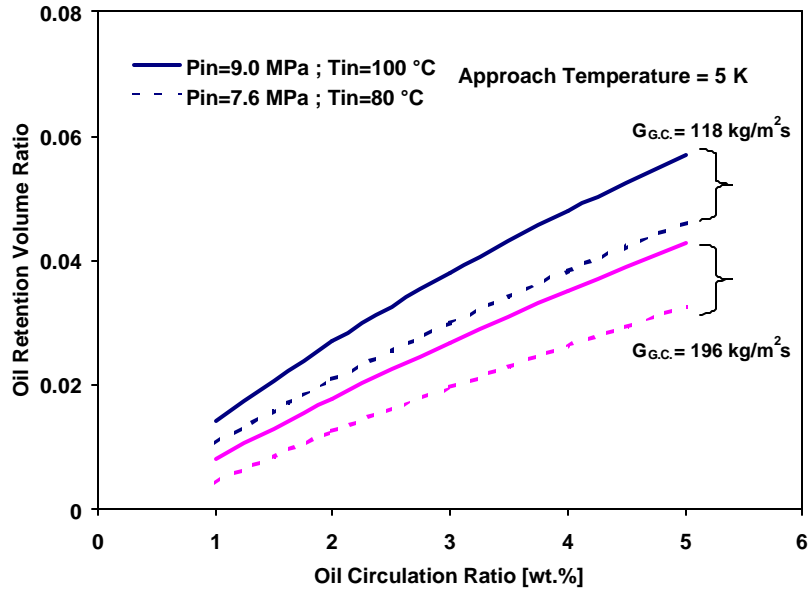


Figure 7.17 Effects of Gas Cooling Pressure

CHAPTER 8 Conclusions and Design Recommendations

The objective of this dissertation is to develop and use methods to experimentally and theoretically clarify the oil retention behavior in CO₂ air-conditioning systems and to provide the recommendations for the suction line and all other heat exchangers to minimize oil retention. This was accomplished with newly developed experimental method and simulations. In this chapter, conclusions of this dissertation are summarized in the order of the experiment and simulation works.

8.1 Conclusions from Experimental Research

8.1.1 Development of an Experimental Facility

An oil injection-extraction method was developed to measure the oil retention within each cycle component. Four different refrigerant mass fluxes, 290, 352, 414, and 559 kg/m²s at the suction line, were tested to examine the effect of the mass flux on oil retention volume ratio. The indoor and outdoor temperatures, where the evaporator and gas cooler would be operated, were set to 27°C and 36.1°C, respectively, while the humidity was fixed around 40% RH in all tests. The test facility for the oil retention was built with two main loops: a refrigeration loop and an oil loop. The refrigeration loop consisted mainly of a compressor driven by an electric motor, a gas cooler, a manual expansion valve, and an evaporator. The oil loop consisted of a gear pump, a mass flow meter, an oil extractor, an oil accumulator, and an oil reservoir. A separate oil loop was installed to serve the following two purposes: injection of the oil to the test section at the

desired oil circulation ratio as well as extraction of the oil from the test section and measuring the oil amount extracted.

8.1.2 Experimental Results

The experimental test results for the oil retention of different system components including the suction line, the evaporator, and the gas cooler are summarized as follows.

- As the oil circulation ratio increases, the oil retention volume in the heat exchanger and suction line also increases.
- For the refrigerant mass flux, $290 \text{ kg/m}^2\text{s}$ at the suction line, the oil retention volume ratio in the evaporator is around 0.09 to 0.11 for 1 to 5 wt.% of oil circulation ratio.
- For the higher refrigerant mass flux, $559 \text{ kg/m}^2\text{s}$ at the suction line, 0.04 to 0.06 of the oil retention volume ratio is obtained in the evaporator for 1 to 5 wt.% of oil circulation ratio. In the higher refrigerant mass flux, the oil retention in the suction line is not significant.
- The oil retention volume ratio in the gas cooler is less than 0.05 of the total oil amount charged initially.
- The oil retention in the gas cooler is quite small because of high CO_2 density, low oil viscosity, and low oil surface tension.
- Higher inlet vapor quality results in higher oil retention in the evaporator.
- 16% and 10% of the total oil amount charged initially is retained in heat exchangers at 5 wt.% of oil circulation ratio for the refrigerant mass fluxes, $290 \text{ kg/m}^2\text{s}$ and $414 \text{ kg/m}^2\text{s}$, respectively. The oil retention in heat

exchangers is noticeable amount. Therefore this behavior should be accounted for.

- The oil distribution in the CO₂ air-conditioning systems was experimentally analyzed.
- For the higher refrigerant mass flux, less oil volume is retained in the heat exchangers and this also results in a lower pressure drop penalty factor.
- The effect of oil on pressure drop was found to be most significant at high vapor qualities and superheat region where the local oil mass fractions are the highest.

8.2 Conclusions from the Modeling Efforts

8.2.1 Modeling of Oil Retention in the Suction Line and Heat Exchangers

An analytical model to estimate the oil retention in the suction line was developed while assuming an annular flow regime. In this analysis of CO₂ and oil flow in the suction line, the interfacial friction factor was expressed as a function of the CO₂ gas Reynolds number as well as the dimensionless oil film thickness. In the case of heat exchangers, void fraction models were used to estimate the oil retention. Due to property changes during the phase change, the heat exchangers were divided into several segments and the oil retention in the heat exchangers was obtained with the oil fraction and the length of corresponding segment.

8.2.2 Modeling Results

The analytical model was validated with experimental results, and parametric studies were conducted in the suction line and heat exchangers. Modeling results are summarized as follows:

- Most simulation results in the suction line are bounded by $\pm 20\%$ from experimental results.
- The simulation results using the void fraction models by Hughmark (1962) and Premoli *et al.* (1971) are bounded by $\pm 20\%$ with experimental results of oil retention in the evaporator and the gas cooler.
- The oil retention decreases with the increase of solubility because the CO₂/oil mixture viscosity reduces as the CO₂ solubility increases.
- For the design of a suction line, the tube size should be carefully considered while balancing the effect of a refrigerant pressure drop and the oil retention.
- Higher superheating at the suction line causes less oil retention than lower superheating.
- High superheating at the evaporator outlet results in high oil retention. Oil tends to be retained more in the superheated region because the local liquid film viscosity is higher than in other regions.
- Low inlet vapor quality is preferable to reduce the oil retention in the evaporator because reduced oil viscosity can be used.
- In the gas cooler, most oil is retained at the second half of the gas cooler since it reduces the average liquid viscosity.

- Low approach temperature at the end of the gas cooler and high gas cooling pressure result in higher oil retention because of the oil viscosity and CO₂ density.

8.3 Recommended Design Guidelines

Based on the understanding on oil retention behavior in CO₂ air-conditioning systems, recommendations for design guidelines for suction line and heat exchangers to minimize oil retentions are proposed as follows.

8.3.1 Suction line

To minimize the oil retention in the suction line, first of all, a high refrigerant flow rate is required to enhance the refrigerant drag force exerted on the oil. Other recommendations to minimize the oil retention are summarized as follows:

- Total length of the suction line should be short.
- Higher suction line temperature is recommended.
- Using an oil that has higher CO₂ solubility is recommended.
- A small diameter tube in the suction line is recommended while balancing the pressure drop penalty.

8.3.2 Heat Exchangers

The header design is important in minimizing the oil retention in the heat exchangers. Recommendations suggested for the heat exchangers are as follows:

- ❑ Upward flow in the vertical header should be avoided. Otherwise, a small outlet header is recommended to enhance the high refrigerant velocity to carry oil film vertically upward.
- ❑ To prevent oil trapping at the vertical header, it is recommended that the exit port be installed at the lower part of the header in case of the vertical header as shown in (a) and (b) of Figure 8.1.
- ❑ Vertical downward flow in the microchannel tubes with horizontal headers as shown in (c) of Figure 8.1 is recommended.
- ❑ In the evaporator, low vapor quality at the evaporator inlet and low superheating at the evaporator outlet are recommended.
- ❑ In the gas cooler, higher gas cooling pressure is not recommended.

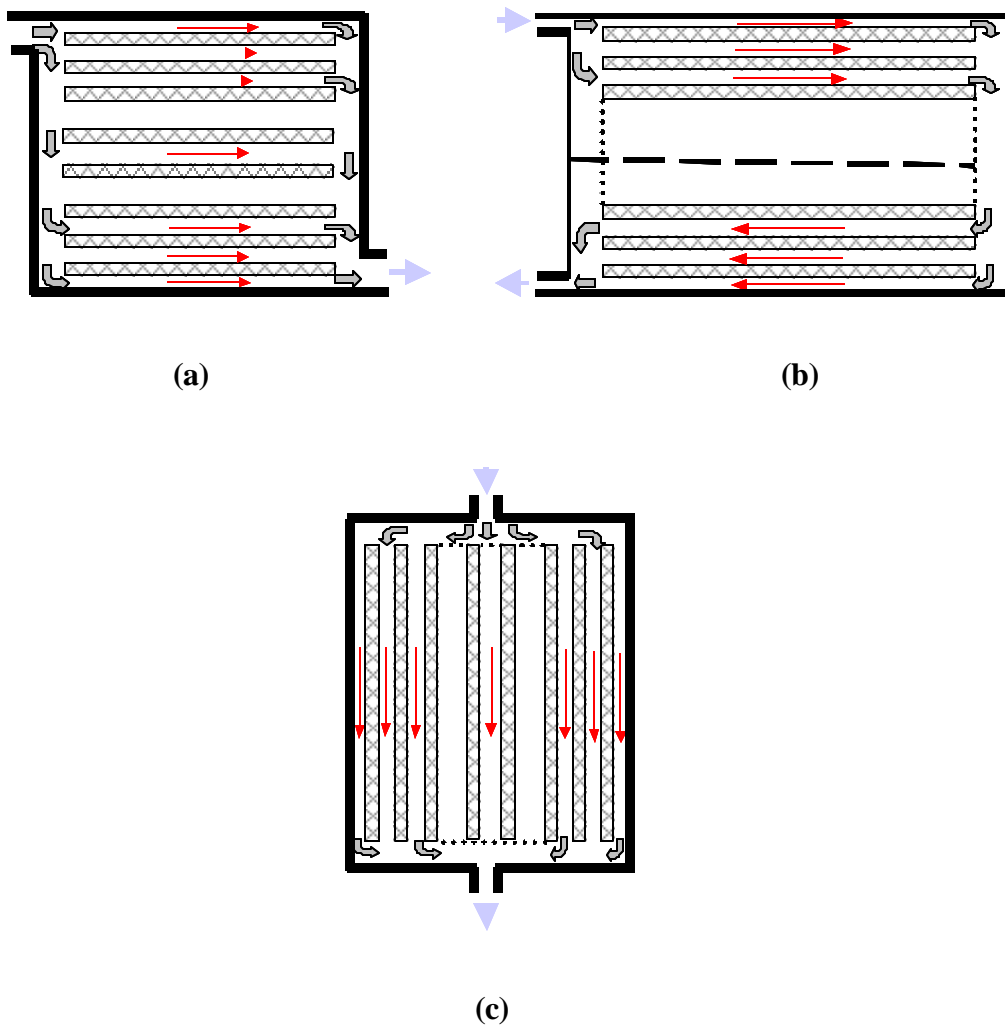


Figure 8.1 Proposed Designs of Heat Exchangers

CHAPTER 9 Future Work

This study has investigated oil retention in CO₂ air-conditioning systems. However, this study is only the beginning step towards understanding oil behavior in other refrigeration and air-conditioning systems. Suggested future works below are to provide better understanding of oil behavior so that the system can be designed properly.

- ❑ Investigation of oil retention characteristics in CO₂ refrigeration systems that have low temperature levels.
- ❑ Experimental work on oil retention with different types of oil such as POE, PAO, or MO.
- ❑ Investigation of oil migration during the transient mode.
- ❑ Investigation of oil retention with respect to the shape or flow direction of microchannel tubes and headers.
- ❑ Improvement of simulation tools to predict oil retention.
- ❑ Flow visualization of refrigerant /oil mixture in a microchannel heat exchanger.
- ❑ Investigation of header effect of heat exchangers on oil retention.
- ❑ Experimental work on oil retention in HFC refrigerants.

Appendix A Summary of Oil Retention Tests

Table A.1 Oil Injection at the Evaporator Outlet

Test Number	1	2	3	4	5
Injection Port	Evaporator outlet	Evaporator outlet	Evaporator outlet	Evaporator outlet	Evaporator outlet
Ref. MFR (g/s)	13.6	13.4	13.5	13.5	13.5
Oil MFR (g/s)	0.09	0.10	0.11	0.17	0.26
OCR (wt. %)	0.6	0.7	0.8	1.3	1.9
$P_{\text{gas cooler inlet}}$ (MPa)	7.8	7.7	7.8	7.8	7.8
$P_{\text{evap. inlet}}$ (MPa)	3.9	3.9	4.0	4.0	3.9
$T_{\text{gas cooler inlet}}$ (°C)	75.8	75.0	75.1	75.2	75.2
$T_{\text{gas cooler outlet}}$ (°C)	36.3	36.3	36.1	36.2	36.4
$T_{\text{evap. outlet}}$ (°C)	14.8	14.8	15.4	15.4	15.2
T_{suction} (°C)	15.5	15.4	16.0	16.0	15.8
$X_{\text{inlet vapor}}$	0.8	0.8	0.8	0.8	0.8
Oil Retention (ml)	14.5	16.1	13.7	18.9	29.5

Table A.1 Oil Injection at the Evaporator Outlet (Continued)

Test Number	6	7	8	9	10
Injection Port	Evaporator outlet	Evaporator outlet	Evaporator outlet	Evaporator outlet	Evaporator outlet
Ref. MFR (g/s)	13.6	13.6	13.6	13.5	13.4
Oil MFR (g/s)	0.36	0.57	0.60	0.74	0.83
OCR (wt. %)	2.6	4.0	4.3	5.2	5.8
$P_{\text{gas cooler inlet}}$ (MPa)	7.8	7.8	7.7	7.7	7.7
$P_{\text{evap. inlet}}$ (MPa)	3.9	4.0	3.9	3.9	3.9
$T_{\text{gas cooler inlet}}$ (°C)	75.5	75.3	75.2	75.4	75.9
$T_{\text{gas cooler outlet}}$ (°C)	36.2	36.2	36.2	36.2	36.4
$T_{\text{evap. outlet}}$ (°C)	15.3	15.9	14.7	16.4	17.8
T_{suction} (°C)	15.9	16.4	15.4	16.8	17.9
$X_{\text{inlet vapor}}$	0.8	0.8	0.8	0.8	0.8
Oil Retention (ml)	33.1	35.9	42.9	37.8	38.9

Table A.1 Oil Injection at the Evaporator Outlet (Continued)

Test Number	11	12	13	14	15
Injection Port	Evaporator outlet	Evaporator outlet	Evaporator outlet	Evaporator outlet	Evaporator outlet
Ref. MFR (g/s)	13.5	13.5	17.1	17.0	16.7
Oil MFR (g/s)	0.86	0.98	0.21	0.38	0.47
OCR (wt. %)	5.9	6.8	1.3	2.2	2.7
$P_{\text{gas cooler inlet}}$ (MPa)	7.7	7.7	8.2	8.3	8.1
$P_{\text{evap. inlet}}$ (MPa)	3.9	3.9	4.0	4.0	3.9
$T_{\text{gas cooler inlet}}$ (°C)	75.6	75.2	85.9	86.5	86.1
$T_{\text{gas cooler outlet}}$ (°C)	36.3	36.2	37.3	37.1	36.7
$T_{\text{evap. outlet}}$ (°C)	17.2	17.0	13.1	12.7	13.3
T_{suction} (°C)	17.4	17.2	13.5	13.1	13.6
$X_{\text{inlet vapor}}$	0.8	0.8	0.7	0.7	0.7
Oil Retention (ml)	38.7	42.7	13.0	21.2	26.1

Table A.1 Oil Injection at the Evaporator Outlet (Continued)

Test Number	16	17	18	19	20
Injection Port	Evaporator outlet	Evaporator outlet	Evaporator outlet	Evaporator outlet	Evaporator outlet
Ref. MFR (g/s)	17.0	17.0	17.0	20.4	20.6
Oil MFR (g/s)	0.54	0.80	1.10	0.23	0.33
OCR (wt. %)	3.1	4.5	6.3	1.1	1.6
$P_{\text{gas cooler inlet}}$ (MPa)	8.2	8.2	8.1	8.7	8.7
$P_{\text{evap. inlet}}$ (MPa)	4.0	4.0	3.9	3.9	3.9
$T_{\text{gas cooler inlet}}$ (°C)	86.7	86.5	86.4	91.0	89.2
$T_{\text{gas cooler outlet}}$ (°C)	37.1	37.0	36.9	39.2	39.2
$T_{\text{evap. outlet}}$ (°C)	13.4	13.7	16.0	12.0	11.8
T_{suction} (°C)	13.7	13.9	16.0	12.4	12.4
$X_{\text{inlet vapor}}$	0.7	0.7	0.7	0.6	0.6
Oil Retention (ml)	26.8	31.6	40.9	9.9	17.2

Table A.1 Oil Injection at the Evaporator Outlet (Continued)

Test Number	21	22	23	24	25
Injection Port	Evaporator outlet	Evaporator outlet	Evaporator outlet	Evaporator outlet	Evaporator outlet
Ref. MFR (g/s)	20.9	20.7	20.2	20.5	27.4
Oil MFR (g/s)	0.65	0.74	0.80	1.17	0.44
OCR (wt. %)	3.0	3.5	3.8	5.4	1.6
$P_{\text{gas cooler inlet}}$ (MPa)	8.8	9.0	8.7	9.0	9.2
$P_{\text{evap. inlet}}$ (MPa)	4.0	4.0	3.9	4.0	3.9
$T_{\text{gas cooler inlet}}$ (°C)	89.4	92.3	90.5	91.0	100.1
$T_{\text{gas cooler outlet}}$ (°C)	39.4	40.4	39.0	40.1	38.1
$T_{\text{evap. outlet}}$ (°C)	12.7	12.6	12.9	13.0	9.7
T_{suction} (°C)	12.9	12.7	13.1	13.0	9.9
$X_{\text{inlet vapor}}$	0.6	0.6	0.6	0.6	0.5
Oil Retention (ml)	22.0	27.1	29.9	34.5	17.2

Table A.1 Oil Injection at the Evaporator Outlet (Continued)

Test Number	26	27	28	29	30
Injection Port	Evaporator outlet	Evaporator outlet	Evaporator outlet	Evap.outlet (w/ SLHX)	Evap.outlet (w/ SLHX)
Ref. MFR (g/s)	27.2	26.9	26.7	13.7	14.0
Oil MFR (g/s)	0.75	0.78	1.19	0.10	0.32
OCR (wt. %)	2.7	2.8	4.3	0.7	2.3
$P_{\text{gas cooler inlet}}$ (MPa)	9.2	9.2	9.2	7.7	7.7
$P_{\text{evap. inlet}}$ (MPa)	3.8	3.8	3.7	3.9	4.0
$T_{\text{gas cooler inlet}}$ (°C)	100.1	100.8	100.5	88.5	88.6
$T_{\text{gas cooler outlet}}$ (°C)	38.2	38.3	38.2	35.9	36.0
$T_{\text{evap. outlet}}$ (°C)	9.4	10.1	9.9	12.6	13.1
T_{suction} (°C)	9.5	10.0	9.9	13.3	13.6
$X_{\text{inlet vapor}}$	0.5	0.5	0.5	0.7	0.7
Oil Retention (ml)	20.8	24.7	27.7	10.2	21.8

Table A.1 Oil Injection at the Evaporator Outlet (Continued)

Test Number	31	32	33	34
Injection Port	Evap.outlet (w/ SLHX)	Evap.outlet (w/ SLHX)	Evap.outlet (w/ SLHX)	Evap.outlet (w/ SLHX)
Ref. MFR (g/s)	13.3	14.4	13.9	13.5
Oil MFR (g/s)	0.35	0.48	0.60	0.69
OCR (wt. %)	2.5	3.2	4.1	4.8
$P_{\text{gas cooler inlet}}$ (MPa)	7.6	7.6	7.7	7.7
$P_{\text{evap. inlet}}$ (MPa)	3.9	4.0	4.0	3.9
$T_{\text{gas cooler inlet}}$ (°C)	85.4	85.8	86.3	86.8
$T_{\text{gas cooler outlet}}$ (°C)	35.8	35.9	35.9	36.0
$T_{\text{evap. outlet}}$ (°C)	13.8	13.9	13.9	14.3
T_{suction} (°C)	13.8	14.3	14.2	14.7
$X_{\text{inlet vapor}}$	0.7	0.7	0.7	0.7
Oil Retention (ml)	26.2	27.5	36.0	37.0

Table A.2 Oil Injection at the Evaporator Inlet

Test Number	35	36	37	38	39
Injection Port	Evaporator inlet	Evaporator inlet	Evaporator inlet	Evaporator inlet	Evaporator inlet
Ref. MFR (g/s)	13.8	13.7	13.8	13.8	13.6
Oil MFR (g/s)	0.20	0.42	0.56	0.62	0.8
OCR (wt. %)	1.4	3.0	4.1	4.3	5.6
$P_{\text{gas cooler inlet}}$ (MPa)	7.8	7.8	7.8	7.8	7.7
$P_{\text{evap. inlet}}$ (MPa)	4.0	4.0	4.0	4.0	4.0
$T_{\text{gas cooler inlet}}$ (°C)	75.1	75.1	75.3	75.0	75.0
$T_{\text{gas cooler outlet}}$ (°C)	36.4	36.2	36.5	36.1	36.1
$T_{\text{evap. outlet}}$ (°C)	15.4	15.5	15.7	15.6	15.8
T_{suction} (°C)	16.2	16.3	16.4	16.3	16.5
$X_{\text{inlet vapor}}$	0.8	0.8	0.8	0.8	0.8
Oil Retention (ml)	46.0	58.0	67.3	66.0	69.6

Table A.2 Oil Injection at the Evaporator Inlet (Continued)

Test Number	40	41	42	43	44
Injection Port	Evaporator inlet	Evaporator inlet	Evaporator inlet	Evaporator inlet	Evaporator inlet
Ref. MFR (g/s)	17.2	17.2	17.2	16.7	16.9
Oil MFR (g/s)	0.10	0.63	0.87	0.87	0.92
OCR (wt. %)	0.6	3.6	4.8	5.0	5.2
$P_{\text{gas cooler inlet}}$ (MPa)	8.3	8.2	8.2	8.1	8.1
$P_{\text{evap. inlet}}$ (MPa)	4.0	3.9	4.1	4.0	4.1
$T_{\text{gas cooler inlet}}$ (°C)	86.4	87.0	86.9	87.1	86.3
$T_{\text{gas cooler outlet}}$ (°C)	37.5	37.1	37.4	37.1	37.4
$T_{\text{evap. outlet}}$ (°C)	13.7	13.9	14.2	14.6	14.6
T_{suction} (°C)	14.3	14.5	14.7	15.0	15.0
$X_{\text{inlet vapor}}$	0.7	0.7	0.7	0.7	0.7
Oil Retention (ml)	22.1	49.6	56.0	56.1	63.9

Table A.2 Oil Injection at the Evaporator Inlet (Continued)

Test Number	45	46	47	48	49
Injection Port	Evaporator inlet	Evaporator inlet	Evaporator inlet	Evaporator inlet	Evaporator inlet
Ref. MFR (g/s)	20.6	20.3	20.3	20.2	20.6
Oil MFR (g/s)	0.3	0.50	0.92	1.07	1.30
OCR (wt. %)	1.4	2.4	4.3	5.0	5.9
$P_{\text{gas cooler inlet}}$ (MPa)	8.7	8.5	8.5	8.5	8.6
$P_{\text{evap. inlet}}$ (MPa)	4.0	4.0	4.0	4.0	4.0
$T_{\text{gas cooler inlet}}$ (°C)	90.3	89.5	90.0	89.6	89.6
$T_{\text{gas cooler outlet}}$ (°C)	39.3	38.7	38.7	38.7	39.0
$T_{\text{evap. outlet}}$ (°C)	12.4	12.4	12.7	12.9	13.2
T_{suction} (°C)	13.1	13.0	13.2	13.4	13.6
$X_{\text{inlet vapor}}$	0.6	0.6	0.6	0.6	0.6
Oil Retention (ml)	24.9	28.3	48.4	51.9	57.0

Table A.2 Oil Injection at the Evaporator Inlet (Continued)

Test Number	50	51	52	53	54
Injection Port	Evaporator inlet	Evaporator inlet	Evaporator inlet	Evaporator inlet	Evap. inlet (w/ SLHX)
Ref. MFR (g/s)	27.4	26.6	26.9	27.0	13.4
Oil MFR (g/s)	0.34	0.98	0.93	1.51	0.16
OCR (wt. %)	1.2	3.5	3.4	5.3	1.2
$P_{\text{gas cooler inlet}}$ (MPa)	9.2	9.1	9.2	9.2	7.7
$P_{\text{evap. inlet}}$ (MPa)	4.0	4.0	4.0	4.0	4.0
$T_{\text{gas cooler inlet}}$ (°C)	99.9	100.6	100.6	101.1	85.9
$T_{\text{gas cooler outlet}}$ (°C)	38.3	37.9	38.2	38.0	36.0
$T_{\text{evap. outlet}}$ (°C)	8.6	9.2	9.8	8.9	14.1
T_{suction} (°C)	9.1	9.5	10.4	9.2	14.9
$X_{\text{inlet vapor}}$	0.5	0.5	0.5	0.5	0.7
Oil Retention (ml)	24.4	42.2	35.6	44.8	29.4

Table A.2 Oil Injection at the Evaporator Inlet (Continued)

Test Number	55	56	57	58
Injection Port	Evap. inlet (w/ SLHX)	Evap. inlet (w/ SLHX)	Evap. inlet (w/ SLHX)	Evap. inlet (w/ SLHX)
Ref. MFR (g/s)	13.5	13.7	13.7	13.5
Oil MFR (g/s)	0.45	0.53	0.78	0.10
OCR (wt. %)	3.2	3.7	5.4	0.7
$P_{\text{gas cooler inlet}}$ (MPa)	7.7	7.7	7.7	7.7
$P_{\text{evap. inlet}}$ (MPa)	4.0	4.0	4.0	4.0
$T_{\text{gas cooler inlet}}$ (°C)	85.1	85.7	86.5	85.9
$T_{\text{gas cooler outlet}}$ (°C)	36.3	35.9	36.1	36.0
$T_{\text{evap. outlet}}$ (°C)	14.6	14.5	14.8	14.1
T_{suction} (°C)	15.3	15.1	15.3	14.9
$X_{\text{inlet vapor quality}}$	0.7	0.7	0.7	0.7
Oil Retention (ml)	47.1	57.2	65.8	27.0

Table A.3 Oil Injection at the Gas Cooler Inlet

Test Number	59	60	61	62	63
Injection Port	Gas Cooler inlet	Gas Cooler inlet	Gas Cooler inlet	Gas Cooler inlet	Gas Cooler inlet
Ref. MFR (g/s)	13.3	13.2	13.5	13.2	13.3
Oil MFR (g/s)	0.25	0.35	0.49	0.75	0.88
OCR (wt. %)	1.9	2.6	3.5	5.4	6.2
$P_{\text{gas cooler inlet}}$ (MPa)	7.7	7.7	7.8	7.6	7.7
$P_{\text{evap. inlet}}$ (MPa)	3.9	3.9	4.0	3.9	3.8
$T_{\text{gas cooler inlet}}$ (°C)	78.9	76.2	85.5	87.9	84.4
$T_{\text{gas cooler outlet}}$ (°C)	36.2	36.1	77.9	78.9	76.6
$T_{\text{evap. outlet}}$ (°C)	15.0	15.6	15.7	16.3	15.8
T_{suction} (°C)	16.0	16.6	16.5	16.9	16.6
Oil Retention (ml)	58.0	60.6	74.6	81.7	87.1

Table A.3 Oil Injection at the Gas Cooler Inlet (Continued)

Test Number	64	65	66	67	68
Injection Port	Gas Cooler inlet	Gas Cooler inlet	Gas Cooler inlet	Gas Cooler inlet	Gas Cooler inlet
Ref. MFR (g/s)	13.5	20.2	19.0	20.0	19.0
Oil MFR (g/s)	0.94	0.2	0.21	0.50	0.70
OCR (wt. %)	6.5	1.0	1.1	2.4	3.6
$P_{\text{gas cooler inlet}}$ (MPa)	7.7	8.2	8.6	8.7	8.3
$P_{\text{evap. inlet}}$ (MPa)	3.9	4.0	3.8	3.8	4.0
$T_{\text{gas cooler inlet}}$ (°C)	86.0	89.9	90.6	90.9	88.8
$T_{\text{gas cooler outlet}}$ (°C)	77.8	37.2	38.8	38.6	37.3
$T_{\text{evap. outlet}}$ (°C)	15.9	12.4	12.0	12.0	12.7
T_{suction} (°C)	16.6	13.0	12.7	12.7	13.1
Oil Retention (ml)	98.1	23.9	22.3	40.1	44.3

Table A.3 Oil Injection at the Gas Cooler Inlet (Continued)

Test Number	69	70
Injection Port	Gas Cooler inlet	Gas Cooler inlet
Ref. MFR (g/s)	19.0	19.0
Oil MFR (g/s)	10.6	0.48
OCR (wt. %)	5.6	2.5
$P_{\text{gas cooler inlet}}$ (MPa)	8.1	8.4
$P_{\text{evap. inlet}}$ (MPa)	3.9	4.0
$T_{\text{gas cooler inlet}}$ (°C)	90.1	90.0
$T_{\text{gas cooler outlet}}$ (°C)	36.9	37.7
$T_{\text{evap. outlet}}$ (°C)	13.3	12.7
T_{suction} (°C)	13.6	13.1
Oil Retention (ml)	63.0	31.8

References

- AHRAE Handbook and Product Directory, 1976, Systems, American Society of Heat, Refrigerating and Air Conditioning Engineers, New York, NY.
- AHRAE Handbook of Refrigeration Systems and Applications, 1994, American Society of Heat, Refrigerating and Air Conditioning Engineers, Atlanta, GA.
- Alofs, D. J. and M. M. Hassan, 1990, Influence of Oil on Pressure Drop in Refrigerant Compressor Suction Lines, *ASHRAE Transactions*, 96: 249-255.
- Beckwith, T., R.D. Marangoni, and J.H. Lienhard, 1992, *Mechanical Measurement*, 5th ed, Addison-Wesley Publishing Co., Reading, MA.
- Bharathan, D. and G. B. Wallis, 1983, Air-Water Countercurrent Annular Flow, *International Journal of Multiphase Flow*, 9(4): 349-366.
- Biancardi, F. R., H. H. Michels, T. H. Sienel, and D. R. Randy, 1996, Study of Lubrication Circulation in HVAC Systems, *The Air-Conditioning and Refrigeration Technology Institute*, ARTI MCLR Project Number 665-53100.
- Blankenberger, P. L., A. S. Miller, and T. A. Shedd, 2002, Oil Film Behavior Near the Onset of Flow Reversal in Immiscible Gas/Liquid Vertical Annular Flow, *In Proc. 9th International Refrigeration Conference at Purdue*, R12-3, Purdue University, IN.
- Butterworth, D.A., 1975, A Comparison of Some Void Fraction Relationships for Co-Current Gas-Liquid Flow, *International Journal of Multiphase Flow*, 1: 845-850.
- Casciaro, S., and J.R. Thome, 2001, Thermal Performance of Flooded Evaporators, Part 2: Review of Void Fraction, Two-Phase Pressure Drop, and Flow Pattern Studies, *ASHRAE Transactions*, 107: 919-930.
- Caverstri, R. C., J. Munk and M. Menning, 1994, Solubility, Viscosity, and Density Measurements of Refrigerant-Lubricant Mixtures- Part II: Polyalkylene Glycols with R-134a, *ASHRAE Transactions*, 100(2): 231-238.
- Coddington, R., and R. Macian, 2002, A Study of the Performance of Void Fraction Correlations Used in the Context of Drift-Flux Two-Phase Flow Models, *Nuclear Engineering and Design*, 215: 199-216.
- Collier, J.G. and J.R. Thome, 1994, *Convective Boiling and Condensation*, 3rd ed, Clarendon Press, Oxford.

- Compressor Protective Devices, Tech Tips of Oil Separators, http://www.henrytech.com/techtips_pdfs/HT-TT4.pdf, Henry Technology.
- Cooper, W. D., 1971, Influence of Oil-Refrigerant Relationship on Oil Return, *ASHRAE Symposium Bulletin*, 6-10.
- Eckels, S. J. and M. B. Pate, 1991, An Experimental Comparison of Evaporation and Condensation Heat Transfer Coefficient for HFC-134a and CFC-12, *International Journal of Refrigeration*, 14: 70-77.
- Fore, L.B., S.G. Beus, and R.C. Bauer, 2000, Interfacial Friction in Gas-Liquid Annular Flow: Analogies to Full and Transition Roughness, *International Journal of Multiphase Flow*, 26: 1755-1769.
- Fukano, T. and A. Kariyasaki, 1993, Characteristics of Gas-Liquid Two-Phase Flow in a Capillary Tube, *Nuclear Engineering and Design*, 141: 59-68.
- Fukano, T. and T. Furukawa, 1998, Prediction of the Effects of Liquid Viscosity on Interfacial Shear Stress and Frictional Pressure Drop in Vertical Upward Gas-Liquid Annular Flow, *International Journal of Multiphase Flow*, 24: 587-603.
- Fukuta, M., T. Yanagisawa, K. Sawai, and Y. Ogi, 2000, Flow Characteristics of Oil Film in Suction Line of Refrigeration Cycle, *In Proc. 8th International Refrigeration Conference at Purdue*, 273-280. Purdue University, IN.
- Fung, K. and S. G. Sundaresan, 1994, Study of Oil Return Characteristics in a Display Case Refrigeration System. Comparison of Different Lubricants for a HFC-Blend Refrigerant, *In Proc. 5th International Refrigeration Conference at Purdue*, 121-128, Purdue University, IN.
- Gnielinski, V., 1976, New equations for Heat and Mass Transfer in Turbulent Pipe and Channel Flow, *International Journal of Chemical Engineering*, 16: 359-368.
- Grebner, J. J. and R. R. Crawford, 1993, The Effects of Lubricant on Evaporator Capacity for Systems Using Mixtures of R-12/Mineral Oil and R-134a/Symthetic Oil, *ASHRAE Transactions*, 99: 380-386.
- Green G. H., 1971, The Effect of Oil on Evaporator Performance, *ASHRAE Symposium Bulletin*, 23-27.
- Hauk, A. and E. Weidner, 2000, Thermodynamic and Fluid-Dynamic Properties of Carbon Dioxide with Different Lubricants in Cooling Circuits for Automobile Application, *Industrial & Engineering Chemistry Research*, 39: pp. 4646-4651.
- Hughmark, G.A., 1962, Holdup in Gas-Liquid Flow, *Chemical Engineering Progress*, 58(4): 62-65.

Hurlburt, E. T. and T. A. Newell, 2000, Prediction of the Circumferential Film Thickness Distribution in Horizontal Annular Gas-Liquid Flow, *Transactions of ASME Journal of Fluid Engineering*, 122: 396-402.

Hwang, Y., 1997, Comprehensive Investigation of Carbon Dioxide Refrigeration Cycle, Ph.D. Thesis, University of Maryland, College Park, MD

Hwang, Y., J. P. Lee, R. Radermacher, and R. H. Pereira, 2000, An Experimental Investigation on Flow Characteristics of Refrigerant/Oil mixture in Vertical Upward Flow, *In Proc. 8th International Refrigeration Conference at Purdue*, 265-272. Purdue University, IN.

Hwang, Y., L. Cremaschi, R. Radermacher, T. Hirata, Y. Ozaki, and T. Hotta, 2002, Oil Circulation Ratio Measurement in CO₂ Cycle, *In Proc. New Technologies in Commercial Refrigeration*, University of Illinois, IL.

Jacobs, M. L, F. C. Scheideman, S. M. Kazem and N. A. Macken, 1976, Oil Transport by Refrigerant Vapor, *ASHRAE Transactions*, 82: 318-329.

Kawaguchi, Y., M. Takesue, M. Kaneko, and T. Tazaki, 2000, Performance Study Refrigerating Oil with CO₂, *2000 SAE Automotive Alternative Refrigerant System Symposium*, Scottsdale, AZ.

Kesim, S. C., K. Albayrak and A. Ileri, 2000, Oil Entrainment in Vertical Refrigerant Piping, *International Journal of Refrigeration*, 23: 626-631.

Khor, S. H., M. A. Mendes-Tatis and G. F. Hewitt, 1997, One-Dimensional Modeling of Phase Holdups in Three-Phase Stratified Flow, *International Journal of Multiphase Flow*, 23(5): 885-897.

Kruse, H. H. and M. Schroeder, 1984. Fundamentals of Lubrication in Refrigerating Systems and Heat Pumps. *ASHRAE Transactions*, 90 Part 2B: 763-783.

Lee, J.P., Y. Hwang, R. Radermacher, and S. S. Mehendale, 2001, Experimental Investigations on Oil Accumulation Characteristics in a Vertical Suction Line, *In Proc. of ASME IMECE 2001, Vol. 3, AES 23607*, New York, NY.

Li, H. and T. E. Rajewski, 2000, Experimental Study of Lubricant Candidates for the CO₂ Refrigeration System, *In Proc. 8th International Refrigeration Conference at Purdue*, 409-416. Purdue University, IN.

Lockhart, R.W., and R.C. Martinelli, 1949, Proposed Correlation of Data for Isothermal Two-Phase, Two-Component Flow in Pipes, *Chemical Engineering Progress*, 45:39-48.

Lorentzen, G. and J. Pettersen, 1993, A New, Efficient and Environmentally Benign System for Car Air-Conditioning, *International Journal of Refrigeration*, 16(1): 4-12.

- Luninski, Y., D. Barnea and Y. Taitel, 1983, Film Thickness in Horizontal Annular Flow, *The Canadian Journal of Chemical Engineering*, 61: 621-626.
- Macken, N. A., F. C. Scheideman and M. L. Jacobs, 1979, Pressure Loss and Liquid transport of Oil-Refrigerant Mixtures in Suction and Discharges Lines, *ASHRAE Transactions*, 85(2): 77 –92.
- Mehendale, S. S. and R. Radermacher, 2000, Experimental and Theoretical Investigation of Annular Film Flow Reversal in a Vertical Pipe: Application to Oil Return in Refrigeration Systems, *International Journal of HVAC & R Research*. 6(1): 55-74.
- Mehendale, S. S., 1998, Experimental and Theoretical Investigation of Annular Film Flow Reversal in a Vertical Pipe, Ph.D. Thesis, University of Maryland, College Park, MD.
- Moriyama, K. and A. Inoue, 1992, The Thermohydraulic Characteristics of Two-Phase Flow in Extremely Narrow Channels (The Friction Pressure Drop and Heat Transfer of Boiling Two-Phase Flow, Analytical Model), *Heat Transfer- Japanese Research*, 21(8): 838-856.
- Newton, C. H., M. Behnia, and J.A., Reizes, 1999, The Effect of Liquid Viscosity on Gas Wall and Interfacial Shear Stress in Horizontal Two-Phase Pipe Flow, *Chemical Engineering Science*, 54:1071-1079.
- Nidegger, E., J. R. Thome, and D. Favrat, 1997, Flow Boiling and Pressure Drop Measurements for R-134a/Oil Mixtures Part 1 - Evaporation in a Microfin Tube, *International Journal of HVAC & R Research*, 3(1): 38-53.
- Nino, V.G., P.S. Hrnjak, and T.A. Newell, 2002, Analysis of Void Fraction in Microchannels, *In Proc. 9th International Refrigeration Conference at Purdue*, R10-3. Purdue University, IN.
- Oliemans, R. V. A., B. F. M. Pots, and N. Trompe, 1986, Modeling of Annular Dispersed Two-Phase Flow in Vertical Pipes, *International Journal of Multiphase Flow*, 12(5): 711-732.
- Omega Handbook and Encyclopedia of Flow & Level, 2000, Omega Engineering Inc., Stamford, CT.
- Peles, Y. P. and S. Haber, 2000, A Steady State, One Dimensional, Model for Boiling Two Phase Flow in Triangular Micro-Channel, *International Journal of Multiphase Flow*, 26: 1095-1115.
- Petterson, J., 2003, Two-Phase Flow Pattern, Heat Transfer, and Pressure Drop in Microchannel Vaporization of CO₂, *ASHRAE Transactions*, 109: CH-03-8-1.
- Popovic, P., 1999, Investigation and Analysis of Lubricant Effects on the Performance of an HFC-134a Refrigeration System, Ph.D. Thesis, Iowa State University, Ames, IA

Preissner, M., 2001, Carbon Dioxide Vapor Compression Cycle Improvements with Focus on Scroll Expanders, Ph.D. Thesis, University of Maryland, College Park, MD.

Premoli, A., D. Francesco, and A. Prina, 1971, A Dimensionless Correlation for Determining the Density of Two-Phase Mixtures, *Lo Termotecnica* 25: 17-26.

Reyes-Gavilan, J., G. T. Flak and T. R. Tritcak, 1996, Lubricant Return Comparison of Naphthenic and Polyol Ester Oils in R-134a Household Refrigeration Applications, *ASHRAE Transactions*, 102(2): 180-185.

Rice, C.K., 1987, The Effect of Void Fraction Correlation and Heat Flux Assumption on Refrigerant Charge Inventory Predictions, *ASHRAE Transactions*, 93: 341-367.

Riedle, K. J., N. A. Macken and S. W. Gouse, Jr., 1972, Oil Transport by Refrigerant Vapor: A Literature Survey and Proposed Analytical Model, *ASHRAE Transactions*, 78: 124-133.

Scheideman, F. C. and N. A., Macken, 1975, Pressure Loss of Refrigerant-Oil Mixtures in Horizontal Pipes, *ASHRAE Transactions*, 81: 235 –249.

Seeton, C., J. Fahl and D. Henderson, 2000, Solubility, Viscosity, Boundary Lubrication and Miscibility of CO₂ and Synthetic Lubricants. *In Proc. 8th International Refrigeration Conference at Purdue*, 417-424. Purdue University, IN.

Short, G, and R. Cavestri, 1992, High-Viscosity Ester Lubricants for Alternative Refrigerant, *ASHRAE Transactions*, 98: 785–795.

Skouloudis, A. N. and J. Wijrtz, 1993, Film-Thickness, Pressure-Gradient, and Turbulent Velocity Profiles in Annular Dispersed Flows, *Journal of Fluid Engineering*, 115: 264-269.

Sumida, Y., Nakayame, M., Suzuki, S., and Kawaguchi, S., 1998, Alkylbenzene for Split Air Conditioner with R-410A Part 2: Oil Return Characteristics, *In Proc. 1998 International Compressor Engineering Conference at Purdue*, 471-476, Purdue University, IN.

Sunami, M., K. Takigawa, and S. Suda, 1994, New Immiscible Refrigeration Lubricant for HFCs, *In Proc. 5th International Refrigeration Conference at Purdue*, 129-134, Purdue University, IN.

Sunami, M., K. Takigawa, and S. Suda, and U. Sasaki, 1995, New Immiscible Refrigeration Lubricant For HFCs, *ASHRAE Transactions*, 101: 940–946.

Sunami, M., Shimomura, Y., Sawada, K., Fukunaga, Y., and Sasaki, U., 1998, Compressor Durability Tests with AB and HFCs, *In Proc. 7th International Refrigeration Conference at Purdue*, 355-360, Purdue University, IN.

- Sundaresan, S. G. and R. Radermacher, 1996, Oil Return Characteristics of Refrigerant Oils in Split Heat Pump System, *ASHRAE Journal*, 38(8): 57-61.
- Taitel, Y., and Dukler, A.E., 1976, A Model for Predicting Flow Regime Transitions in Horizontal and Near Horizontal Gas-Liquid Flow, *AIChE*, 22: 47-55.
- Taitel, Y., D. Barnea and J. P. Brill, 1995, Stratified Three Phase Flow in Pipes, *International Journal of Multiphase Flow*, 21(1): 53-60.
- Tatara, R. A., P. Payvar, 2000, Effects of Oil on Boiling of Replacement Refrigerants Flowing Normal to a Tube Bundle - Part II: R-134a, *ASHRAE Transactions*, 106: 786-791.
- Tomas, R. H. P. and H. T. Pham, 1992, Solubility and Miscibility of Environmentally Safer Refrigerant/Lubricant Mixtures, *ASHRAE Transactions*, 98: 783-788.
- Triplett, K.A., S.M. Ghiaasiaan, S.I. Abdel-Khalik, and D.L. Sadowski, 1999, Gas-Liquid Two-Phase Flow in Microchannels Part I: Two-Phase Flow Patterns, *International Journal of Multiphase Flow*, 25: 377-394.
- Vaughn, R. S., 1971, Refrigeration Compressors, Lubricating Oil, and Refrigerant-An Uneasy Trio, *ASHRAE Symposium Bulletin*, 14-18.
- Wallis, G. B., 1969, *One-Dimensional Two-Phase Flow*, McGraw-Hill Book Company, N.Y., NY.
- Wallis, G., 1970, Annular Two-Phase Flow, Part I: A Simple Theory, *Transactions of ASME Journal of Basic Engineering*, 92: 59-72.
- Wongwises, S. and W. Kongkiatwanitch, 2001, Interfacial Friction Factor in Vertical Upward Gas-Liquid Annular Two-Phase Flow, *International Communication Heat and Mass Transfer*, 28(3): 323-336.
- Yang, C.Y. and C.C. Shieh, 2001, Flow Pattern of Air-Water and Two-Phase R-134a in Small Circular Tubes, *International Journal of Multiphase Flow*, 27: 1163-1177.
- Yashar, D.A., M.J. Wilson, H.R. Kopke, D.M. Graham, J.C. Chato, and T.A. Newell, 2001, An Investigation of Refrigerant void Fraction in Horizontal, Microfin Tubes, *International Journal of HVAC & R Research*, 7(1): 67-82.
- Yokozeiki, A., 1994, Solubility and Viscosity of Refrigerant-Oil Mixtures, *In Proc. 5th International Refrigeration Conference at Purdue*, 335-340, Purdue University, IN.
- Yokozeiki, A., K. Takigawa, and S. I. Sandler, 2000, Solubility and Viscosity of Hydrofluorocarbon/Alkylbenzene Oil Mixtures, *In Proc. 8th International Refrigeration Conference at Purdue*, 241-247. Purdue University, IN.

Zhao, Y., 2001, Flow Boiling Characteristics of Carbon Dioxide in Microchannels, Ph.D. Thesis, University of Maryland, College Park, MD.

Zhao, Y., M. Molki, M. M. Ohadi and S. V. Dessiatoun, 2000, Flow Boiling of CO₂ in Microchannels, *ASHRAE Transactions*, 106: 437–445.

Zhao, Y., M. Molki, M. M. Ohadi, F. H. R. Franca, and R. Radermacher, 2002, Flow Boiling of CO₂ with Miscible Oil in Microchannels, *ASHRAE Transactions*, 108: 4505.

Zurcher, O., J. R. Thome, and D. Favrat, 1998, In-Tube Flow Boiling of R-407C and R-407C/Oil Mixtures. Part II: Plain Tube Results and Predictions, *International Journal of HVAC & R Research*, 4(4): 373-399.